ANALYSIS AND DESIGN OF A CUK SWITCHING REGULATOR

A THESIS SUBMITTED TO
THE GRADUATE SCHOOL OF NATURAL AND APPLIED SCIENCES
OF
MIDDLE EAST TECHNICAL UNIVERSITY

BY

ZEKIYE GÜNAYDIN

IN PARTIAL FULFILLMENT OF THE REQUIREMENTS
FOR
THE DEGREE OF MASTER OF SCIENCE
IN
ELECTRICAL AND ELECTRONICS ENGINEERING

MAY 2009

Approval of the thesis:

ANALYSIS AND DESIGN OF A CUK SWITCHING REGULATOR

submitted by **Zekiye Günaydın** in partial fulfillment of the requirements for the degree of **Master of Science in Electrical and Electronics Engineering Department, Middle East Technical University** by,

Prof. Dr. Zafer Dursunkaya _____
Dean, Graduate School of **Natural and Applied Sciences**

Prof. Dr. İsmet Erkmen _____
Head of Department, **Elec. Electronics Engineering**

Prof. Dr. Aydın Ersak _____
Supervisor, **Elec. Electronics Engineering Dept., METU**

Examining Committee Members:

Prof. Dr. Muammer Ermiş _____
Elec. Electronics Engineering Dept., METU

Prof. Dr. Aydın Ersak _____
Elec. Electronics Engineering Dept., METU

Assoc. Prof. Dr. Ahmet M. Hava _____
Elec. Electronics Engineering Dept., METU

Assoc. Prof. Timur Aydemir _____
Elec. Electronics Engineering Dept., Gazi University

Günay Şimşek M.Sc. _____
ASELSAN

Date: 04.05.2009

I hereby declare that all information in this document has been obtained and presented in accordance with academic rules and ethical conduct. I also declare that, as required by these rules and conduct, I have fully cited and referenced all material and results that are not original to this work.

Name, Last name :

Signature :

ABSTRACT

ANALYSIS AND DESIGN OF A CUK SWITCHING REGULATOR

GÜNAYDIN, Zekiye

M. S, Department of Electrical and Electronics Engineering

Superivisor: Prof. Dr. Aydın ERSAK

may 2009, 117 pages

This theses analyzes Cuk converter, that is one of the dc to dc switchıng converters. For continuous inductor current mode and discontinuous inductor current mode, stedy state operation is analysied. Characteristic parameters are determined. Through State Space Averge Models, Small Signal Models are obtained. Parasitic Resistance effects on steady state and small signal models are determined. Efficency of the switching converter is derived. Open loop transfer functions for continous and discontinuous inductor curret mode are obtained. Parmeters for small signal behaviour is determined and stability is analysied. Parasitic resistance effects on transfer functions is determined. Therotecial analysis are verified with a simulations of designed converter.

Keywords: Dc-dc, Cuk Converter, discontinuous inductor current mode (DICM), continuous inductor current mode (CICM) , parasitic resistance effects, efficieny, open loop transfer functions .

ÖZ

CUK ANAHTARLAMALI DÖNÜŞTÜRÜCÜNÜN İNCELENMESİ VE TASARIMI

GÜNAYDIN, Zekiye

Yüksek Lisans, Elektrik ve Elektronik Mühendisliği Bölümü

Tez Yöneticisi: Prof. Dr. Aydın ERSAK

mayıs 2009, 117 sayfa

Bu çalışma Cuk anahtarlamalı dc-dc dönüştürücüsünü incelemekedir. Sürekli ve süreksiz andüktans akımları için sürekli hal çalışması incelendi. Karakteristic parametreler belirlendi. Durum uzayı oratalama modelinden yaralanılarak küçük işaret modeli elde edildi. Gerçek elemanlarda var olan dirençlerin sürekli hal çalışmasına ve küçük işaret modeline etkisi belirlendi. Anahtarlamalı dönüştürücünün verimi incelendi. Sürekli ve süreksiz endüktans akımları çalışması için açık çevrim transfer fonksiyonları elde edildi. Küçük işaret davranışı için parametreler belirlendi, karalılık incelendi. Eleman iç dirençlerinin transfer fonksiyonları üzerindeki etkisi belirlendi. Teorik analizler tasarımlanan Cuk dönüştürücünün simülasyonu ile doğrulandı.

Anahtar Kelimeler: Dc-dc, Cuk Dönüştürücü, Süreksiz endüktans akımı çalışması, Sürekli endüktans akımı çalışması, eleman iç dirençlerinin etkisi, verimlilik, açık çavrim transfer fonksiyonu.

TABLE OF CONTENTS

CHAPTER 1

INTRODUCTION

Cuk converter is a switching regulator which yields a variable output voltage from a constant dc supply. Its continuous input inductor current gives a relative advantage against its rivals. This converter has been investigated quite extensively in the literature. There several studies related to its modeling, analysis, and control issues.

Descriptive equations of voltage and current for different operational states of a Cuk converter used, when developing the model of the converter, are given in several papers [12, 13] for continuous inductor current mode operation. The state-space averaged model used to derive the steady-state and the dynamic models of the Cuk converter based on its state space averaged model, are given in [2]. The state-space averaging concept provides a means to obtain models for Cuk converter operating in discontinuous inductor current mode. It is used also to analyze the converter response for continuous inductor current mode. Discontinuous inductor current mode operation of Cuk converter at constant duty ratio makes the application of Cuk converter feasible to be used as power-factor preregulator [5], and parameters for this specific operation are determined in [3] and [4]. Additionally, [16] investigates application of Cuk converter as power-factor preregulator in continuous inductor current mode. It is stated that by special average current mode control technique, Cuk converter in continuous inductor current mode is applicable as power-factor preregulator for high power requirements that can not be provided at discontinuous inductor current mode. Furthermore, there is an additional mode of operation of both Cuk and Sepic converters that is discontinuous (energy transfer) capacitor voltage mode. Similar to the discontinuous inductor current mode of operation, the discontinuous capacitor voltage mode operation makes the application of Cuk converter feasible to be used as power factor preregulator. In [17] discontinuous capacitor voltage mode operation of Cuk converter is studied and

power-factor preregulator applications of discontinuous inductor current mode and discontinuous voltage mode is compared. Efficiency issues related to the Cuk converter are discussed in the literature in comparison with Buck-Boost converter without giving an overall efficiency expression.[1] Stability analysis for Cuk converter is performed through state-space averaged model with Routh–Hurwitz criterion in [14] for closed- and open-loop in continuous input inductor current mode operation. Also in [15] stability for closed- and open-loop in continuous input inductor current mode is analyzed with multifrequency approach.

Application of sliding mode control to Cuk converter is discussed in [13], [12] and [18]. Sliding mode control technique is based on directing state variables of a system to references that compose a surface and is applicable to linear and non liner systems. In [13] the control technique is applied considering the state-space averaged models of the converter with fixed frequency PWM switching. The control technique improves large signal dynamic response and ensures large signal stability. Studies regarding to the improvement of the system stability and optimization of the performance take place in the literature using the sliding mode control technique which also gets rid of the need of decoupling input and output stages of the converter.[12] Another control technique that takes place in applications of Cuk converter is one cycle control.[19, 20] Duty ratio in one cycle control technique is determined by comparing output voltage integration to reference volt-second at each cycle. Current mode control of Cuk converter is analyzed in [21], [22] and [23]. In the papers it is stated that current mode control is stable for limited duty- ratio, where the duty-ratio of operation is determined by reference current. In case the duty ratio limit is exceeded by setting current reference high, alternating variations in duty-ratio is observed and chaotic waveforms are observed. Isolation, integrated magnetics concept and their advantages in Cuk converter is discussed in [24] and [25].

Isolation transformer in Cuk converter is placed by dividing energy transferring capacitor to two. The isolation transformer is placed between the capacitors such as; both of energy transferring capacitors are connected series to transformer windings, one to primary winding and the other to secondary winding. Application of integrated magnetics is feasible only for inductors which have

identical voltage waveforms. Thus for Cuk converter integration is applicable between two inductors, between primary winding of the transformer and input inductor or between secondary winding of the transformer and output inductor. Magnetics integration reduces current ripples at input, output or input and output at the same time regarding to integrated elements. Moreover, zero current ripples can be achieved at input inductor or output inductor by the magnetics integration. Current ripple reduction is important in efficiency and EMI.

The thesis work aims at analyzing and determining the design constraints prevailing the switching of the Cuk converter. Analyses are done for two operating modes of the converter; continuous input inductor current mode, and discontinuous input inductor current mode. Analyses in these modes of operations use a state-space averaged model of the Cuk converter developed as described in [2]. These analyses involve the use of steady-state and dynamic (small signal) models of the converter to determine the responses of the converter when operating in either of the operational modes. The stability analysis and the investigation of the dynamic behavior of the converter use the transfer functions that are defined in the thesis as dynamic conversion ratios.

The thesis considers effects of parasitic resistances related to several parameters of the Cuk converter as well. The related analysis is given following the ideal case analysis. With a designed Cuk converter simulations will be performed to go through theoretical analyses.

In the thesis second chapter covers continuous input inductor current mode analysis. Voltage and current equations for states are derived. Using criteria such as; the volt-second balancing for inductors, and current-charge balancing for capacitors, steady-state equations are obtained. The steady-state and dynamic models are developed in state-space.

Third chapter deals with discontinuous input inductor current mode analysis. Likewise in the continuous mode of operation again, the voltage and current equations for states are obtained. Critical parameters for discontinuous inductor current mode are determined. State-space averaged models of the converter are

derived for the steady-state and dynamic analyses. Operational criterion and parameters of the converter model are rearranged so that the converter is analyzed as a Power Factor Preregulator.

In fourth chapter effects of parastic resistances will be determined. State-space averaged models are modified with parasitic resistances for both operating modes. Modifications are extended to steady state and dynamic models as well for both operating modes.

Efficiency considerations for Cuk converter are evaluated in fifth chapter. Parasitic resistance and switching of real elements are sources of losses. A MOSFET is considered as the real switch in Cuk converter. Switching losses of a diode and MOSFET as well as those related to inductors are investigated in [8] and [9].

Sixth chapter investigates the stability and the dynamic behavior of the converter. Using the small signal models obtained in second, third, and fourth chapters, the dynamic voltage conversion-ratios, and control to output conversion ratios are obtained in both operating modes. Effect of parasitic resistances on the dynamic conversion-ratios is also evaluated.

In the last chapter simulation results are examined. A cuk converter has been designed for simulation purposes. The simulations have been conducted for the continuous inductor current mode operation. When discontinuous inductor current mode operation is considered the simulated converter is modified accordingly and simulations are performed for discontinuous inductor current mode and the power factor preregulator application. The dynamic conversion-ratios of the circuits are obtained. Stability analysis and dynamic behaviors are examined for discontinuous and continuous inductor current modes. Parasitic resistances are also evaluated for stability and dynamic behavior in continuous and discontinuous inductor current mode operation.

CHAPTER 2

ANALYSIS FOR CONTINUOUS INDUCTOR CURRENT MODE OPERATION

Cuk converter is a switched mode converter. Schematic of the Cuk converter is shown in Fig. 2.1. During the operation the switch S_1 switches on and off at a frequency ' f_S ', with a period 'T' and duty ratio'k' within the period T determined by an externally applied control signal.

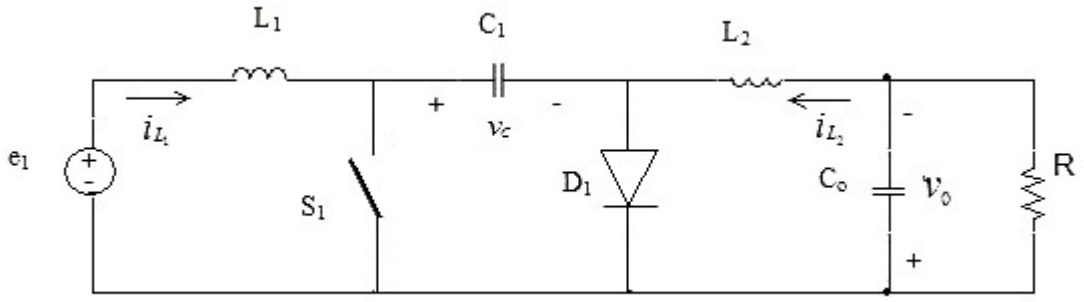

Fig. 2.1 Cuk converter

2.1 Separate Analysis of Two States

Continuous conduction mode operation implies than inductor currents do not fall to zero at any instant within the period.

In the subsequent analysis parasitic resistances are negligibly small, and all elements are supposed ideal.

The operation of the converter within the period T can be divided into two states for continuous conduction mode operation;

State for S1 is ‘on’, when $0 < t < T_{on}$

State for S1 is ‘off’, when $T_{on} < t < T$

where $k = \frac{T_{on}}{T} \Rightarrow T_{on} = kT$ and $k' = 1 - k$

2.1.1 State S_1 ‘off’, $kT < t < T$

The circuit is divided into two separate meshes as seen in Fig. 2.2. When S1 is off, the energy storage capacitor C_1 in the left hand mesh is charged through L_1 and D_1 in this time interval. Diode D_1 common to both meshes is forward biased in this time interval. L_2 and C_o in the right hand mesh transfer their stored energies, left from the previous time interval during the steady-state operation, to the load R over D_1 again. One can write the following equations governing the operation in this state as;

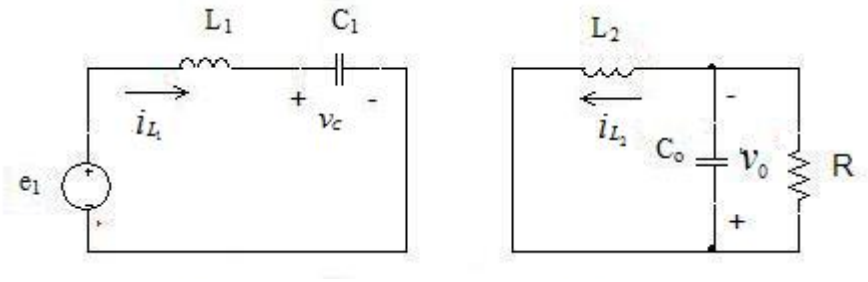

Fig. 2.2 The Cuk converter equivalent circuit in state for S_1 is off

$$\frac{di_{L_1}}{dt} = \frac{e_1 - v_C}{L_1}$$

$$\frac{dv_C}{dt} = \frac{i_{L_1}}{C} \qquad (2.1)$$

in the left hand mesh,

$$\frac{di_{L_2}}{dt} = -\frac{v_0}{L_2}$$

$$\frac{dv_0}{dt} = \frac{1}{C_0}(i_{L_2} - \frac{v_0}{R}) \qquad (2.2)$$

in the right hand mesh.

Current passing through D_1 is the sum of input and output inductor currents:

$$i_{D_1} = i_{L_1} + i_{L_2} \qquad (2.3)$$

2.1.2 State S_1 'on', $0 < t < kT$

In the state S_1 is on the converter circuit takes the form shown in Fig.2.3. Similar to the 'off' state equivalent circuit there are two separate meshes again. In the left hand mesh the input inductor L_1 stores energy from the source over S_1 during the time interval. The energy storage capacitor C_1 is now in the right hand mesh and it transfers stored energy, over S_1, to the load R, and energy storing elements L_2 and C_o. Due to the inappropriate voltage polarity of the charge on the capacitor C_1 diode D_1 is reverse biased and therefore off. The common path between the two meshes is provided by S_1 this time. One can write the following equations governing the operation in this state as;

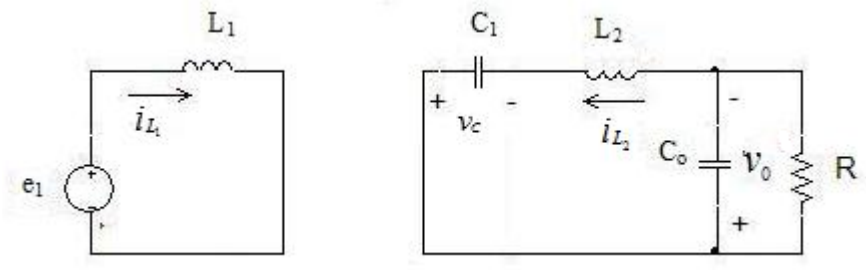

Fig. 2.3 The Cuk converter equivalent circuit in state for S_1 is on

$$\frac{di_{L_1}}{dt} = \frac{e_1}{L_1} \qquad (2.4)$$

in the left hand mesh, and

$$\frac{dv_{C_1}}{dt} = -\frac{i_{L_2}}{C_1}$$

$$\frac{di_{L_2}}{dt} = \frac{(v_{C_1} - v_0)}{L_2} \tag{2.5}$$

$$\frac{dv_0}{dt} = \frac{1}{C_0}(i_{L_2} - \frac{v_0}{R})$$

in the right hand mesh.

Current passing through S_1 is the sum of input and output inductor currents:

$$i_{S_1} = i_{L_1} + i_{L_2} \tag{2.6}$$

Main energy transferring element in the Cuk converter is the capacitor C_1. The terminal of C_1 connected to the negative terminal of the supply alternates in each state. It is the negative terminal of C_1 for the state S_1 is off, the positive terminal for the state S_1 is on. It was declared in [1] that this property in the connection of C_1 is the cause of the inversion of the output voltage, v_o.

2.2 Steady State Operation

Note that the integral of the voltage v_{Li} on an inductor L_i i=1,2 within a switching period T is equal to zero when it operates in steady state. Thus if the voltage changes polarity within a cycle, the volt-second balance is to be maintained. This yields,

$$\begin{aligned} &\int_0^T L_i \frac{di_{L_i}}{dt} dt = 0 \\ &L_i(i_{L_i}(T) - i_{L_i}(0)) = 0 \qquad i = 1,2 \\ &i_{L_i}(T) = i_{L_i}(0) \end{aligned} \tag{2.7}$$

the result indicating that the inductor current magnitudes at the beginning and at the end of a cycle are equal.

Similarly, the integral of the current i_C through a capacitor C_1 within a switching period T is equal to zero when it operates in steady-state. Thus, if the current changes direction within a cycle, the ampere-second balance is to be maintained. This yield,

$$\begin{aligned} &\int_0^T i_{C_1}\,dt = 0 \\ &\int_0^T C_1 \frac{dv_{C_1}}{dt} dt = 0 \\ &C_1(v_{C_1}(T) - v_{C_1}(0)) = 0 \\ &v_{C_1}(T) = v_{C_1}(0) \end{aligned} \tag{2.8}$$

the result indicating that the capacitor voltage magnitudes at the beginning and at the end of a cycle are equal.

(2.4) and (2.5) can be written in incremental form as (2.9), (2.10), and (2.11); ΔI_{L1} , ΔI_{L2} , and Δv_{C1} can then be defined as peak-to-peak ripple magnitudes of the respective variables.

$$\begin{aligned} &\frac{\Delta I_{L_1}}{\Delta t} = \frac{e_1}{L_1} \qquad with \quad \Delta t = kT \\ &\Delta I_{L_1} = \frac{e_1}{L_1 f_S} k \end{aligned} \tag{2.9}$$

$$\begin{aligned} &\frac{\Delta I_{L_2}}{\Delta t} = \frac{v_{C_1} - v_0}{L_2} \qquad with \quad \Delta t = kT \\ &\Delta I_{L2} = \frac{v_{C_1} - v_0}{L_2 f_S} k \end{aligned} \tag{2.10}$$

$$\begin{aligned} &\frac{\Delta v_{C_1}}{\Delta t} = -\frac{I_{L_2}}{C_1} \qquad with \quad \Delta t = kT \\ &\Delta v_{C_1} = \frac{I_{L_2}}{C_1 f_S} k \end{aligned} \tag{2.11}$$

The output voltage ripple is the ripple on the voltage of the capacitor C_o. Since the load current ripple is negligibly small then $\Delta I_{L_2} = \Delta I_{C_0}$ must follow. As can

be followed from the trace of i_{Co}, Fig. 2.4, the charging current for C_o flows only for half a period T/2. Therefore, the average value for this current is

$$\begin{aligned} I_{C_0} &= (\Delta I_{C_0} / 2) / 2 \\ &= \Delta I_{L_2} / 4 \end{aligned} \quad . \tag{2.12}$$

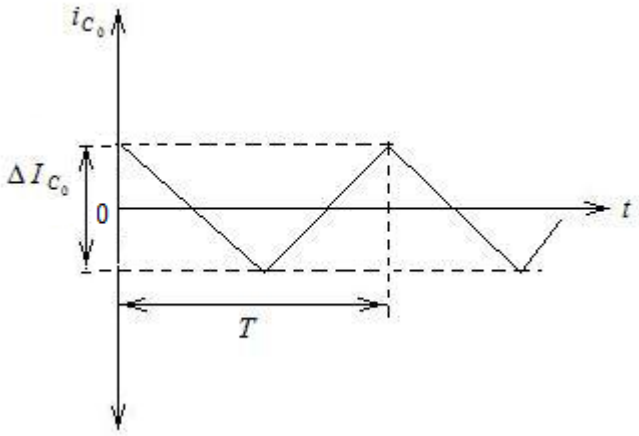

Fig. 2.4 Current of Output capacitor C_0

Thus the incremental change on the voltage of the capacitor C_o due to the average charging current I_{Co} is expressed as in [7];

$$\begin{aligned} \Delta v_{C_0} &= \frac{1}{C_0} \int_0^{T/2} I_{C_0} dt \\ &= \frac{1}{C_0} \int_0^{T/2} \frac{\Delta I_{L_2}}{4} dt = \frac{\Delta I_{L_2}}{8 f_S C_0} \end{aligned}$$

and substituting (2.10) we have result in [7]:

$$\Delta v_{C_0} = \frac{(v_{C_1} - v_0)}{8 L_2 C_0 f_S{}^2} k \tag{2.13}$$

Voltages applied to inductances during switching period are considered nearly constant. Since the volt-second increase in the period S_1 is 'on' must be equal to the volt-second decrease in the period S_1 is 'off' that means volt-second rise and fall in the voltage on an inductor must be balanced over a period T. Upper case

letters representing the steady state values of the respective variables this balance for the inductor L_1 gives (2.14) ;

$$\begin{aligned} &\int_0^{kT} E_1 dt + \int_{kT}^{T} (E_1 - V_{C_1}) dt = 0 \\ &E_1 kT + (E_1 - V_{C_1})(1-k)T = 0 \\ &E_1 T - V_{C_1}(1-k)T = 0 \\ &E_1 = (1-k)V_{C_1} \end{aligned} \tag{2.14}$$

Volt second balancing for second inductor leads;

$$\begin{aligned} &\int_0^{kT} (V_{C_1} - V_0) dt + \int_{kT}^{T} (-V_0) dt = 0 \\ &(V_{C_1} - V_0)kT + (-V_0)(1-k)T = 0 \\ &V_{C_1} kT - V_0 T = 0 \\ &V_{C_1} k = V_0 \end{aligned} \tag{2.15}$$

Considering currents drawn from the capacitor constant the rise and fall of the voltage on the capacitor C_1 must also be balanced over a period T as given in (2.16).

$$\begin{aligned} &\int_0^{kT} I_{L_1} dt - \int_{kT}^{T} I_{L_2} dt = 0 \\ &I_{L1} kT - I_{L_2}(1-k)T = 0 \\ &I_{L_1} k = I_{L_2}(1-k) \end{aligned} \tag{2.16}$$

With the help of (2.3), average current for the diode D_1 , I_{D_1} is averaged value of the sum of the average input and the average output inductor currents I_{L_1}, I_{L_2} over a period kT.

$$\begin{aligned} &I_{D_1} = (I_{L_1} + I_{L_2})k \\ &I_{D_1} = (I_{L_2} \frac{(1-k)}{k} + I_{L_2})k \\ &I_{D_1} = I_{L_2} \end{aligned} \tag{2.17}$$

Also from (2.6) average current for the switch S_1, I_{S_1} is expressed with average input and output inductor currents I_{L_1}, I_{L_2} as follows;

$$
\begin{aligned}
I_{S_1} &= (I_{L_1} + I_{L_2})(1-k) \\
I_{S_1} &= (I_{L_1} + I_{L_1}\frac{k}{(1-k)})(1-k) \\
I_{S_1} &= I_{L_1}
\end{aligned}
\tag{2.18}
$$

2.3 Steady State and Dynamic Models

State-space averaging method is used to model the power stages of dc-to-dc switching converters. It combines two main power stage modelling approaches, state-space and averaging methods between which correlation is little. The method was proposed by Middlebrook R.D., Cuk Slobodan in [2].

State-space averaging method provides single representation for entire period as stated in [2]. According to the averaging method dynamic and static equations are averaged. For $0 < t < kT$ interval equations are multiplied by 'k', and for $kT < t < T$ interval equations are multiplied by 'k' =(1-k)' for averaging the system variables.

$$k(\frac{di_{L_1}}{dt} = \frac{e_1}{L_1}) + (1-k)(\frac{di_{L_1}}{dt} = \frac{e_1 - v_{C_1}}{L_1})$$

$$k(\frac{dv_{C_1}}{dt} = -\frac{i_{L_2}}{C_1}) + (1-k)(\frac{dv_{C_1}}{dt} = \frac{i_{L_1}}{C_1})$$

$$k(\frac{di_{L_2}}{dt} = \frac{v_{C_1} - v_0}{L_2}) + (1-k)(\frac{di_{L_2}}{dt} = -\frac{v_0}{L_2})$$

$$k(\frac{dv_0}{dt} = \frac{1}{C_0}(i_{L_2} - \frac{v_0}{R})) + (1-k)(\frac{dv_0}{dt} = \frac{1}{C_0}(i_{L_2} - \frac{v_0}{R})) \tag{2.19}$$

By summing these resulting equations the average state-space representation is obtained. Variables that take place in the model are averaged variables for a switching period. Averaging method is applied in (2.19) and (2.20).

$$\frac{di_{L_1}}{dt} = \frac{e_1}{L_1} - \frac{(1-k)v_{C_1}}{L_1}k$$

$$\frac{dv_{C_1}}{dt} = -\frac{ki_{L_2}}{C_1} + \frac{(1-k)i_{L_1}}{C_1}$$

$$\frac{di_{L_2}}{dt} = \frac{kv_{C_1}}{L_2} - \frac{v_0}{L_2}$$

$$\frac{dv_0}{dt} = \frac{i_{L_2}}{C_0} - \frac{v_0}{C_0 R} \tag{2.20}$$

‘This model is the basic model which is the starting model for all other (steady state and dynamic model) derivations.’ stated in [2].

Variables in the state space averaged model can be represented as summation of steady state and perturbed variables. In steady state operation variables are constant. This means that derivatives for steady state variables in model equations are zero. Steady state variables are represented by upper case and perturbed variables are represented by lower case with a cap ‘^’ on top then,

$$e_1 = E_1 + \hat{e}_1$$

$$i_{L_1} = I_{L_1} + \hat{i}_{L_1}$$

$$v_{C_1} = V_{C_1} + \hat{v}_{C_1}$$

$$i_{L_2} = I_{L_2} + \hat{i}_{L_2}$$

$$v_o = V_o + \hat{v}_o$$

$$k = K + \hat{k} \tag{2.21}$$

New representation of the state space averaged model is given in (2.18). The system is nonlinear, includes product of time dependent perturbed variables.

It is supposed that perturbed values are too small from steady state values. Thus by neglecting terms including product of time dependent (perturbed) variables

the system is linearized. The linear equations are given in (2.23). It is a linearized small-signal low-frequency model.

$$\frac{d\hat{i}_{L_1}}{dt} = \frac{E_1}{L_1} - \frac{(1-K)V_{C_1}}{L_1} + \frac{\hat{e}_1}{L_1} - \frac{(1-K)\hat{v}_{C_1}}{L_1} + \frac{V_{C_1} + \hat{v}_{C_1}}{L_1}\hat{k}$$

$$\frac{d\hat{v}_{C_1}}{dt} = -\frac{KI_{L_2}}{C_1} + \frac{(1-K)I_{L_1}}{C_1} - \frac{K\hat{i}_{L_2}}{C_1} + \frac{(1-K)\hat{i}_{L_1}}{C_1} - \frac{I_{L_1} + I_{L_2}}{C_1}\hat{k} - \frac{\hat{i}_{L_1} + \hat{i}_{L_2}}{C_1}\hat{k}$$

$$\frac{d\hat{i}_{L_2}}{dt} = \frac{KV_{C_1}}{L_2} - \frac{V_0}{L_2} + \frac{K}{L_2}\hat{v}_{C_1} - \frac{1}{L_2}\hat{v}_0 + \frac{(V_{C_1} + \hat{v}_{C_1})}{L_2}\hat{k}$$

$$\frac{d\hat{v}_0}{dt} = \frac{I_{L_2}}{C_0} - \frac{V_0}{C_0 R} + \frac{\hat{i}_{L_2}}{C_0} - \frac{\hat{v}_0}{C_0 R} \qquad (2.22)$$

$$\frac{d\hat{i}_{L_1}}{dt} = \frac{E_1}{L_1} - \frac{(1-K)V_{C_1}}{L_1} + \frac{\hat{e}_1}{L_1} - \frac{(1-K)\hat{v}_{C_1}}{L_1} + \frac{V_{C_1}}{L_1}\hat{k}$$

$$\frac{d\hat{v}_{C_1}}{dt} = -\frac{KI_{L_2}}{C_1} + \frac{(1-K)I_{L_1}}{C_1} - \frac{K\hat{i}_{L_2}}{C_1} + \frac{(1-K)\hat{i}_{L_1}}{C_1} - \frac{I_{L_1} + I_{L_2}}{C_1}\hat{k}$$

$$\frac{d\hat{i}_{L_2}}{dt} = \frac{KV_{C_1}}{L_2} - \frac{V_0}{L_2} + \frac{K}{L_2}\hat{v}_{C_1} - \frac{1}{L_2}\hat{v}_0 + \frac{V_{C_1}}{L_2}\hat{k}$$

$$\frac{d\hat{v}_0}{dt} = \frac{I_{L_2}}{C_0} - \frac{V_0}{C_0 R} + \frac{\hat{i}_{L_2}}{C_0} - \frac{\hat{v}_0}{C_0 R} \qquad (2.23)$$

According to [2] steady state and dynamic models are combined in (2.23). After separation, steady-state (2.24) and dynamic (2.26) models are obtained. From steady state model the relation between input and output variables are derived and given in (2.25). It is consistent with relations derived due to volt second balance and ampere second balance.

$$0 = \frac{E_1}{L_1} - \frac{(1-K)V_{C_1}}{L_1} + \frac{\hat{e}_1}{L_1}$$

$$0 = -\frac{KI_{L_2}}{C_1} + \frac{(1-K)I_{L_1}}{C_1}$$

$$0 = \frac{KV_{C_1}}{L_2} - \frac{V_0}{L_2}$$

$$0 = \frac{I_{L_2}}{C_0} - \frac{V_0}{C_0 R} \tag{2.24}$$

$$E_1 = (1-K)V_{C_1};\ I_{L_2} = \frac{(1-K)}{K} I_{L_1}$$

$$V_0 = KV_{C_1};\ I_{L_2} = \frac{V_0}{R}$$

$$V_0 = \frac{K}{(1-K)} E_1;\ V_{C_1} = E_1 + V_0 \tag{2.25}$$

The relation between variables expressed in (2.21) is dependent on duty ratio K and the load resistance only as stated in [2]. L_1, C_1, L_2, C_o storage element values do not affect steady state operation point.

$$\frac{d\hat{i}_{L_1}}{dt} = \frac{\hat{e}_1}{L_1} - \frac{(1-K)\hat{v}_{C_1}}{L_1} + \frac{V_{C_1}}{L_1}\hat{k}$$

$$\frac{d\hat{v}_{C_1}}{dt} = -\frac{K\hat{i}_{L_2}}{C_1} + \frac{(1-K)\hat{i}_{L_1}}{C_1} - \frac{I_{L_1} + I_{L_2}}{C_1}\hat{k}$$

$$\frac{d\hat{i}_{L_2}}{dt} = \frac{K}{L_2}\hat{v}_{C_1} - \frac{1}{L_2}\hat{v}_0 + \frac{V_{C_1}}{L_2}\hat{k}$$

$$\frac{d\hat{v}_0}{dt} = \frac{\hat{i}_{L_2}}{C_0} - \frac{\hat{v}_0}{C_0 R} \tag{2.26}$$

Dynamic model given in (2.26) includes variable $\hat{k}$. Perturbations in duty ratio k can be observed in both open loop and closed loop systems. For closed loop systems, model is modified by substituting feedback loop relation between k and output voltage v_0.

(2.27) is the matrix representation of (2.26).

$$\begin{bmatrix} \frac{d\hat{i}_{L_1}}{dt} \\ \frac{d\hat{v}_{C_1}}{dt} \\ \frac{d\hat{i}_{L_2}}{dt} \\ \frac{d\hat{v}_0}{dt} \end{bmatrix} = \begin{bmatrix} 0 & -\frac{(1-K)}{L_1} & 0 & 0 \\ \frac{(1-K)}{C_1} & 0 & -\frac{K}{C_1} & 0 \\ 0 & \frac{K}{L_2} & 0 & -\frac{1}{L_2} \\ 0 & 0 & \frac{1}{C_o} & -\frac{1}{C_o R} \end{bmatrix} \begin{bmatrix} \hat{i}_{L_1} \\ \hat{v}_{C_1} \\ \hat{i}_{L_2} \\ \hat{v}_0 \end{bmatrix} + \begin{bmatrix} \frac{1}{L_1} \\ 0 \\ 0 \\ 0 \end{bmatrix} \hat{e}_1 + \begin{bmatrix} \frac{V_C}{L_1} \\ -\frac{(I_{L_1} + I_{L_2})}{C_1} \\ \frac{V_{C_1}}{L_2} \\ 0 \end{bmatrix} \begin{bmatrix} \hat{k} \end{bmatrix} \quad (2.27)$$

The system has two sources of perturbation, voltage source perturbations $\hat{e}_1$ and duty ratio perturbations $\hat{k}$.

CHAPTER 3

ANALYSIS FOR DISCONTINUOUS INDUCTOR CURRENT MODE

General condition for discontinuous inductor mode operation at dc to dc converters is zero current passing through the inductor for a period of a cycle. Whereas Cuk converter operates in discontinuous inductor current mode if the output inductor current reverses direction and becomes equal to input inductor current within a switching period. Thus the third state is observed in the period 'T'. Two of states are similar with the states of continuous conduction mode. ON OFF state combinations of the switch and the diode determine states of discontinuous conduction mode.

3.1 Separate Analysis of the Three State

The three state operation definition needs at least two duty ratios. Duty ratio k defines the ratio of on position of switch S_1. Duty ratio k_1 defines the ratio of on position of the diode D_1. In the continuous conduction mode operation the diode D_1 is on until the end of a cycle, so there is no need to the second duty ratio.

State S_1 on, D_1 off $\quad 0 < t < T_{on}$

State S_1 off, D_1 on $\quad T_{on} < t < T_{don}$

State S_1 off, D_1 off $\quad T_{don} < t < T$

where $k = \frac{T_{on}}{T} \Rightarrow T_{on} = kT$, $k_1 = \frac{T_{don} - T_{on}}{T} \Rightarrow T_{don} = (k + k_1)$ and $k' = 1 - (k + k_1)$

Combination of State S_1 on, D_1 off and State S_1 off, D_1 represents similar operation to continuous conduction mode.

3.1.1 State S_1 on, D_1off $0 < t < kT$

The circuit operation at this state is similar with the operation of the state S_1 on of the continuous conduction mode. The equivalent circuit for this state is given in Fig. 3.2. It is same with the equivalent circuit at state S_1 on, Fig. 2.3.The only difference between the states is; the output inductor current is negative at the beginning of the state S_1 on, D_1 off while it is a positive for continuous conduction mode operation. The analysis made in the part 2.1.2 is valid for this state too.

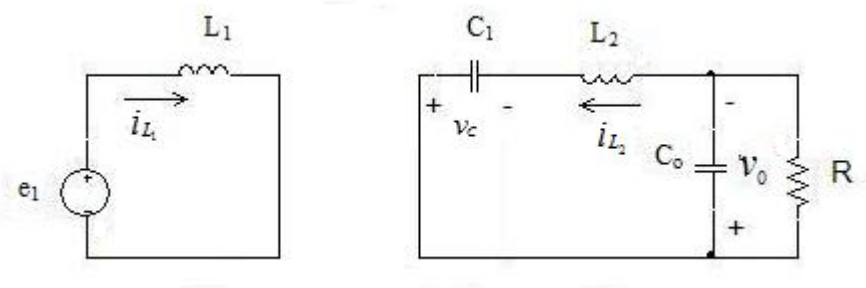

Fig. 3.1 The Cuk converter equivalent circuit in state S_1 on, D_1 off.

$$\frac{di_{L_1}}{dt} = \frac{e_1}{L_1} \tag{3.1}$$

in the left hand mesh, and

$$\frac{dv_{C_1}}{dt} = -\frac{i_{L_2}}{C_1}$$

$$\frac{di_{L_2}}{dt} = \frac{v_{C_1}}{L_2} - \frac{v_0}{L_2}$$

$$\frac{dv_0}{dt} = \frac{i_{L_2}}{C_0} - \frac{v_0}{C_0 R} \tag{3.2}$$

in the right hand mesh.

Current passing through D_1 is the sum of input and output inductor currents:

$$i_{S_1} = i_{L_1} + i_{L_2} \tag{3.3}$$

3.1.2 State S_1 off, D_1 on $kT < t < (k + k_1)T$

The operation of this state is also similar to the operation of the state S_1 off of the continuous conduction mode. The equivalent circuit for this state is given in Fig. 3.2. It is same with the equivalent circuit at state S_1 off, Fig. 2.2. The differences between these states are duration and the value of output inductor current at the end of the state. In the discontinuous conduction mode, state S_1 off, D_1 on ends before the cycle ends. Whereas the state S_1 off ends at the end of a cycle in the continuous conduction mode operation. Also output inductor current value is positive at the end of the state for continuous conduction mode operation but it has negative value at the end for discontinuous conduction mode operation.

The analysis made in the part 2.1.1 is valid for this state too.

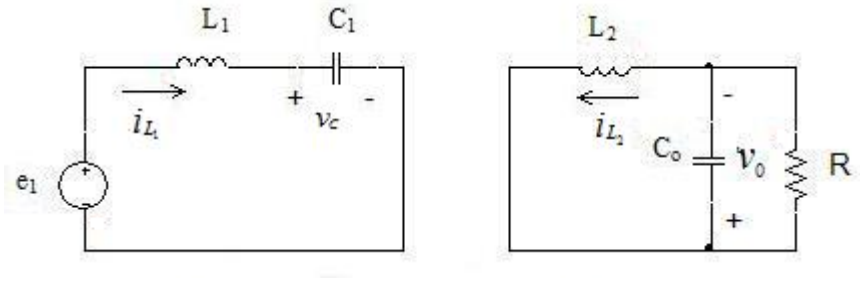

Fig. 3.2 The Cuk converter equivalent circuit in state S_1 off, D_1 on

$$\frac{di_{L_1}}{dt} = \frac{e_1 - v_{C_1}}{L_1}$$

$$\frac{dv_{C_1}}{dt} = \frac{i_{L_1}}{C_1} \tag{3.4}$$

in the left hand mesh,

$$\frac{di_{L_2}}{dt} = -\frac{v_0}{L_2}$$

$$\frac{dv_0}{dt} = \frac{1}{C_0}(i_{L_2} - \frac{v_0}{R}) \qquad (3.5)$$

in the right hand mesh.

Current passing through D_1 is the sum of input and output inductor currents:

$$i_{D_1} = i_{L_1} + i_{L_2} \qquad (3.6)$$

3.1.3 State S_1 off, D_1 off $(k + k_1)T < t < T$

The circuit is not separated to meshes in the state S_1 off, D_1 off as it is in the other states. The equivalent circuit is given in Fig. 3.2. This state starts when the current i_D of the diode D_1 become zero. The zero current passing through the diode D_1 causes the diode D_1 to be reversed biased. At this state the switch S_1 is also off. The switch S_1 is turned on at the end of switching period T. This means that input inductor current i_{L_1} is equal to reverse directed output inductor current i_{L_2} and common current is circulating through L_1, C_1 and L_2.

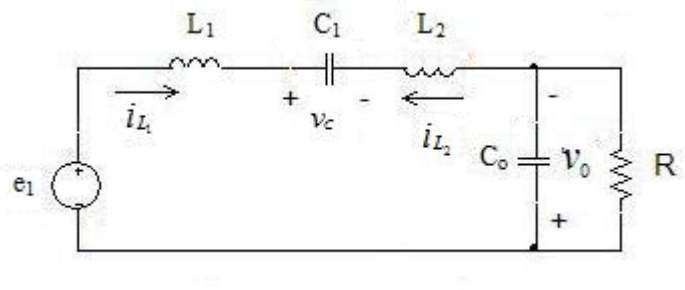

Fig. 3.2 The Cuk converter equivalent circuit in state S_1 off, D_1 on

One can write the following equations governing the operation in this state as;

$$i_{L_1} = -i_{L_2} \tag{3.7}$$

$$v_{L_1} + v_{L_2} = e_1 + v_0 - v_{C_1} \tag{3.8}$$

The combined behaviour of the first two states is similar with continuous conduction mode operation. Considering steady state operation, average voltage of the energy transferring capacitor for state S_1 off, D_1 on and state S_1 on, D_1 off is equal to sum of input and output voltages. Current i_{L_1} keeps charging energy transferring capacitor C_1, but the capacitor voltage increase is negligibly small for the state S_1 off, D_1 off. C_1 is large enough to provide nearly constant voltage within a period. Thus it is considered constant and following equation is valid:

$$\frac{dv_{C_1}}{dt} = 0 \tag{3.9}$$

Also i_{L_1} discharges output capacitor C_0, but the capacitor voltage decrease because of i_{L_1} is negligibly small for the state S_1 off, D_1 off and it is ignored. C_0 is large enough to provide nearly constant voltage within a period.

$$\frac{dv_{C_0}}{dt} = 0 \tag{3.10}$$

As a result voltage across inductors within the state S_1 off, D_1 off is zero, given in (3.11).

$$v_{L_1} + v_{L_2} = e_1 + v_0 - v_{C_1} = 0 \tag{3.11}$$

Thus, for steady state operation current flowing at the third state is constant, freewheeling current and it is expressed as;

$$i_{L1} = -i_{L2} = I_f \tag{3.12}$$

This result in

$$\frac{di_{L_1}}{dt} = \frac{di_{L_2}}{dt} = 0 \tag{3.13}$$

3.2 Steady State Operation

In Fig. 3.3 the waveforms of input and output currents within a period for steady state discontinuous conduction mode is shown.

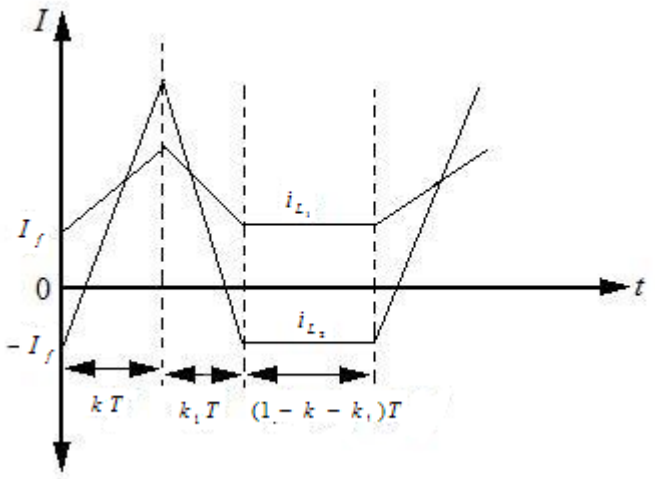

Fig. 3.3 Input and output inductor current waveforms within a period for steady state discontinuous conduction mode.

In the case when voltages v_i across the inductors L_i, i=1,2 changes polarity, for steady state operation voltage balancing for each L_i, i=1,2 is required within a period T. By applying (2.5) volt-second balancing at discontinuous conduction mode operation following results are obtained.

These results imply that the inductor current magnitudes are same at the beginning of a cycle, at the instant $(k+k_1)T$ within a cycle and at the end of a cycle.

$$\int_0^T v_{L_i} dt = 0$$

$$\int_0^T L_i \frac{di_{L_i}}{dt} dt = 0$$

$$\int_0^{(k+k_1)T} L_i \frac{di_{L_i}}{dt} dt + \int_{(k+k_1)T}^{T} L_i \frac{di_{L_i}}{dt} dt = 0$$

$$i_{L_i}(0) = i_{L_i}((k+k_1)T) = i_{L_i}(T) \tag{3.14}$$

(3.14) also implies that magninute of current increment at kT is equal to magnutude of current decrement at k_1T . Thus, derivative equivalents of input and output currents in (3.1), (3.2), (3.3) and (3.4) are modified by substituting incremental variables such that;

$$\frac{\Delta I_{L_1}}{\Delta t} = \frac{e_1}{L_1}$$

$$\Delta I_{L_1} = \frac{e_1}{L_1 f_s} k \qquad \text{where } \Delta t = kT$$

$$\frac{\Delta I_{L_1}}{\Delta t} = \frac{v_{C_1} - e_1}{L_1} \qquad \text{where } \Delta t = k_1T \tag{3.15}$$

$$\Delta I_{L_1} = \frac{v_{C_1} - e_1}{L_1 f_s} k_1$$

$$\frac{\Delta I_{L_2}}{\Delta t} = \frac{v_{C_1} - v_0}{L_1} \qquad \text{where } \Delta t = kT$$

$$\Delta I_{L_2} = \frac{v_{C_1} - v_0}{L_1 f_s} k$$

$$\frac{\Delta I_{L_2}}{\Delta t} = \frac{v_0}{L_1} \qquad \text{where } \Delta t = k_1T$$

$$\Delta I_{L_2} = \frac{v_0}{L_1 f_s} k_1 \tag{3.16}$$

According to (3.14) at steady state operation for each inductor decrement and increment of currents within a period are equal. Upper case letters represent steady state operation values of varibles. This yields,

$$\Delta I_{L_1} = \frac{V_{C_1} - E_1}{L_1 f_s} K_1 = \frac{E_1}{L_1 f_s} K$$

$$\Delta I_{L_2} = \frac{V_{C_1} - V_0}{L_2 f_s} K = \frac{V_0}{L_2 f_s} K_1 \tag{3.17}$$

(3.17) provides determination of the relation between input and output variables.

$$\begin{aligned} V_C &= \frac{(K_1 + K)}{K_1} E_1 \\ V_C &= \frac{(K + K_1)}{K} V_0 \end{aligned} \tag{3.18}$$

As stated earlier for steady state operation at discontinuous conduction mode voltage of energy transferring capacitor is the sum of input and output voltages. Note that this result is satisfied since the voltage increase of the energy transferring capacitor is negligible small at the state S_1 off, D_1 off.

$$V_{C_1} = E_1 + V_0 \tag{3.19}$$

Also the relation between output and input voltages are derived as the ratio of duty ratios K, K_1.

$$\frac{V_0}{E_1} = \frac{K}{K_1} \tag{3.20}$$

Considering %100 efficiency, power equality is given in (3.21).

$$E_1 I_{L_1} = V_0 I_{L_2} \tag{3.21}$$

Relation of input and output current is obtained from (3.22), by substituting input and output voltage relation.

$$\frac{I_{L_1}}{I_{L_2}} = \frac{K}{K_1} \tag{3.22}$$

According to the Fig. 3.3 and (3.11) average input and output currents for a period can be obtained as given in [5] ;

$$i_{L_1} = \frac{e_1}{2L_1 f_S} k(k+k_1) + I_f$$

$$i_{L_2} = \frac{e_1}{2L_2 f_S} k(k+k_1) - I_f \tag{3.23}$$

According to the capacitor charge balance at steady state the total charge of the capacitor for a period must be zero, as indicated in (2.6). Thus the energy transfering capacitor C_1 maintains the ampere-second balance as the other capacitor. Considering the current waveforms given in Fig. 3.3, and (2.6) the charge balancing for C_1 is represented in (3.24). The circulating current value I_f given in (3.25) is the result of (3.24). Voltage increase of energy transferring capacitor because I_f at the state S_1 off, D_1 off is not ignored.

$$-\int_0^{KT} i_{L_2} dt + \int_{KT}^{(K+K_1)T} i_{L_1} dt + \int_{(K+K_1)T}^{T} I_f dt = 0$$

$$-\left(-\int_0^{I_f \frac{L_2}{V_{L_2}}} i_{L_2} dt + \int_{I_f \frac{L_2}{V_{L_2}}}^{KT} i_{L_2} dt\right) + \int_{KT}^{(K+K_1)T} i_{L_1} dt + \int_{(K+K_1)T}^{T} I_f dt = 0$$

$$I_f{}^2 \frac{L_2}{2V_{L_2}} - \frac{1}{2}(\Delta I_{L_2} - I_f)(KT - I_f \frac{L_2}{V_{L_2}}) + \frac{1}{2}\Delta I_{L_1} K_1 T + I_f (1-K-K_1)T = 0 \tag{3.24}$$

$$-\frac{1}{2}\Delta I_{L_2} KT + \frac{1}{2}\Delta I_{L_2} I_f \frac{L_2}{V_{L_2}} + \frac{1}{2} I_f KT + \frac{1}{2}\Delta I_{L_1} K_1 T + I_f (1-K-K_1)T = 0$$

$$\frac{1}{2}\Delta I_{L_1} K_1 T - \frac{1}{2}\Delta I_{L_2} KT + I_f \left[\frac{1}{2}\Delta I_{L_2} \frac{L_2}{V_{L_2}} - \frac{1}{2} KT + (1-K_1)T\right] = 0$$

(3.24) leads;

$$I_f = \frac{\frac{1}{2}\Delta I_{L_1} KT - \frac{1}{2}\Delta I_{L_2} K_1 T}{\left[\frac{1}{2}\Delta I_{L_2}\frac{L_2}{V_{L_2}} - \frac{1}{2}KT + (1-K_1)T\right]} \tag{3.25}$$

By substituting ripple current equivalents (3.15), (3.16) for steady state operation in (3.25) circulating current I_f equivalent is modified as (3.26). V_{L_2} is replaced with its equivalent value E_1 at a period $(0, kT)$.

$$I_f = \frac{\frac{1}{2}\frac{E_1}{L_2 f_S}K^2 - \frac{1}{2}\frac{V_0}{L_1 f_S}K_1^{\,2}}{(1-K_1)} \tag{3.26}$$

The circulating current I_f is predicted that has positive value for the defined direction and defined discontinuous inductor current mode operation.

In the case of I_f is negative, input inductor current will be reversed while output inductor current flows in the same direction. It means that higher current ripple is on the input inductor and also on the source current. This is undesired case. To reduce ripples from source additional filtering is needed. This method is inefficient, since output filtering already exists. The inequality (3.27) must be satisfied to provide positive I_f.

$$\begin{aligned}
&\frac{1}{2}\frac{E_1}{L_2 f_S}K^2 > \frac{1}{2}\frac{V_0}{L_1 f_S}K_1^{\,2} \\
&\frac{E_1}{L_2}K^2 > \frac{V_0}{L_1}K_1^{\,2} \\
&L_1 > \frac{V_0}{E_1}\frac{K_1^{\,2}}{K^2}L_2 \\
&L_1 > (\frac{E1}{V_0})L_2
\end{aligned} \tag{3.27}$$

It is suggested in [3] that input and output inductor values not to be at the same degree. To avoid high ripples at input side the condition of the input and output inductor relation (3.27) is modified as given in [3];

$$L_1 >> (\frac{E_1}{V_0})L_2 \tag{3.28}$$

3.2.1 Criteria for Discontinuous Inductor Current Mode Operation

For discontinuous inductor current mode operation durations for three states are defined in the previous part. General relation between them is defined as follows:

$$(k + k_1)T < T \tag{3.29}$$

At a period $[T, k_1 T]$, input and output currents i_{L_1}, i_{L_2} are flowing through the diode as stated in part 3.1.2. For a Cuk converter operating in discontinuous inductor current mode, average value of diode current $I_{D(disc)}$ for a period $(k+k_1)T$ is equal to average value of output inductor current $I_{L_2(disc)}$ for the same period. One can write the following according to (3.6) The relation (3.22) is valid for the averaged variables at a period $(k+k_1)T$.

$$\begin{aligned} I_{D(disc)} &= (I_{L_2(disc)} + I_{L_1(disc)})K_1 \\ &= (I_{L_2(disc)} + \frac{K}{K_1} I_{L_2(disc)})K_1 \\ &= I_{L_2(disc)}(K + K_1) \end{aligned} \tag{3.30}$$

where $(K + K_1) = 1$ *for* $I_{D(disc)}, I_{L_2(disc)}, I_{L_1(disc)}$.

Since the effect of circulating current I_f on the output capacitor voltage is ignored, average output current I_0 for a whole period T is equal to output inductor current I_{L_2} averaged for a period.

$$I_{D(disc)}(K + K_1) = I_D$$

$$I_{L_2(disc)}(K + K_1) = I_{L_2} \quad \textit{for a period T.}$$

$$I_D = I_{L_2} = \frac{V_0}{R} \quad \textit{for a period T.} \tag{3.31}$$

Peak value of the diode current is the sum of input and output peak values. Thus the steady state value of peak diode current as stated in [4] is

$$\begin{aligned} i_{Dpeak} &= \frac{e_1}{L_1} KT + I_f + \frac{e_1}{L_2} KT - I_f \\ i_{Dpeak} &= \frac{e_1}{L_{eq}} KT \end{aligned} \tag{3.32}$$

where $L_{eq} = \dfrac{L_1 L_2}{L_1 + L_2}$

The average value of diode current i_D is obtained as follows;

$$\begin{aligned} I_D &= \frac{i_{Dpeak} k_1 T}{2T} \\ I_D &= \frac{e_1 k k_1 T}{2L_{eq}} = \frac{{e_1}^2 k^2 T}{2.v_0 L_{eq}} \end{aligned} \tag{3.33}$$

From (3.31) and (3.33) one can write the following equation;

$$\begin{aligned} \frac{{E_1}^2 K^2 T}{2.V_0 L_{eq}} &= \frac{V_0}{R} \\ \frac{R K^2 T}{2L_{eq}} &= \frac{{V_0}^2}{{E_1}^2} \end{aligned} \tag{3.34}$$

where $\dfrac{V_0}{E_1} = M$ is 'voltage conversion ratio' between input voltage E_1 and outputaverage voltage V_0 .Then the equivalent representation for duty ratio K, (3.35) is obtained.

$$K = \sqrt{\frac{2L_{eq}}{RT} M^2} = M\sqrt{\frac{2L_{eq}}{RT}} \tag{3.35}$$

$\frac{2L_{eq}}{RT}$ is defined as conduction parameter as defined in [4] and is denoted by K_a. (3.20) provides another equivalent reperesantation for M such as;

$$M = \frac{V_0}{E_1} = \frac{K}{K_1} \tag{3.36}$$

By substituting (3.36) in (3.35) the duty ratio K_1 is obtained as following;

$$K_1 = \sqrt{K_a} \tag{3.37}$$

where K_a is conduction parameter and defided for (3.35).

As a result duty-ratio K_1 is dependent to physical parameters L_1, L_2, load current and switching period. Variations of input voltage and duty ratio K do not affect the duty ratio K_1.

By substituting K and K_1 equivalents in equation (3.29) the following criteria is obtained for steady state discontinuous conduction mode operation.

$$\begin{aligned} &(K + \frac{E_1}{V_0} K) < 1 \\ &K(1 + \frac{1}{M}) < 1 \Rightarrow K < \frac{M}{1+M} \end{aligned} \tag{3.38}$$

From (3.36)-(3.38) conduction parameter K_a is found as;

$$K_a < \frac{1}{(1+M)^2} \tag{3.39}$$

The transition point between discontinuous and continuous conduction mode operations is the equivalence of the criteria (3.38), that is

$$K = \frac{M}{1+M} \tag{3.40}$$

By substituting the conduction parameter K_a in the transition point criteria, critical conduction parameter $K_{a,crt}$ equivalent becomes as follows;

$$K_{a,crt} = \frac{1}{(1+M)^2} \tag{3.41}$$

Since the voltage conversion ratio, M is greater than zero, the critical conduction parameter, $K_{a,crt}$ is always smaller than 1.

$$K_{a,crt} < 1 \tag{3.42}$$

3.3 Steady State and Dynamic Models

State space averaging method is applicable to multi state configurations. Discontinuous conduction mode operation is a three state configuration. Application of the method to a multi state configuration is similar with the application to a two state configuration. The method is multiplying each state-space equation with the duty ratio of its interval and summing resultant equations. The model derivation is given in (3.43). Resultant model is given in (3.44)

$$\begin{aligned}
&\mathrm{k}\left(\frac{di_{L_1}}{dt} = \frac{e_1}{L_1}\right) + \mathrm{k}_1\left(\frac{di_{L_1}}{dt} = \frac{e_1 - v_{C_1}}{L_1}\right) \\
&\mathrm{k}\left(\frac{dv_{C_1}}{dt} = -\frac{i_{L_2}}{C_1}\right) + \mathrm{k}_1\left(\frac{dv_{C_1}}{dt} = \frac{i_{L_1}}{C_1}\right) \\
&\mathrm{k}\left(\frac{di_{L_2}}{dt} = \frac{v_{C_1} - v_0}{L_2}\right) + \mathrm{k}_1\left(\frac{di_{L_2}}{dt} = -\frac{v_0}{L_2}\right) \\
&\mathrm{k}\left(\frac{dv_0}{dt} = \frac{1}{C_0}\left(i_{L_2} - \frac{v_0}{R}\right)\right) + \mathrm{k}_1\left(\frac{dv_0}{dt} = \frac{1}{C_0}\left(i_{L_2} - \frac{v_0}{R}\right)\right)
\end{aligned} \tag{3.43}$$

State space averaged model aims to represent the behaviour with a single equation for entire period. Therefore as stated in [6], the model represents the behaviour of variables averaged for a switching period. Since state space averaged model is the model for low frequency behaviour, the averaged representations for variables do not cause to ignore any characteristic related with low frequency

behaviour. In (3.44) i_{L_1}, i_{L_2}, v_{C_1}, v_0 are averaged values for a switching period. i_{L_1}, i_{L_2} are given in (3.23).

$$\frac{di_{L_1}}{dt} = \frac{e_1}{L_1} - \frac{k_1}{k+k_1}\frac{v_{C_1}}{L_1}$$

$$\frac{dv_{C_1}}{dt} = -\frac{k}{k+k_1}\frac{i_{L_2}}{C_1} + \frac{k_1}{k+k_1}\frac{i_{L_1}}{C_1}$$

$$\frac{di_{L_2}}{dt} = \frac{k}{k+k_1}\frac{v_{C_1}}{L_2} - \frac{v_0}{L_2}$$

$$\frac{dv_0}{dt} = \frac{1}{C_0}(i_{L_2} - \frac{v_0}{R}) \qquad (3.44)$$

Operation at steady state means that perturbed values for all variables and derivatives of variables are zero. From (3.44) the steady state model is obtained and given in (3.45). Uper case letters represents steady state operating point values.

$$0 = \frac{E_1}{L_1} - \frac{K_1}{K+K_1}\frac{V_{C_1}}{L_1}$$

$$0 = -\frac{K}{K+K_1}\frac{I_{L_2}}{C_1} + \frac{K_1}{K+K_1}\frac{I_{L_1}}{C_1}$$

$$0 = \frac{K}{K+K_1}\frac{V_{C_1}}{L_2} - \frac{V_0}{L_2}$$

$$0 = \frac{1}{C_0}(I_{L_2} - \frac{V_0}{R}) \qquad (3.45)$$

As a result of (3.45) the relationships between steady state variables, input voltage E_1, output voltage V_0, input current I_{L_1}, output current I_{L_2} and voltage of energy transferring capacitor V_{C_1} are as follows:

$$E_1 = \frac{K_1}{K+K_1}V_{C_1};\ V_0 = \frac{K}{K+K_1}V_{C_1} \Rightarrow E_1 + V_0 = V_{C_1}$$

$$\frac{I_{L_1}}{I_{L_2}} = \frac{K}{K_1} \quad ; \quad I_{L_2} = \frac{V_0}{R} \qquad (3.46)$$

Relationships in (3.46) are same with (3.18), (3.19), (3.20) and (3.22), obtained for steady-state operation.

The model obtained in (3.44) is nonlinear. Small signal model is obtained by linearizing the model (3.44) around the steady state operating point. Averaged small signal variables, in other words perturbed variables are represented by cap '^' on the lower case representation of the variables. The model is given in (3.47).

$$\frac{d\hat{i}_{L_1}}{dt} = \frac{\hat{e}_1}{L_1} - \frac{K_1}{(K+K_1)}\frac{\hat{v}_{C_1}}{L_1} + \frac{K_1}{(K+K_1)^2}\frac{V_{C_1}\hat{k}}{L_1} - \frac{K}{(K+K_1)^2}\frac{V_{C_1}\hat{k}_1}{L_1}$$

$$\frac{d\hat{v}_{C_1}}{dt} = -\frac{K}{K+K_1}\frac{\hat{i}_{L_2}}{C_1} + \frac{K_1}{K+K_1}\frac{\hat{i}_{L_1}}{C_1} + \frac{K_1}{(K+K_1)^2}\frac{(I_{L_2}-I_{L_1})\hat{k}}{C_1} - \frac{K}{(K+K_1)^2}\frac{(I_{L_2}-I_{L_1})\hat{k}_1}{C_1}$$

$$\frac{d\hat{i}_{L_2}}{dt} = \frac{K}{K+K_1}\frac{\hat{v}_{C_1}}{L_2} - \frac{\hat{v}_0}{L_2} - \frac{K_1}{(K+K_1)^2}\frac{V_{C_1}\hat{k}}{L_2} + \frac{K}{(K+K_1)^2}\frac{V_{C_1}\hat{k}_1}{L_2} \qquad (3.47)$$

$$\frac{d\hat{v}_0}{dt} = \frac{1}{C_0}(\hat{i}_{L_2} - \frac{\hat{v}_0}{R})$$

(3.48) is the matrix representation of (3.47).

$$\begin{bmatrix} \frac{d\hat{i}_{L_1}}{dt} \\ \frac{d\hat{v}_{C_1}}{dt} \\ \frac{d\hat{i}_{L_2}}{dt} \\ \frac{d\hat{v}_0}{dt} \end{bmatrix} = \begin{bmatrix} 0 & \frac{K_1}{(K+K_1)L_1} & 0 & 0 \\ \frac{K_1}{(K+K_1)C_1} & 0 & -\frac{K}{(K+K_1)C_1} & 0 \\ 0 & \frac{K}{(K+K_1)L_2} & 0 & -\frac{1}{L_2} \\ 0 & 0 & \frac{1}{C_0} & -\frac{1}{C_0 R} \end{bmatrix} \begin{bmatrix} \hat{i}_{L_1} \\ \hat{v}_{C_1} \\ \hat{i}_{L_2} \\ \hat{v}_0 \end{bmatrix} + \begin{bmatrix} \frac{1}{L_1} \\ 0 \\ 0 \\ 0 \end{bmatrix} \hat{e}_1$$

$$+ \begin{bmatrix} \frac{K_1}{(K+K_1)^2}\frac{V_{C_1}}{L_1} \\ \frac{K_1}{(K+K_1)^2}\frac{(I_{L_2}-I_{L_1})}{C_1} \\ -\frac{K_1}{(K+K_1)^2}\frac{V_{C_1}}{L_2} \\ 0 \end{bmatrix} \hat{k} + \begin{bmatrix} -\frac{K}{(K+K_1)^2}\frac{V_{C_1}}{L_1} \\ -\frac{K}{(K+K_1)^2}\frac{(I_{L_2}-I_{L_1})}{C_1} \\ \frac{K}{(K+K_1)^2}\frac{V_{C_1}}{L_2} \\ 0 \end{bmatrix} \hat{k}_1 \qquad (3.48)$$

According to (3.48) there are three sources of perturbation: perturbation voltage source $\hat{e}_1$, perturbation of duty ratio of the switch S_1 $\hat{k}$ and perturbation $\hat{k}_1$.

$$\begin{bmatrix} \frac{d\hat{\hat{i}}_{L_1}}{dt} \\ \frac{d\hat{\hat{v}}_{C_1}}{dt} \\ \frac{d\hat{\hat{i}}_{L_2}}{dt} \\ \frac{d\hat{\hat{v}}_0}{dt} \end{bmatrix} = \begin{bmatrix} 0 & \frac{K_1}{(K+K_1)L_1} & 0 & 0 \\ \frac{K_1}{(K+K_1)C_1} & 0 & -\frac{K}{(K+K_1)C_1} & 0 \\ 0 & \frac{K}{(K+K_1)L_2} & 0 & -\frac{1}{L_2} \\ 0 & 0 & \frac{1}{C_0} & -\frac{1}{C_0 R} \end{bmatrix} \begin{bmatrix} \hat{\hat{i}}_{L_1} \\ \hat{\hat{v}}_{C_1} \\ \hat{\hat{i}}_{L_2} \\ \hat{\hat{v}}_0 \end{bmatrix}$$

$$+ \begin{bmatrix} \frac{1}{L_1} \\ 0 \\ 0 \\ 0 \end{bmatrix} \hat{e}_1 + \begin{bmatrix} \frac{K_1}{(K+K_1)^2} \frac{V_{C_1}}{L_1} \\ \frac{K_1}{(K+K_1)^2} \frac{(I_{L_2} - I_{L_1})}{C_1} \\ -\frac{K_1}{(K+K_1)^2} \frac{V_{C_1}}{L_2} \\ 0 \end{bmatrix} \hat{k} \qquad (3.49)$$

Variations in $\hat{k}_1$ is dependent according to (3.29) to switching frequency and load. Thus $\hat{k}_1$ is not independent variable, variations in $\hat{k}_1$ are observed while switching frequency and output load perturbs. In analysis load and switching frequency perturbations is not considered. Thus (3.48) is modified and (3.49) is obtained.

3.4 Application of Cuk Converter as Power Factor Preregulator

Ac to dc converters such as bridge rectifier has output voltage with high ripple. A simple method to reduce ripples is adding a filter capacitor. Unfortunately the simple method cause high, narrow current pulses. That means high harmonic currents are observed on the utility line. The desired case is utility current to be without harmonics and in phase with utility voltage as stated in [5].

The alternative method to regulate output voltage of ac to dc converter is using power factor preregulator circuits that are based on dc to dc converters. Important property of the circuits is improving power factor of utility line.

One of the dc to dc converters used as power factor preregulator is Cuk converter operating in discontinuous inductor current mode.

The expected operation of the pre regulator is to provide almost unity power factor. Therefore the converter's input impedance must have resistive characteristics.

At discontinuous conduction mode operation the sum of average input and output currents are given in equation (3.50) according to [5].

$$i_{L1} + i_{L2} = \frac{1}{2}\frac{e_1}{L_{eq} f_s} k(k + k_1) \tag{3.50}$$

By substituting equation $i_{L2} = \frac{k_1}{k} i_{L1}$ modified equation for average input current is obtained as given in [6].

$$i_{L1} = \frac{1}{2}\frac{k^2}{L_{eq} f_s} e_1 \quad \text{where } R_{in} = \frac{2L_{eq} f_s}{k^2} \tag{3.51}$$

In (3.51) it is obviously shown that for a constant duty cycle k and constant switching frequency f_s, R_{in} is constant and averaged input current i_{L1} and supply voltage e_1 are in the same phase. As stated in [5] Cuk converter behaves as an ideal current shaper, and performs current shaping automatically with no control when operating in DICM.

Critical conduction parameter are derived in the following lines according to the flow in [3].

Output filtering of Cuk converter provides nearly constant output voltage v_0.

$$v_0 \approx V_0 \tag{3.52}$$

Input voltage waveform of the Cuk converter while it is used as power factor preregulator is half sinusoidal pulses. Thus input voltage is defined as

$$e_1 = V_1 \left|\sin(wt)\right| \tag{3.53}$$

Thus conversion ratio m is as obtained follows:

$$m = \frac{v_0}{e_1} = \frac{V_0}{V_1|\sin(wt)|} = \frac{M}{|\sin(wt)|} \qquad \text{where } M = \frac{V_0}{V_1} \tag{3.54}$$

As a result conversion ratio m varies according to the input voltage variation. It has minimum M value at $wt = \pi/2$ and maximum infinity at $wt = 0$ and $wt = \pi$.

(3.52) is substituted in (3.51) and input current is obtained as

$$i_{L_1} = \frac{1}{2}\frac{k^2}{L_{eq} f_s} V_1 |\sin(wt)| \Rightarrow I_{L_1} = \frac{1}{2}\frac{k^2}{L_{eq} f_s} V_1 \tag{3.55}$$

Assuming %100 efficiency load current is

$$i_0 = \frac{V_1 I_{L_1}}{V_0} \sin^2(wt) \tag{3.56}$$

Thus the load value seen by the converter is

$$r = \frac{{V_0}^2}{V_1 I_{L_1} \sin^2(wt)} \tag{3.57}$$

Also input and output power equivalence can be expressed with input voltage and current RMS values and output resistance:

$$\frac{V_1 I_{L_1}}{2} = \frac{{V_0}^2}{R} \tag{3.58}$$

As a result modified (3.58) is given as

$$r = \frac{R}{2\sin^2(wt)} \tag{3.59}$$

(3.59) evidently express that load seen by the converter varies according to the input voltage variation. It has minimum $R/2$ value at $wt = \pi/2$ and maximum infinity at $wt = 0$ and $wt = \pi$.

As stated in [3] since input voltage is constantly changing with a frequency two times of line frequency, converter is not operating at its steady state conditions.

(3.35) is modified by substituting variable load resistance r to obtain variable expression for conduction parameter k_a.

$$k_a = \frac{2L_{eq}}{rT} = 2\frac{2L_{eq}}{RT}\sin^2(wt) = 2K_a\sin^2(wt) \tag{3.60}$$

Also by modifying (3.41) with (3.54) $k_{a,crt}$ expression with variable conversion ratio is obtained (3.61).

$$k_{a,crt} = \frac{\sin^2(wt)}{(|\sin(wt)| + M)^2} \tag{3.61}$$

Condition for discontinuous conduction mode operation is

$$k_a < k_{a,crt} \tag{3.62}$$

By substituting (3.60) and (3.61) in (3.62) discontinuous inductor current mode operation criteria for parmeter K_a is obtained.

$$K_a < \frac{1}{2(|\sin(wt)| + M)^2} \tag{3.63}$$

Since $|\sin(wt)| \le 1$, the right hand part of (3.63) has its smallest value for $|\sin(wt)| = 1$. Thus the criteria that provides dscontinuous inductor current mode operation for entire half sinusoidal period is

$$K_a < \frac{1}{2(1+M)^2} \tag{3.56}$$

(3.35) is modified with variable conversion ratio m and variable conduction parmeter to obtain an expression for duty ratio K for the switch S_1.

$$K = m\sqrt{k_a} = \frac{M}{|\sin(wt)|}\sqrt{2K_a}\,|\sin(wt)| = \sqrt{2}M\sqrt{K_a} \tag{3.57}$$

As a result Cuk converter, operating at discontinuous conduction mode with constant duty-ratio K, has a resistive characteristic. That povides high power factor at the utility.

CHAPTER 4

PARASITIC RESISTANCE EFFECTS

4.1 Source of Parasitic Resistances

4.1.1 Parasitic Resistance in Inductor

Currents passing through inductors of Cuk Converters are not purely dc. They have both ac and dc components. So, resistance characteristic of inductances must be modeled for dc and ac. Winding resistance for dc is expressed as

$$R = \rho \frac{l}{A} \tag{4.1}$$

where l is length of conductor, A is cross sectional area of conductor, ρ is resistivity. In case of ac current resistance characteristics differ because of 'skin effect' and 'proximity effect'. Ac current passing through a conductor causes magnetic flux induction. This magnetic flux according to Lenz Law induces eddy current in a conductor, which lowers current density in a centre so current density accrues at outer part of a conductor. Thus ac current tends to flow at a surface of a conductor. This is called in literature 'skin effect'.

It was stated in [8] that according to Maxwell equation maximum current density is at the surface of a conductor and decays exponentially. As stated in [8] length, most of current passes through is called 'skin depth' and for sinusoidal current with frequency f skin depth is given as:

$$\delta = \sqrt{\frac{\rho}{\pi \mu f}} \tag{4.2}$$

where ρ is resistivity of the material, μ is permeability and is equal to μ_0 for copper conductor. In (4.2) it is obviously shown that δ depth for a specific conductor depends on current frequency. 'skin depth' decreases with increase of frequency.

Also it is stated in [8] that penetration depth of copper conductors at 500 kHz is approximately equal to diameter of AWG #40 conductor and at 10 kHz to diameter of AWG #22.

An ac resistance for a conductor is given in [8] as:

$$R_{ac} = \frac{h}{\delta} R \qquad for\ h >> \delta \tag{4.3}$$

where *h* is thickness of conductor and R is dc resistance given in (4.1).

Magnetic flux induced by ac current passing through a conductor, causes eddy current induction in an adjoining conductor too. This is 'proximity effect'.

It is stated in [8] proximity effect causes increase of partial current at least 2 times in a conductor while net flowing current remains constant. Eddy currents in coils of inductor increases losses according to proximity effect and is source of additional parasitic resistance series to an inductor.

According to [8] 'skin effect' and 'proximity effect' are effective in case of high current where using multi layer windings are necessary, especially in high frequency converters.

In Cuk Converter, for continuous conduction mode the ripples of input and output current are required small enough to consider currents as constant. Current with a %10 ripple has RMS value 1.05 times average current I. Even in high switching frequency 'skin effect' and 'proximity effect' can be neglected.

For discontinuous induction current mode operation output inductor current ripple is generally higher than the average output inductor current. Thus especially for high frequency operations 'skin effect' and 'proximity effect' is considerable.

4.1.2 Parasitic Resistance in Capacitor

A capacitor is an element consists of parallel plates or films that are electrical conductors and insulating layer through them. Wires, the plates and the insulator are not ideal and have resistances. These resistances are the cause of parasitic voltage drop. It is stated in [9] that in a capacitor model insulator resistor is represented with parallel resistor to an ideal capacitor, resistance of plates and wire is represented with a series resistance. According to [9] in a capacitor standard model, all resistances are modeled with a single resistance called 'equivalent series resistance' or 'ESR'. In [9] 'ESR' is given as:

$$ESR = R_{wp} + \frac{1}{w^2 R_{ins} C^2} \tag{4.4}$$

where R_{wp} *is* resistance of wire and plates and R_{ins} is resistance of insulator, w is switching frequency in radians. R_{ins} is the property dependent to insulator. As stated in [9] ESR is a non linear frequency dependent resistance and it decreases with increasing switching frequency. Also it was stated in [9] that ESR is the basic specification for a capacitor and in general the value, given by manufacturers is for 120 Hz.

For a capacitor dissipation factor (*df*) or loss tangent (tan δ) is defined as in [9]:

$$df / \tan\delta = \frac{R}{X}$$

$$= \frac{ESR}{\frac{1}{wC}} = (ESR)wC \tag{4.5}$$

[9] states that the dissipation factor or loss tangent is also supplied by manufacturer.

4.1.3 Parasitic Resistances in Power Semiconductors

Cuk converter contains two semiconductors; a switch and a diode which replaces a second switch. In Cuk converter both semiconductors are used as switching devices. Switching devices have two states on and off at their regular operation.

As stated in [9] at on states, while current passes through a real switching element, small voltage drop is observed. Also at off state while voltage across a real switch is blocked, small current passes through a switch.

Transition between on and off states is another stage exists at operation of a real switch and it is called commutation stage according to [9]. The commutation stage is important and considered for loss calculations.

4.1.3.1 Diode

On and off state modeling of real switches is called static modeling. Real switch static model influences characteristics of power converters.

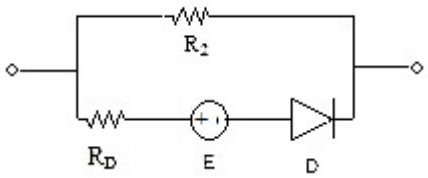

Fig. 4.1 On- off state model of a diode

A model for a real diode is given in [9] as illustrated in Fig. 4.1. In the model D represents an ideal diode. According to a diode v-i characteristic, constant voltage drop at on state operation is observed. This is modeled with dc voltage source E. The linear part of on state v-i characteristic is represented by the resistor R_D. Off state operation is modeled with a resistor R_2. Current passing through R_2 at off state is significantly small. As stated in [9] off state current do not cause considerably high losses. The overall efficiency is affected less than % 0.1 according to [9]. Thus it is

emphasized in [9] that for power electronics a diode is preferred to be modeled with on state characteristic. Thus modified model is given in Fig. 4.2.

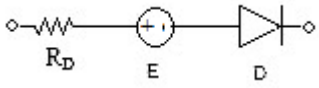

Fig. 4.2 Model of a diode, off state current is ignored.

4.1.3.2 Power MOSFET

As a switching semiconductor in analysis of Cuk converter, a mosfet is considered. Power MOSFET's are widely used in application. According to [9] static model of a MOSFET is given in Fig. 4.3. In the model in [9] an ideal switch is represented with an ideal SCR. The model in [9] is modified by replacing ideal SCR with ideal switch. For the proposed operation an ideal switch meets the function of an ideal SCR.

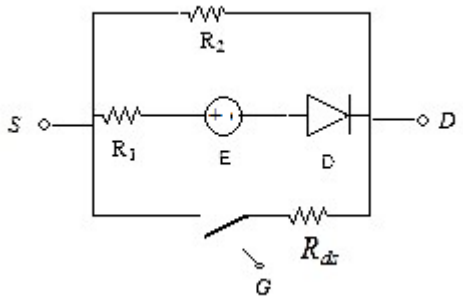

Fig. 4.3 Static model of a MOSFET

According to a MOSFET forward operation, voltage current characteristic given in Fig. 4.4 from the origin are nearly linear. Thus forward operation is modeled with a resistance R_{ds} series to an ideal switch in Fig. 4.3.

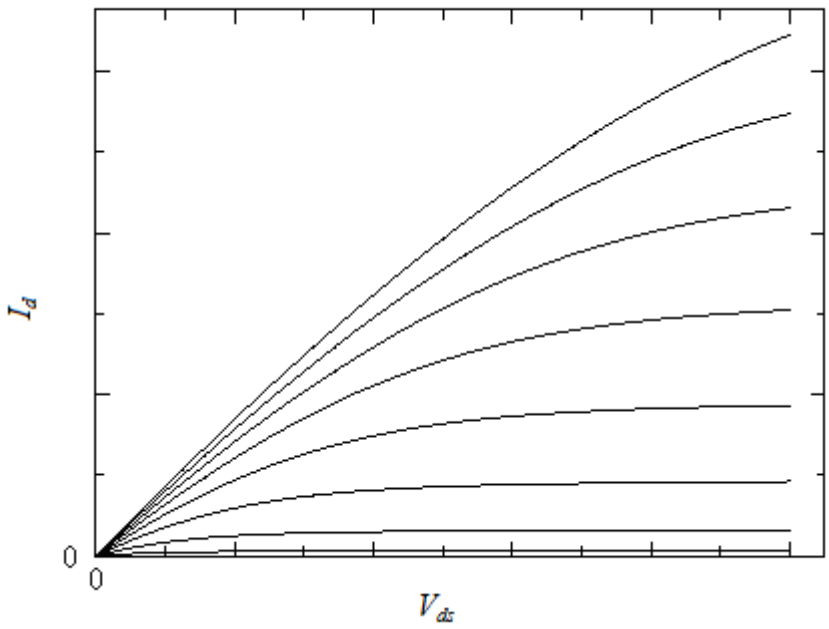

Figure 4.4. MOSFET Forward characteristic

For a linear operation of a MOSFET, voltage drop V_{ds} across it is small. Slope of characteristics is dependent on magnitude of the control signal V_G . Thus the series resistance R_{ds} is related with V_G. G in Fig. 4.4 represents gate of a MOSFET where control signal is applied.

Reverse direction operation of a MOSFET is dominated by a reverse diode that internally exists. It is represented in the model of a MOSFET by parallel reverse diode mode. For reverse direction operation, in case of gate signal is on, voltage drop across a MOSFET is smaller than both voltage drop of internal diode and voltage drop of R_{ds}. R_2, off state resistance of a diode is generally ignored in the model of a MOSFET.

Voltage on the MOSFET is positive for regular operation of Cuk converter. Thus in modeling of parasitic resistances in Cuk converter reverse direction operation of a MOEFET is ignored.

4.2 Modeling of Cuk Converter with Parasitic Resistances

A Cuk converter circuit model with series parasitic resistances is given in Fig. 4.5.

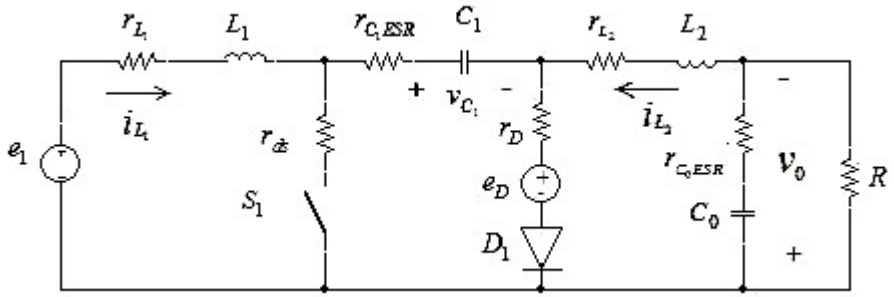

Fig. 4.5 Cuk Converter Circuit with parasitic resistances. +,-

4.2.1 Steady State and Dynamic Models for Continuous Inductor Current Mode

Operation way of a Cuk converter remains as explained in case of deal elements. (2.1), (2.2), (2.3) and (2.4) is modified to obtain representation with series parasitic resistances. e_D is constant forward voltage drop of diode and it is about 0.7-0.8 V.

State S_1 'off', $kT < t < T$

$$\frac{di_{L_1}}{dt} = \frac{e_1}{L_1} - \frac{v_{C_1}}{L_1} - \frac{e_D}{L_1} - \frac{(r_{L_1} + r_{C_1ESR})i_{L_1}}{L_1} - \frac{r_D(i_{L_1} + i_{L_2})}{L_1}$$

$$\frac{dv_{C_1}}{dt} = \frac{i_{L_1}}{C_1} \qquad (4.6)$$

$$\frac{di_{L_2}}{dt} = -\frac{r_D(i_{L_1}+i_{L_2})}{L_2} - \frac{r_{L_2}i_{L_2}}{L_2} - \frac{v_0}{L_2} - \frac{e_D}{L_2}$$

$$\frac{dv_0}{dt} = \frac{R}{C_0(R+r_{C_0ESR})}(i_{L_2} - \frac{v_0}{R}) + \frac{r_{C_0ESR}R}{r_{C_0ESR}+R}\frac{di_{L_2}}{dt} \tag{4.7}$$

State S_1 'on', $0 < t < kT$

$$\frac{di_{L_1}}{dt} = \frac{e_1}{L_1} - \frac{r_{L_1}i_{L_1}}{L_1} - \frac{r_{ds}(i_{L_1}+i_{L_2})}{L_1}$$

$$\frac{dv_{C_1}}{dt} = -\frac{i_{L_2}}{C_1} \tag{4.8}$$

$$\frac{di_{L_2}}{dt} = \frac{v_{C_1}}{L_2} - \frac{v_0}{L_2} - \frac{r_{L_2}i_{L_2}}{L_2} - \frac{r_{C_1ESR}i_{L_2}}{L_2} - \frac{r_{ds}(i_{L_1}+i_{L_2})}{L_2}$$

$$\frac{dv_0}{dt} = \frac{R}{C_0(R+r_{C_0ESR})}(i_{L_2} - \frac{v_0}{R}) + \frac{r_{C_0ESR}R}{r_{C_0ESR}+R}\frac{di_{L_2}}{dt} \tag{4.9}$$

With the help of (4.6), (4.7), (4.8) and (4.9) state space average model is obtained as follows:

$$\frac{di_{L_1}}{dt} = \frac{e_1}{L_1} - \frac{r_{L_1}i_{L_1}}{L_1} - \frac{kr_{ds}(i_{L_1}+i_{L_2})}{L_1} - \frac{(1-k)(v_{C_1}+e_D)}{L_1} - \frac{(1-k)(r_{C_1ESR})i_{L_1}}{L_1} - \frac{(1-k)r_D(i_{L_1}+i_{L_2})}{L_1}$$

$$\frac{dv_{C_1}}{dt} = -\frac{ki_{L_2}}{C_1} + \frac{(1-k)i_{L_1}}{C_1}$$

$$\frac{di_{L_2}}{dt} = \frac{kv_{C_1}}{L_2} - \frac{kr_{ds}(i_{L_1}+i_{L_2})}{L_2} - \frac{kr_{C_1ESR}i_{L_2}}{L_2} - \frac{(1-k)r_D(i_{L_1}+i_{L_2})}{L_2} - \frac{(1-k)e_D}{L_2} - \frac{r_{L_2}i_{L_2}}{L_2} - \frac{v_0}{L_2}$$

$$\frac{dv_0}{dt} = \frac{R}{C_0(R+r_{C_0ESR})}(i_{L_2} - \frac{v_0}{R}) + \frac{r_{C_0ESR}R}{r_{C_0ESR}+R}\frac{di_{L_2}}{dt} \tag{4.10}$$

4.2.1.1 Steady State Model for Continuous Inductor Current Mode

From (4.10) steady state model is obtained by implying steady state condition $dx/dt = 0$, where 'x' are variables. Obtained model is given in (4.11). Steady state variables are expressed with upper case letters.

$$0 = \frac{E_1}{L_1} - \frac{r_{L_1} I_{L_1}}{L_1} - \frac{Kr_{ds}(I_{L_1} + I_{L_2})}{L_1} - \frac{(1-K)(V_{C_1} + e_D)}{L_1} - \frac{(1-K)(r_{C_1 ESR}) I_{L_1}}{L_1} - \frac{(1-K) r_D (I_{L_1} + I_{L_2})}{L_1}$$

$$0 = -\frac{K I_{L_2}}{C_1} + \frac{(1-K) I_{L_1}}{C_1}$$

$$0 = \frac{K V_{C_1}}{L_2} - \frac{Kr_{ds}(I_{L_1} + I_{L_2})}{L_2} - \frac{Kr_{C_1 ESR} I_{L_2}}{L_2} - \frac{(1-K) r_D (I_{L_1} + I_{L_2})}{L_2} - \frac{(1-K) e_D}{L_2} - \frac{r_{L_2} I_{L_2}}{L_2} - \frac{V_0}{L_2}$$

$$0 = \frac{R}{C_0 (R + r_{C_0 ESR})} (I_{L_2} - \frac{V_0}{R}) \tag{4.11}$$

One can obtain steady state equivalents for variables from (4.11) as following:

$$E_1 = r_{L_1} I_{L_1} + Kr_{ds}(I_{L_1} + I_{L_2}) + (1-K)(V_{C_1} + e_D) + (1-K)(r_{C_1 ESR}) I_{L_1} + (1-K) r_D (I_{L_1} + I_{L_2}) \tag{4.12}$$

$$I_{L_1} = \frac{K}{(1-K)} I_{L_2} \tag{4.13}$$

$$V_{C_1} = \frac{1}{K}(Kr_{ds}(I_{L_1} + I_{L_2}) + Kr_{C_1 ESR} I_{L_2} + (1-K) r_D (I_{L_1} + I_{L_2}) + (1-K) e_D + r_{L_2} I_{L_2} + V_0) \tag{4.14}$$

$$I_{L_2} = \frac{V_0}{R} \tag{4.15}$$

Conversion of input and output current (4.13) and output current equivalent (4.15) are equal to ideal case current conversion and output current equivalent given in (2.25). This is because switching loss effects on the current are ignored. From (2.17) and (2.18) (4.16) and (4.17) are obtained.

$$K(I_{L_1} + I_{L_2}) = I_{L_1} \tag{4.16}$$

$$(1-K)(I_{L_1} + I_{L_2}) = I_{L_2} \tag{4.17}$$

Thus substituting (4.16) and (4.17) into (4.12) and (4.14) E_1 and V_{C_1} as follows:

$$E_1 = r_{L_1} I_{L_1} + r_{ds} I_{L_1} + (1-K)(V_{C_1} + e_D) + (1-K)(r_{C_1ESR}) I_{L_1} + r_D I_{L_2} \tag{4.18}$$

$$V_{C_1} = \frac{1}{K}(r_{ds} I_{L_1} + K r_{C_1ESR} I_{L_2} + r_D I_{L_2} + (1-K) e_D + r_{L_2} I_{L_2} + V_0) \tag{4.19}$$

In (4.18) and (4.19) all I_{L_1} are replaced with its equivalent given in (4.13). As a result;

$$E_1 = \frac{K}{(1-K)} I_{L_2}(r_{L_1} + r_{ds} + (1-K)(R_{C_1ESR}) + \frac{(1-K)}{K} r_D) + (1-K)(V_{C_1} + e_D) \tag{4.20}$$

$$V_{C_1} = I_{L_2}(\frac{1}{(1-K)} r_{ds\_on} + r_{C_1ESR} + \frac{1}{K} r_D + \frac{1}{K} r_{L_2}) + \frac{(1-K)}{K} e_D + \frac{1}{K} V_0 \tag{4.21}$$

By substituting (4.21) in (4.20) and replacing I_{L_2} with its equivalent given in (4.15), steady-state input and output voltage conversion ratio M_{CON} is obtained as;

$$\frac{V_0}{E_1} = \frac{K}{1-K} \frac{1}{\left[\frac{1}{R}(\frac{K^2}{(1-K)^2} r_{L_1} + \frac{K}{(1-K)^2} r_{ds} + \frac{1}{1-K} r_D + \frac{K}{1-K} r_{C_1ESR} + r_{L_2}) + \frac{e_D}{V_0} + 1\right]} \tag{4.22}$$

The steady state conversion ratio, M_{CON} appears as multiplication of ideal conversion ratio in (2.25) and parasitic effect. Parasitic resistances, clearly cause reduction in the conversion ratio. All parasitic resistances, except the output capacitor parasitic resistance r_{C_0ESR}, affect the conversion ratio of the converter.

Variation of M_{CON} with duty ratio K is shown in Fig. 4.6. It is an exponential variation.

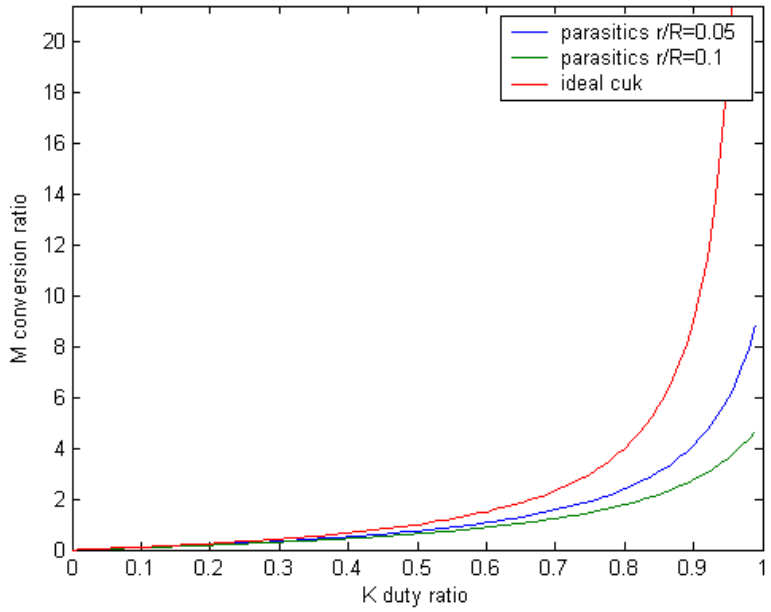

Fig. 4.6 Steady- state variation of conversion ratio M_{CON} with duty ratio K

It is stated in [10] that output voltage ripple is equal to ripple voltage caused by 'r_{C_0ESR}' in the case of '$C_0 r_{C_0ESR}$' is greater than half of maximum state duration $(\frac{(1-K_{\min})}{2}, \frac{K_{\max}}{2})$.

$$\Delta V_0 = r_{C_0ESR} \Delta I_{L_2} \tag{4.23}$$

where ΔI_{L_2} is given in 2.10 for ideal case. If C_0 provides lower time constant than required in the condition peak to peak voltage ripple is greater than (4.23).

4.2.1.2 Dynamic Model for Continuous Inductor Current Mode

Dynamic or small signal model expresses behavior of a system near steady state operating point. By linearizing model in (4.10) in the vicinity of steady state operating point E_1, V_0, I_{L1}, I_{L2}, K dynamic model is obtained.

$$\frac{d\hat{i}_{L_1}}{dt} = \frac{\hat{e}_1}{L_1} - \frac{r_{L_1} + Kr_{ds} + (1-K)r_{C_1ESR} + (1-K)r_D}{L_1}\hat{i}_{L_1} - \frac{(1-K)}{L_1}\hat{v}_{C_1} -$$

$$\frac{Kr_{ds} + (1-K)r_D}{L_1}\hat{i}_{L_2} + \frac{V_{C_1} + e_D + r_{C_1ESR}I_{L_1} + (r_D - r_{ds})(I_{L_1} + I_{L_2})}{L_1}\hat{k}$$

$$\frac{d\hat{v}_{C_1}}{dt} = -\frac{\hat{k}I_{L_2}}{C_1} - \frac{K\hat{i}_{L_2}}{C_1} - \frac{I_{L_1}\hat{k}}{C_1} + \frac{(1-K)\hat{i}_{L_1}}{C_1}$$

$$\frac{d\hat{i}_{L_2}}{dt} = -\frac{Kr_{ds} + (1-K)r_D}{L_2}\hat{i}_{L_1} + \frac{K}{L_2}\hat{v}_{C_1} - \frac{r_{L_2} + Kr_{ds} + Kr_{C_1ESR} + (1-K)r_D}{L_2}\hat{i}_{L_2} -$$

$$\frac{\hat{v}_0}{L_2} + \frac{V_{C_1} - r_{C_1ESR}I_{L_2} + (r_D - r_{ds})(I_{L_2} + I_{L_2}) + e_D}{L_2}\hat{k}$$

$$\frac{d\hat{v}_0}{dt} = \frac{R}{C_0(R + r_{C_0ESR})}(\hat{i}_{L_2} - \frac{\hat{v}_0}{R}) + \frac{r_{C_0ESR}R}{r_{C_0ESR} + R}\frac{d\hat{i}_{L_2}}{dt} \qquad (4.24)$$

Matrix representation of the small signal model is

$$\begin{bmatrix} \frac{d\hat{i}_{L_1}}{dt} \\ \frac{d\hat{v}_{C_1}}{dt} \\ \frac{d\hat{i}_{L_2}}{dt} \\ \frac{d\hat{v}_0}{dt} \end{bmatrix} = \begin{bmatrix} -\frac{r_{L_1} + Kr_{ds} + (1-K)r_{C_1ESR} + (1-K)r_D}{L_1} & -\frac{(1-K)}{L_1} & -\frac{Kr_{ds} + (1-K)r_D}{L_1} & 0 \\ \frac{(1-K)}{C_1} & 0 & -\frac{K}{C_1} & 0 \\ -\frac{Kr_{ds} + (1-K)r_D}{L_2} & \frac{K}{L_2} & -\frac{r_{L_2} + Kr_{ds} + Kr_{C_1ESR} + (1-K)r_D}{L_2} & -\frac{1}{L_2} \\ -\frac{r_{C_0ESR}R}{r_{C_0ESR} + R}\frac{Kr_{ds} + (1-K)r_D}{L_2} & \frac{r_{C_0ESR}R}{r_{C_0ESR} + R}\frac{K}{L_2} & A & B \end{bmatrix} \begin{bmatrix} \hat{i}_{L_1} \\ \hat{v}_{C_1} \\ \hat{i}_{L_2} \\ \hat{v}_0 \end{bmatrix} +$$

$$\begin{bmatrix} \frac{1}{L_1} \\ 0 \\ 0 \\ 0 \end{bmatrix} [\quad] + \begin{bmatrix} \frac{V_{C_1} + e_D + r_{C_1ESR}I_{L_1} + (r_D - r_{ds})(I_{L_1} + I_{L_2})}{L_1} \\ -\frac{(I_{L_1} + I_{L_2})}{C_1} \\ \frac{V_{C_1} + (r_D - r_{ds})(I_{L_1} + I_{L_2}) - r_{C_1ESR}I_{L_2} + e_D}{L_2} \\ \frac{r_{C_0ESR}R}{r_{C_0ESR} + R}(\frac{V_{C_1} + (r_D - r_{ds})(I_{L_1} + I_{L_2}) - r_{C_1ESR}I_{L_2} + e_D}{L_2}) \end{bmatrix} [\quad] \qquad (4.25)$$

where;

$$A=\frac{R}{C_0(R+r_{C_0ESR})}-\frac{r_{C_0ESR}R}{r_{C_0ESR}+R}\left(\frac{r_{L_2}+Kr_{ds}+Kr_{C_1ESR}+(1-K)r_D}{L_2}\right) \tag{4.26}$$

$$B=-\left(\frac{R}{C_0(R+r_{C_0ESR})}+\frac{r_{C_0ESR}R}{L_2(r_{C_0ESR}+R)}\right. \tag{4.27}$$

In (4.24) output voltage derivative $d\hat{v}_0/dt$ is related to deriavaive of output inductor current $d\hat{i}_{L_2}/dt$. To obtain expression for output voltage derivative $d\hat{v}_0/dt$ related to only $i_{L_1}, v_{C_1}, i_{L_2}, v_0$ variables, equivalent of $d\hat{i}_{L_2}/dt$ in (4.24) is substitued in the expression of $d\hat{v}_0/dt$ in (4.24). Resultant expression for $d\hat{v}_0/dt$ is given in the matrix representation (4.25).

The model with parasitic resistances (4.25) has two sources of perturbations as in the ideal model, they are; the input voltage perturbation $\hat{e}_1$ and the duty ratio perturbation $\hat{k}$.

4.2.2 Steady State and Dynamic Models for Discontinuous Inductor Current Mode

(3.1) – (3.5) equations are modified to involve parasitic resistance determined in Fig. 4.5.

State S_1 'off', $kT<t<(k+k_1)T$

$$\frac{di_{L_1}}{dt}=\frac{e_1}{L_1}-\frac{v_{C_1}}{L_1}-\frac{e_D}{L_1}-\frac{(r_{L_1}+r_{C_1ESR})i_{L_1}}{L_1}-\frac{r_D(i_{L_1}+i_{L_2})}{L_1}$$

$$\frac{dv_{C_1}}{dt}=\frac{i_{L_1}}{C_1} \tag{4.28}$$

$$\frac{di_{L_2}}{dt}=-\frac{r_D(i_{L_1}+i_{L_2})}{L_2}-\frac{r_{L_2}i_{L_2}}{L_2}-\frac{v_0}{L_2}-\frac{e_D}{L_2}$$

$$\frac{dv_0}{dt}=\frac{R}{C_0(R+r_{C_0ESR})}\left(i_{L_2}-\frac{v_0}{R}\right)+\frac{r_{C_0ESR}R}{r_{C_0ESR}+R}\frac{di_{L_2}}{dt} \tag{4.29}$$

State S_1 'on', $0 < t < kT$

$$\frac{di_{L_1}}{dt} = \frac{e_1}{L_1} - \frac{r_{L_1} i_{L_1}}{L_1} - \frac{r_{ds}(i_{L_1} + i_{L_2})}{L_1}$$

$$\frac{dv_{C_1}}{dt} = -\frac{i_{L_2}}{C_1} \tag{4.30}$$

$$\frac{di_{L_2}}{dt} = \frac{v_{C_1}}{L_2} - \frac{v_0}{L_2} - \frac{r_{L_2} i_{L_2}}{L_2} - \frac{r_{C_1 ESR} i_{L_2}}{L_2} - \frac{r_{ds}(i_{L_1} + i_{L_2})}{L_2}$$

$$\frac{dv_0}{dt} = \frac{R}{C_0(R + r_{C_0 ESR})}(i_{L_2} - \frac{v_0}{R}) + \frac{r_{C_0 ESR} R}{r_{C_0 ESR} + R}\frac{di_{L_2}}{dt} \tag{4.31}$$

Variations in variables at stage $(k + k_1)T < t < T$ are ignored also in case with parasitic resistances, because of same approximations stated in ideal case analysis. From (4.28), (4.29), (4.30) and (4.31) state space average model representation is obtained.

$$\frac{di_{L_1}}{dt} = \frac{e_1}{L_1} - \frac{r_{L_1} i_{L_1}}{L_1} - \frac{k}{(k + k_1)}\frac{r_{ds}(i_{L_1} + i_{L_2})}{L_1} - \frac{k_1}{(k + k_1)}\frac{(v_{C_1} + e_D)}{L_1} -$$

$$\frac{k_1}{(k + k_1)}\frac{r_{C_1 ESR} i_{L_1}}{L_1} - \frac{k_1}{(k + k_1)}\frac{r_D(i_{L_1} + i_{L_2})}{L_1}$$

$$\frac{dv_{C_1}}{dt} = -\frac{k}{(k + k_1)}\frac{i_{L_2}}{C_1} + \frac{k_1}{(k + k_1)}\frac{i_{L_1}}{C_1}$$

$$\frac{di_{L_2}}{dt} = \frac{k}{(k + k_1)}\frac{v_{C_1}}{L_2} - \frac{k}{(k + k_1)}\frac{r_{ds}(i_{L_1} + i_{L_2})}{L_2} - \frac{k}{(k + k_1)}\frac{r_{C_1 ESR} i_{L_2}}{L_2} -$$

$$\frac{k_1}{(k + k_1)}\frac{r_D(i_{L_1} + i_{L_2})}{L_2} - \frac{k_1}{(k + k_1)}\frac{e_D}{L_2} - \frac{r_{L_2} i_{L_2}}{L_2} - \frac{v_0}{L_2}$$

$$\frac{dv_0}{dt} = \frac{R}{C_0(R + r_{C_0 ESR})}(i_{L_2} - \frac{v_0}{R}) + \frac{r_{C_0 ESR} R}{r_{C_0 ESR} + R}\frac{di_{L_2}}{dt} \tag{4.32}$$

4.2.2.1 Steady State Model for Discontinuous Inductor Current Mode

By setting variations in variables in (4.32) to zero one can obtain following relations for steady state operation. Upper case variables represent values for steady state operating point.

$$0 = E_1 - r_{L_1} I_{L_1} - \frac{Kr_{ds}(I_{L_1} + I_{L_2})}{(K + K_1)} - \frac{K_1(V_{C_1} + e_D)}{(K + K_1)} - \frac{Kr_{C_1ESR} I_{L_1}}{(K + K_1)} - \frac{K_1 r_D (I_{L_1} + I_{L_2})}{(K + K_1)}$$

$$0 = -\frac{K}{(K + K_1)} I_{L_2} + \frac{K_1}{(K + K_1)} I_{L_1}$$

$$0 = \frac{K}{(K + K_1)} V_{C_1} - \frac{Kr_{ds}(I_{L_1} + I_{L_2})}{(K + K_1)} - \frac{Kr_{C_1ESR} I_{L_2}}{(K + K_1)} - \frac{K_1 r_D (I_{L_1} + I_{L_2})}{(K + K_1)} - \frac{K_1 e_D}{(K + K_1)} - r_{L_2} I_{L_2} - V_0$$

$$0 = \frac{R}{C_0 (R + r_{C_0ESR})} (I_{L_2} - \frac{V_0}{R}) \tag{4.33}$$

which when rearranged gives;

$$E_1 = r_{L_1} I_{L_1} + \frac{Kr_{ds}(I_{L_1} + I_{L_2}) + K_1(V_{C_1} + e_D) + K_1 r_{C_1ESR} I_{L_1} + K_1 r_D (I_{L_1} + I_{L_2})}{(K + K_1)} \tag{4.34}$$

$$I_{L_1} = \frac{K}{K_1} I_{L_2} \tag{4.35}$$

$$V_{C_1} = \frac{1}{K}(Kr_{ds}(I_{L_1} + I_{L_2}) + Kr_{C_1ESR} I_{L_2} + K_1 r_D (I_{L_1} + I_{L_2}) + K_1 e_D + (K + K_1) r_{L_2} I_{L_2} + (K + K_1) V_0) \tag{4.36}$$

$$I_{L_2} = \frac{V_0}{R} \tag{4.37}$$

Conversion of input and output current (4.35) and output current equivalent (4.37) are equal to ideal case current conversion and output current equivalent given in (3.22). This is also because switching loss effects on the current are ignored.

By substituting (4.35), (4.36) and (4.37) in (4.34) input and output voltage conversion ratio M_{DISC} is obtained as following:

$$\frac{V_0}{E_1} = \frac{K}{K_1} \frac{1}{(\frac{1}{R}(\frac{K^2}{K_1^2} r_{L_1} + \frac{K(K+K_1)}{K_1^2} r_{ds} + \frac{(K+K_1)}{K_1} r_D + \frac{K}{K_1} r_{C_1 ESR} + r_{L_2}) + \frac{e_D}{V_0} + 1)} \quad (4.38)$$

Steady-state variation of conversion-ratio, M_{DISC} with duty ratio K is shown in Fig. 4.7. Variation characteristics are nearly linear. For higher parasitic resistances characteristic lines have smaller slope. Also for small k_1 conversion ratio increases.

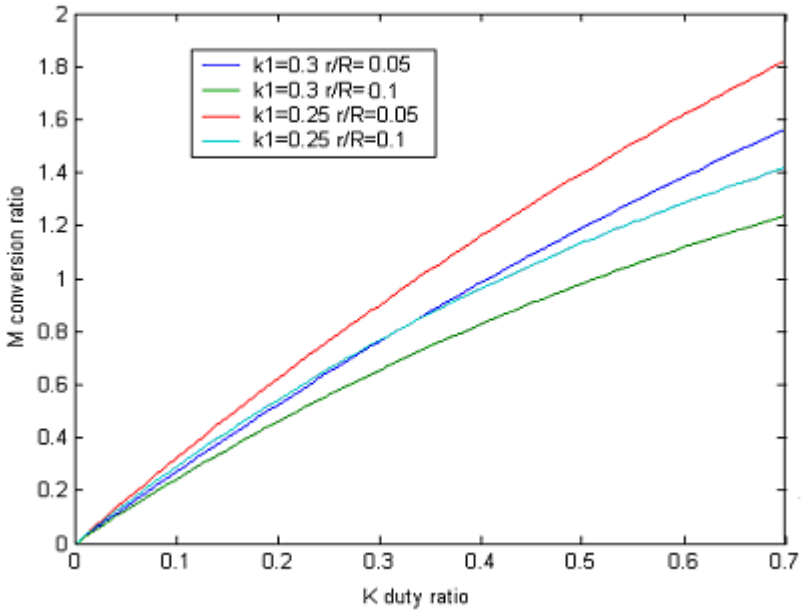

Fig. 4.7 Steady-state variation of conversion ratio M_{DISC} with duty ratio K

All parasitic resistances except output capacitor parasitic resistance r_{C_0ESR} appear at the conversion ratio expression.

Output ripple expression (4.23) with stated conditions for continuous inductor current mode is valid for discontinuous inductor current mode too. ΔI_{L_2} for discontinuous inductor current mode is given in (3.16) for ideal case. Output current ripple is high from average output current for discontinuous inductor current mode. Therefore capacitors with low ESR values for high current ripples are preferreable.

4.2.2.2 Dynamic Model for Discontinuous Inductor Current Mode

The method to obtain dynamic model as applied in previous parts is linearizing the model in the vicinity of steady state operation. The model in (4.41) is a dynamic model obtained by modifying (4.32) by substituting di_{L_2}/dt in (4.32) in the equivalent of dv_0/dt in (4.32) and linearizing the modified (4.32).

(4.41) do not contain $\hat{k}_1$ as a source of perturbation. Although the variations in $\hat{k}_1$ depends on the switching frequency and load, $\hat{k}_1$ is not an independent variable. Variations in $\hat{k}_1$ are seen while switching frequency and output load are perturbed. In analysis, load and switching frequency perturbations are not considered. Thus in (4.41) $\hat{k}_1$ is not included as a source of perturbation. System has two sources of perturbations; the input voltage perturbations $\hat{e}_1$, and $\hat{k}$.

In (4.41) C and D stand for;

$$C = \frac{R}{C_0(R + r_{C_0ESR})} - \frac{r_{C_0ESR}R}{L_2(r_{C_0ESR} + R)}\left(r_{L_2} + \frac{Kr_{ds} + Kr_{C_1ESR} + K_1r_D}{(K + K_1)}\right) \tag{4.39}$$

$$D = -\left(\frac{R}{C_0(R + r_{C_0ESR})} + \frac{r_{C_0ESR}R}{L_2(r_{C_0ESR} + R)}\right) \tag{4.40}$$

$$\begin{bmatrix} \frac{d\hat{i}_{L_1}}{dt} \\ \frac{d\hat{v}_{C_1}}{dt} \\ \frac{d\hat{i}_{L_2}}{dt} \\ \frac{d\hat{v}_0}{dt} \end{bmatrix} = \begin{bmatrix} -\frac{1}{L_1}(r_{L_1} + \frac{Kr_{ds} + K_1 r_{C_1 ESR} + K_1 r_D}{K + K_1}) & -\frac{K_1}{(K+K_1)L_1} & -\frac{Kr_{ds} + K_1 r_D}{(K+K_1)L_1} & 0 \\ \frac{K_1}{C_1(K+K_1)} & 0 & -\frac{K}{C_1(K+K_1)} & 0 \\ -\frac{Kr_{ds} + K_1 r_D}{L_2(K+K_1)} & \frac{K}{(K+K_1)L_2} & -\frac{1}{L_2}(r_{L_2} + \frac{Kr_{ds} + Kr_{C_1 ESR} + K_1 r_D}{(K+K_1)}) & -\frac{1}{L_2} \\ -\frac{r_{C_0 ESR} R}{r_{C_0 ESR} + R} \frac{Kr_{ds} + K_1 r_D}{L_2(K+K_1)} & \frac{r_{C_0 ESR} R}{r_{C_0 ESR} + R} \frac{K}{(K+K_1)L_2} & C & D \end{bmatrix} \begin{bmatrix} \hat{i}_{L_1} \\ \hat{v}_{C_1} \\ \hat{i}_{L_2} \\ \hat{v}_0 \end{bmatrix} +$$

$$\begin{bmatrix} \frac{1}{L_1} \\ 0 \\ 0 \\ 0 \end{bmatrix} \begin{bmatrix} \hat{v}_1 \end{bmatrix} + \begin{bmatrix} \frac{K_1}{(K+K_1)^2} \frac{V_{C_1} + e_D + r_{C_1 ESR} I_{L_1} + (r_D - r_{ds})(I_{L_1} + I_{L_2})}{L_1} \\ -\frac{K_1}{(K+K_1)^2} \frac{(I_{L_1} + I_{L_2})}{C_1} \\ \frac{K_1}{(K+K_1)^2} \frac{V_{C_1} + e_D + (r_D - r_{ds})(I_{L_1} + I_{L_2}) - r_{C_1 ESR} I_{L_2}}{L_2} \\ \frac{r_{C_0 ESR} R}{r_{C_0 ESR} + R} (\frac{K_1}{(K+K_1)^2} \frac{V_{C_1} + e_D + (r_D - r_{ds})(I_{L_1} + I_{L_2}) - r_{C_1 ESR} I_{L_2}}{L_2}) \end{bmatrix} \begin{bmatrix} \hat{d} \end{bmatrix} \qquad (4.41)$$

CHAPTER 5

EFFICIENCY

5.1 Elements of Losses

Loss in switching regulator are consists of two main parts; loss of parasitic resistances and switching losses.

5.1.1 Parasitic Resistances

Conversion ratios of discontinuous inductor current mode and continuous inductor current mode operations given in (4.38) and (4.22) imply that parasitic resistances are one of a reason for loss.

Considering conversion ratios (4.32) and (4.22) one can derive loss caused by parasitic resistances as following;

For Continuous Inductor Current Mode Operation;

$$\frac{E_1 I_{L_1} - V_0 I_{L_2}}{E_1 I_{L_1}} = \frac{G_1}{G_1 + 1} \tag{5.1}$$

where;

$$G_1 = \frac{1}{R}\left(\frac{K^2}{(1-K)^2} r_{L_1} + \frac{K}{(1-K)^2} r_{ds} + \frac{1}{1-K} r_D + \frac{K}{1-K} r_{C_1 ESR} + r_{L_2}\right) + \frac{e_D}{V_0}$$

For Discontinuous Inductor Current Mode Operation;

$$\frac{E I_{L_1} - V_0 I_{L_2}}{E_1 I_{L_1}} = \frac{G_2}{G_2 + 1} \tag{5.2}$$

where;

$$G_2 = \frac{1}{R}\left(\frac{K^2}{{K_1}^2} r_{L_1} + \frac{K(K+K_1)}{{K_1}^2} r_{ds} + \frac{(K+K_1)}{K_1} r_D + \frac{K}{K_1} r_{C_1 ESR} + r_{L_2}\right) + \frac{e_D}{V_0}$$

In the derivations of (5.1) and (5.2) input and output current conversions are considered ideal as given in (2.25) and (3.22), since switching loss is not considered in this part. $r_{C_0 ESR}$ also causes loss that is not included in (5.1) and (5.2). Average current I_{C_0} passing through the $r_{C_0 ESR}$ in CICM operation as given in (2.12) for half of a period is

$$I_{C_0} = \frac{\Delta I_{C_0}}{4} \tag{5.3}$$

The average current at a period is zero. It means that average current for the first half of a period is equal to negative average current for the second half of a period. Thus the average dissipation on the resistor $r_{C_0 ESR}$ for both halves of a period are equal.

The average dissipation on the $r_{C_0 ESR}$ for a whole period is derived as given in [1];

$$P_{r_{C_0}} = \frac{4}{3} r_{C_0 ESR} {I_{C_0}}^2 \tag{5.4}$$

(5.4) is also valid for discontinuous inductor current mode operation. By neglecting freewheeling current (5.3) also represents average current passing through $r_{C_0 ESR}$ in discontinuous inuctor current mode operaion.

5.1.2 Switching Losses

Switching losses consist of indutor losses related to current ripple and frequency on them and losses of switching elements.

5.1.2.1 Switching Losses of Inductance

Energy of an inductor is stored in the core material. Since it is not ideal and core losses and eddy current losses become considerable because of the current ripple and frequency.

Current flowing through an inductance induce magnetic field H which is the source of flux density B. Relationship between B and H is dependent to the permeability of a core material. For linear part, it is defined as; $B = \mu H$ *where* μ *is permeability*. Non ideal B-H characteristics are different for increasing H and decreasing H. This means that a specific value of flux density B is induced with higher inductance current in ascending part of B-H characteristic compared to that in the decreasing part of B-H characteristics. The difference between current values is the cause of loss. According to [8] energy consumed by core is represented in terms of inductor voltage and current as follows:

$$W = \int_{one\_cyccle} v(t)i(t)dt \tag{5.5}$$

For ideal inductor the energy is equal to zero for a cycle.

According to Faraday's and Ampere's law v(t) and i(t) are replaced with their flux density and magnetic field equivalents. Thus energy given in (5.5) is modified as

$$W = (A_C l_m) \int_{one\_cyccle} HdB \tag{5.6}$$

where A_C is cross sectional area of the core and l_m is the average length of magnetic field versus flux. Integral part of (5.6) corresponds to the area inside of B-H graph given in Fig. 5.1. For low current ripple, loss decreases. The enclosed area in the B-H graph is small. For high ripple seen in discontinuous inductor current mode operation enclosed area increases, thus core loss is high.

As stated in [8] power loss is frequency *f*, times energy lost in a cycle. It is given as follows in [8].

$$P_{core\_loss} = f(A_C l_m) \int_{one\_cyccle} HdB \tag{5.7}$$

Ac flux Φ(t) flowing through a core material causes voltage induction in the core. Since core materials conduct current, currents called 'eddy currents' are flowing because of induced voltages. Frequency of flux Φ(t) is a multiplier in

equivalent equation of induced voltage. In [8] it was stated that for purely resistive core material eddy current magnitude also increases with increase of frequency. For ferrite materials as stated in [8] losses increase in the rate higher than f^2 ,because resistivity of ferrite also increase with *f*. Eddy current losses are reduced by applying some methods. It was stated in [9] that laminations cause the flux to be divided and relatively induced voltage on the core material reduces. This method is applicable to materials with low resistivity. Another technique is using as core material alloy of insulating material and ferromagnetic particles. Saturation density of such a material is lower than pure ferromagnetic material. Also using core material with high resistivity reduces eddy current loss.

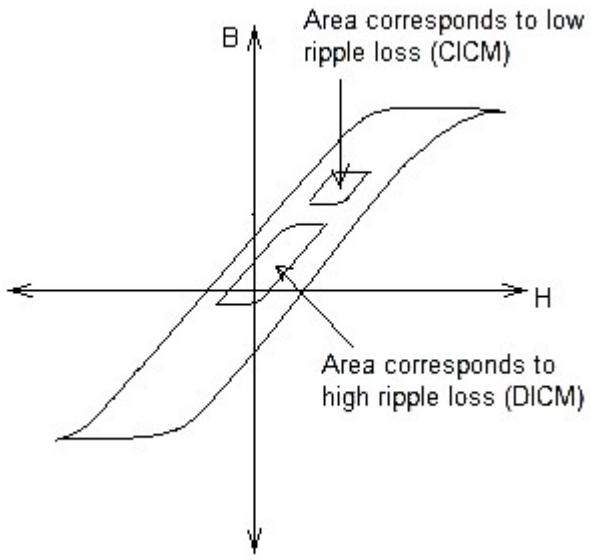

Fig. 5.1 B-H curve and areas that represent core losses.

Total magnetic core loss expression in [9] is given as follows:

$$P_{loss} = P_o f^a B^b \tag{5.8}$$

It is declared in [9] that b in (5.8) is approximately 2 and a in (5.8) is between 1 and 2.

5.1.2.2 Switching Losses of a Diode

A diode is forward biased and conducts current when minority charges are stored in the diode semiconductor p-n junction. A diode is turned off via removing the stored minority charges. In [7] it is stated that in spite of forward diode current reduces to zero, the diode continuous to conduct as long as minority charges exists in the junction. According to [7] the time interval at which stored minority charges are neutralized and recombined is called 'reverse recovery time'. Current-voltage characteristic of a diode for transient operation at reverse recovery time is given in Fig. 5.2 from [8]. As seen from the characteristic charges are removed by negative current. t_r is reverse recovery time. Current passing through the diode at the beginning of turn off transient is I_L.

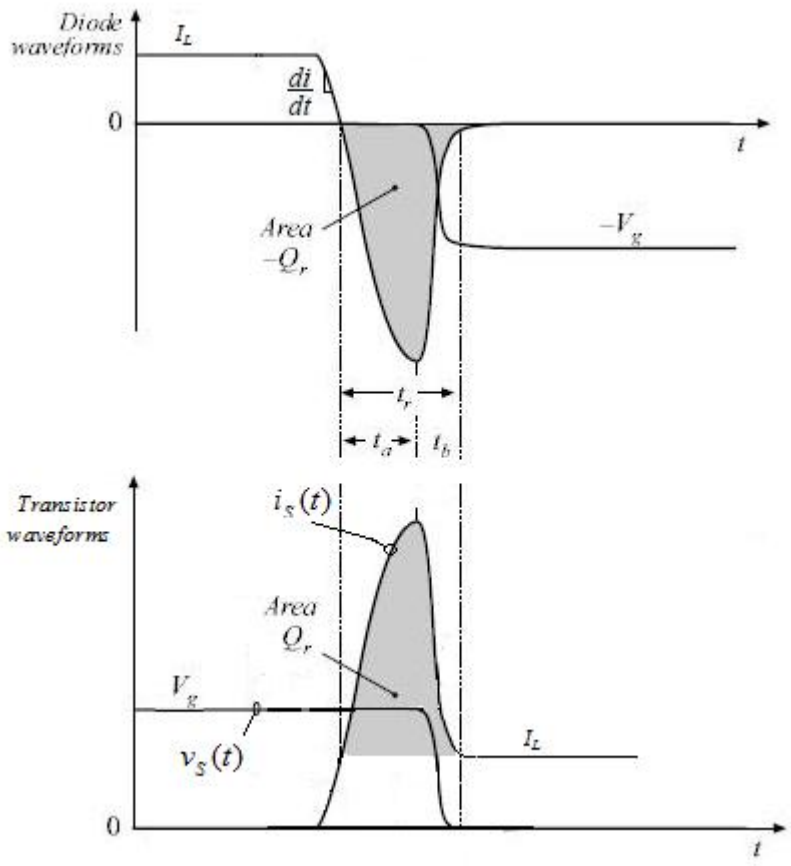

Fig. 5.2 Current-voltage characteristic of a diode for transient operation at reverse recovery time

In [8] it is stated that reverse recovery transient causes switching losses in a switching semiconductor operating in conjunction with the diode in the same converter. A MOSFET is considered as switching semiconductor and it is assumed faster that the diode. According to the buck converter model in [8], turning on the toggled switch MOSFET forces negative current to flow through the diode. Thus the diode minority charges are removed. The increasing rate of reverse current is dependent to both the diode itself and external inductances. Also peak value I_r of the reverse current is related to the rate of increase.

In Fig. 5.2 voltage across a mosfet is V_g. Current passing through the mosfet after transient turn on period is I_L. Stored minority charge is represented by Q_r and is equal to shaded area in Fig. 5.2, area under diode current waveform at t_r reverse recovery time.

Energy dissipation on the mosfet

$$W_D = \int_0^{t_r} v_S(t) i_S(t) dt \tag{5.9}$$

The diode in Cuk converter also causes switching loss on the MOSFET for continuous conduction mode according to the buck converter model explained above. Turning on of the MOSFET applies negative voltage to the diode. Thus it is forced to reverse biases and dissipate power of stored charges on the MOSFET.

However for discontinuous conduction mode operation of Cuk converter this is not valid. The MOSFET is turned on $(1\text{-}k\text{-}k_1)T$ later after the diode is turned off. Thus the diode is not forced by the MOSFET to be reversed biased. The diode becomes reversed biased by removing or neutralizing minority charges with the zero decaying current. Thus for discontinuous inductor current mode operation a diode charge is not dissipated on a toggled switch. Thus diode switching loss does not exist.

For continuous inductor current mode, current I_L passing through the diode at the beginning of turning off is the sum of input and output inductor currents $I_{L1}+I_{L2}$,

where current are considered without ripple. Current passing through the mosfet is $i_S(t)$ and given in (5.10).

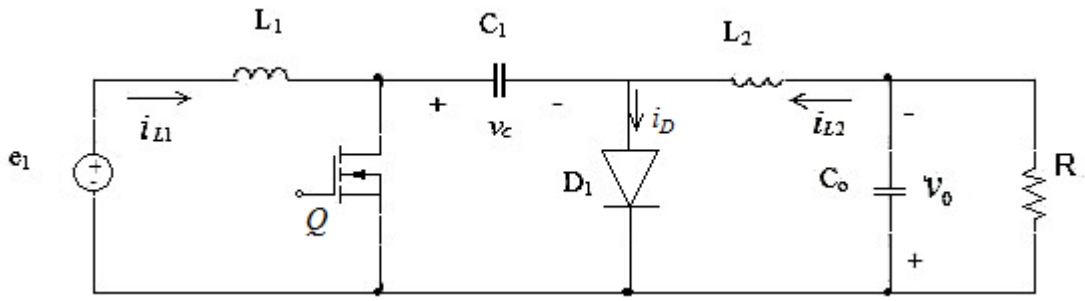

Fig. 5.3 Cuk converter circuit with real switching elements

$$i_S(t) = I_{L_1} + I_{L_2} - i_D(t) \tag{5.10}$$

where $i_D(t)$ is current passing through the diode at transient shown in figure 5.3. Voltage blocked by the mosfet is the sum of input and output voltage, where voltages are considered without ripple. Thus $v_S(t)$ is

$$v_S(t) = E_1 + V_0 \tag{5.11}$$

(5.9) is modified for Cuk converter and dissipated energy in the mosfet for continuous inductor current mode operation is obtained as:

$$W_D = \int_0^{t_r} (E_1 + V_0)(I_{L_1} + I_{L_2} - i_D(t))dt \tag{5.12}$$

$$W_D = (E_1 + V_0)(I_{L_1} + I_{L_2})t_r + (E_1 + V_0)Q_r \tag{5.13}$$

(5.13) represents amount of dissipated energy at a cycle. First term of (5.13) is already considered in MOSFET switching losses. Thus the dissipated energy contribution by a diode is W_{DD}

$$W_{DD} = (E_1 + V_0)Q_r \tag{5.14}$$

Average power is represented as;

$$P_{DD} = \frac{W_{DD}}{T} = W_{DD} f \tag{5.15}$$

where T is switching period, f is a switching frequency.

According to [8] internal junction capacitor C_j causes switching loss. In the analysis junction capacitor loss is ignored.

5.1.2.3 Switching Losses of a MOSFET

For dc-dc converters turn on, turn off transitions of a diode and a transistor are described as follows in [9]: At a state transistor off and diode on inductive current flows through a diode and transistor blocks voltage. After a transistor is driven, current passing through the transistor is set to its nominal value in a time. However diode continuous to conduct a part of the current until transistor current is set to its nominal value. Thus blocked voltage V remains across a transistor at the transient state. When the current of a transistor is set to its nominal value the diode turns off and blocks voltage across the switch. Then switch voltage falls to zero.

At a state, transistor on and diode off, also inductive current flows trough a transistor. At a transition of a transistor, current decreases with high di/dt value, thus negative voltage is induced across the inductor. This causes voltage across the diode to become positive and makes the diode turn on. Then voltage across the diode is transferred across the transistor. As a result transistor transients (on-off and off-on) always take place when blocked voltage V exists across it. It is called 'inductor dominated commutation' in [9].

Transistor commutations of a Cuk Converter are same with the transition model stated above at continuous conduction mode. Switching losses for a MOSFET are calculated according to switching waveforms given for 'inductor dominated commutation' type in Fig. 5.4. At turn off transition of a transistor, turn on transition of not ideal diode because of limited di/dt of a diode causes swinging in inductive

voltages. At turn off transition negative di/dt through inductors increases voltage across the transistor. The situation remains until transition period of a diode starts. It

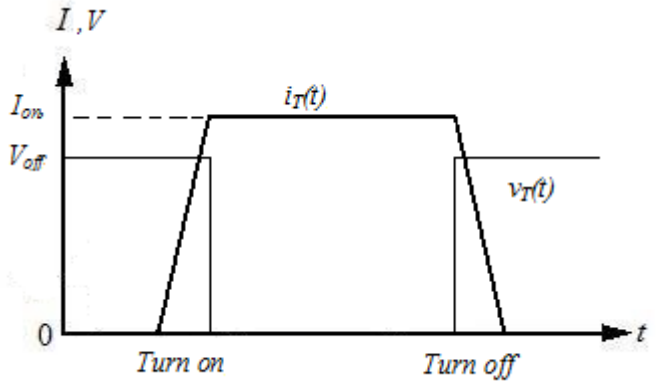

Figure 5.4 Inductor dominated commutation'

is stated in [9] that slow diodes with large inductors cause increase of turn off losses by factors up to %100. In analysis the diode is considered fast enough and additional losses are neglected. It is declared in [9] that a non ideal diode is slower than a transistor and at turn on transition of a transistor di/dt through an inductor is a positive. So voltage across the transistor in transition mode is smaller than a blocked value. This causes reduction in losses. In the analysis since the diode is considered fast enough loss reduction is ignored.

Approximate switching loss of a transistor is given as follows in [9]:

$$W_{switch} = \frac{V_{off} I_{on} (t_{(turn\_on)} + t_{(turn\_off)})}{2} \tag{5.16}$$

(5.16) is equal to blocked voltage across transistor, V_{off} multiplied by area under current waveform at t_{turn_on} and t_{turn_off} given in Fig. 5.4.

For continuous inductor current mode operation, before turn on and after turn off, voltage blocked across a transistor for a Cuk converter is equal to voltage of the energy transfering capacitor C_1. Voltage transition waveforms, at turn on and turn off is given in Fig. 5.4. For steady-state operation, neglecting voltage ripples, voltage of

the capacitor C_1 is equal to summation of input voltage E_1 and output voltage V_0, as given in (2.25). So, blocked voltage across the transistor V_{off} is;

$$V_{off} = E_1 + V_0 \text{ ,for turn on and turn off at continuous inductor current} \quad (5.17)$$

Current passing through a transistor, after turn on and before turn off, is equal to summation of input and output inductor currents for continuous inductor current mode, as given in (2.6). Considering steady-state operation, on state current I_{on} is;

$$I_{on} = I_{L_1} + I_{L_2} \text{ , for turn on and turn off at continuous inductor current} \quad (5.18)$$

Current transition waveforms at turn on and turn off is given in Fig. 5.4. Actually for turn on transition of the transistor, current waveform is affected by the transient operation of the diode and actual transient current is represented by (5.10). However, the diode effect is analyzed in part 5.1.2.2 and only the diode contribution to loss is obtained. Thus to derive the transistor's contribution to switching loss separately, the current for turn on transition is considered as given in Fig. 5.4 by neglecting transient effect of the diode.

By substituting (5.17) and (5.18) in (5.16), switching loss of the transistor for a Cuk converter operating in continuous inductor current mode is;

$$W_{switch} = \frac{(E_1 + V_0)(I_{L_1} + I_{L_2})(t_{(turn\_on)} + t_{(turn\_off)})}{2} \quad (5.19)$$

At discontinuous inductor current mode operation, voltage blocked across a transistor V_{off} after turn off is also equal to voltage of the energy transfering capacitor C_1 and (5.17) is valid. However voltage blocked across a transistor V_{off}, before turn on transition is equal to input voltage E_1, because the converter operates at the state S_1 off, D_1 off.

$$V_{off} = E_1 \text{, for turn on at discontinuous inductor current} \quad (5.20)$$

For discontinuous inductor current mode operation, current passing through the transistor, after turn on and before turn off is also equal to summation of input

and output inductor currents. However ripples for inductor currents in discontinuous inductor current mode is high and (5.18) with state-steady current values is not valid. Thus to obtain accurate expression for the loss, (5.18) is modified by replacing average current values with current values at instants right after turn on and before turn off. For steady-state operation, at the instant before turn off transition input inductor current i_{L_1} and output inductor current i_{L_2} are at their peak values. Thus for turn off transition I_{on} is;

$$I_{on} = I_{L_1 peak} + I_{L_2 peak}\text{, } \textit{for turn off at discontinuous inductor current} \qquad (5.21)$$

For steady state operation, at the instant after turn on transition summation of input inductor current i_{L_1} and output inductor current i_{L_2} is zero, because just ended state is state S_1 off, D_1 off.

$$I_{on} = i_{L_1} + i_{L_2}$$

$$I_{on} = 0 \text{ ,} \textit{for turn on at discontinuous inductor current} \qquad (5.22)$$

Thus for discontinuous inductor current mode switching losses of a transistor is;

$$W_{switch} = \frac{(E_1 + V_0)(I_{L_1 peak} + I_{L_2 peak})t_{(turn\_off)}}{2} \qquad (5.23)$$

The switching loss of a MOSFET at discontinuous inductor current mode is lower than the loss at continuous inductor current mode. (5.23) gives amount of dissipated energy at a cycle. Average power is represented as;

$$P_{switch} = \frac{W_{switch}}{T} = W_{switch} f \qquad (5.24)$$

where T is switching period, f is a switching frequency.

According to [8] internal capacitor C_{ds} effects switching loss. In the analysis C_{ds} loss is ignored.

Also [8] states that internal gate capacitors C_{gs} and C_{gd} causes switching losses. Datasheets of MOSFETs includes gate charge Q_g values instead capacitor values. Thus dissipated energy in terms of charges:

$$W_G = V_{gs} Q_g \tag{5.25}$$

Energy for these capacitors is supplied by gate drive circuit, which is not directly connected to input inductor. In efficiency calculations, input is considered as input inductor current and input voltage and gate energy dissipation is not considered.

5.2 Efficiency of Cuk Converter

As a general rule input power is equal to output power plus loss. Power equivalent for a Cuk converter according to element losses given in previous parts can be expressed as following;

For continuous inductor current mode operation referring to (5.1);

$$E_1 I_{L_1} = V_0 I_{L_2} \frac{(1-K)}{K}(G_1 + 1) + P_{r_{C0}} + P_0 f^a B^b + W_{DD} f + W_{switch} f \tag{5.26}$$

For discontinuous inductor current mode operation referring to (5.2);

$$E_1 I_{L_1} = V_0 I_{L_2} \frac{K_1}{K}(G_2 + 1) + P_{r_{C0}} + P_0 f^a B^b + W_{switch} f \tag{5.27}$$

$P_0 f^a B^b$ in (5.26) and (5.27) represents core loss of both inductances.

In part 5.1.2.2 it is stated that for discontinuous inductor current mode switching losses of a diode do not exist. Thus different from (5.26), (5.27) does not include diode switching loss.The overall efficiency is expressed as;

For continuous inductor current mode operation;

$$\eta = \frac{1}{\frac{(1-K)}{K}(G_1 + 1) + \frac{P_{r_{C0}}}{P_{out}} + \frac{P_0 f^a B^b}{P_{out}} + \frac{W_{DD} f}{P_{out}} + \frac{W_{switch} f}{P_{out}}} \tag{5.28}$$

For discontinuous inductor current mode operation;

$$\eta = \frac{1}{\frac{K_1}{K}(G_2 + 1) + \frac{P_{r_{C0}}}{P_{out}} + \frac{P_0 f^a B^b}{P_{out}} + \frac{W_{switch} f}{P_{out}}} \tag{5.29}$$

where $P_{out} = V_0 I_{L_2}$ for both discontinuous and continuous inductor current mode operation.

(5.28) and (5.29) implies that efficiency of Cuk converter for both operating mode is dependent to the switching frequency.

CHAPTER 6

OPEN LOOP STABILITY ANALYSIS

6.1 Stability Analysis of Cuk Converter with Ideal Elements for Continuous Inductor Current Mode Operation

Continuous inductor current mode small signal model (2.27) is transformed with Laplace transformation. Variable equivalents in Laplace form is given in (6.1).

$$i_{L_1} = \frac{1}{sL_1}\left[-(1-K)v_{C_1} + e_1 + V_{C_1}k\right]$$

$$v_{C_1} = \frac{1}{sC_1}\left[(1-K)i_{L_1} - Ki_{L_2} - (I_{L_1} + I_{L_2})k\right]$$

$$i_{L_2} = \frac{1}{sL_2}\left[Kv_{C_1} - v_0 + V_{C_1}k\right]$$

$$v_0 = \frac{R}{(sC_0R+1)}i_{L_2} \qquad (6.1)$$

where small signal variables are represented with lower case and $E_1, V_{C_1}, K, I_{L_1}, I_{L_2}$ are steady state operating values for related variables. Small signal variables are same with variables of (2.27), but they are represented in (2.27) with '^'over variables. This chapter only deals with small signal variables, thus '^'over variables is removed.

One can write from (6.1) output voltage in terms of input voltage and duty-ratio as following:

$$v_0 = \frac{1}{(1-K)^2(a_0 + a_1.s + a_2s^2 + a_3s^3 + a_4s^4)}\left[K(1-K)e_1 + (d_0 + d_1s + d_2s^2)k\right] \qquad (6.2)$$

where

$$a_0 = 1$$

$$a_1 = \frac{1}{(1-K)^2 R}\left[L_1 K^2 + L_2 (1-K)^2\right]$$

$$a_2 = \frac{1}{(1-K)^2 R} C_0 R\left[L_1 K^2 + L_2 (1-K)^2\right] + \frac{1}{(1-K)^2} C_1 L_1$$

$$a_3 = \frac{1}{(1-K)^2 R} L_1 L_2 C_1$$

$$a_4 = \frac{1}{(1-K)^2} L_1 L_2 C_1 C_0$$

$$d_0 = (1-K) V_{C_1}$$

$$d_1 = -K L_1 (I_{L_1} + I_{L_2})$$

$$d_2 = L_1 C_1 V_{C_1}$$

Voltage conversion ratio *m*, for dynamic operation is defined as output voltage over input voltage while small signal duty-ratio is zero.

$$m = \left.\frac{v_0(s)}{e_1(s)}\right|_{k=0} \tag{6.3}$$

By setting duty-ration k to zero in (6.2), one can derive the dynamic voltage conversion ratio given in (6.4).

$$m = \frac{v_0}{e_1} = \frac{K}{(1-K)(a_0 + a_1.s + a_2 s^2 + a_3 s^3 + a_4 s^4)} \tag{6.4}$$

The system has four poles while it has no zeros. According to the BIBO (Bounded Input Bounded Output) stability for LTI (linear time invariant) systems, dynamic

behaviour is determined by poles of a system. Stability is provided with negative poles.

4.th order equation with coefficients in terms of circuit parameters can be solved approximately. Approximation solution is applied in [11] for 4.th order system. According to the solution 4th order system is represented by multiplication of approximate two second order equations. Condition for approximate separation to two equations is staed in [11] as separate corner frequencies. After separation denominator of (6.4), (6.5) is obtained.

$$(1+\frac{a_1}{a_0}s+\frac{a_2}{a_0}s^2)(1+\frac{a_3}{a_0a_2}s+\frac{a_4}{a_0a_2}s^2) \tag{6.5}$$

Second order denominator is expressed in [8] in the following form:

$$(1+\frac{s}{Qw_0}s+\frac{s^2}{{w_0}^2}) \tag{6.7}$$

where Q is quality factor and w_0 is corner frequency. Q is the magnitude of the transfer function at corner frequency w_0. Thus the condition for separate corner frequencies in terms of (6.5) is expressed as;

$$\frac{a_0}{a_2} << \frac{a_0a_2}{a_4} \tag{6.8}$$

For the transfer function (6.4), separate corner frequency condition is obtained according to (6.8) as following;

$$\frac{1}{C_0L_1\frac{K^2}{(1-.K)^2}+C_0L_2+\frac{1}{(1-.K)^2}C_1L_1} << \frac{K^2}{L_2C_1}+\frac{(1-K)^2}{L_1C_1}+\frac{1}{L_2C_0} \tag{6.9}$$

This yields;

$$1 << \frac{K^4}{(1-K)^2}\frac{C_0L_1}{L_2C_1}+2K^2\frac{C_0}{C_1}+\frac{2K^2}{(1-K)^2}\frac{L_1}{L_2}+(1-K)^2\frac{C_0L_2}{L_1C_1}+\frac{1}{(1-.K)^2}\frac{C_1L_1}{L_2C_0}+2 \tag{6.10}$$

To satisfy (6.10) followings need to be satisfied;

$$C_0 > C_1,\ L_1 > L_2 \text{ and } C_0 L_2 > L_1 C_1 \text{ or } C_0 L_2 < L_1 C_1$$

If (6.9) is not satisfied, poles can be determined with higher order equation solutions. Roots of (6.5), in other words poles are as follows;

$$s_{1,2} = -\frac{a_1}{2a_2}\left[1 \pm \sqrt{1 - \frac{4a_2 a_0}{a_1^{\,2}}}\right] \tag{6.11}$$

$$s_{3,4} = -\frac{a_3}{2a_4}\left[1 \pm \sqrt{1 - \frac{4a_4 a_0 a_2}{a_3^{\,2}}}\right] \tag{6.12}$$

By substituting related coefficients of (6.4) in (6.10) and (6.11) the following pole expressions for the small signal voltage conversion ratio *m* is obtained;

$$s_{1,2} = -\frac{1}{2C_0 R + 2\dfrac{C_1 L_1 R}{L_1 K^2 + L_2 (1-K)^2}}\left[1 \pm \sqrt{1 - 4(1-K)^2 R\left[C_0 R\left[L_1 K^2 + L_2 (1-K)^2\right] + RC_1 L_1\right]\frac{1}{\left[L_1 K^2 + L_2 (1-K)^2\right]^2}}\right] \tag{6.13}$$

where s_{i_1} is defined as the root square term of (6.13) .

$$s_{i_1} = 1 - 4(1-K)^2 R\left[C_0 R\left[L_1 K^2 + L_2 (1-K)^2\right] + RC_1 L_1\right]\frac{1}{\left[L_1 K^2 + L_2 (1-K)^2\right]^2}$$

$$s_{3,4} = -\frac{1}{2C_0 R}\left[1 \pm \sqrt{1 - 4\frac{C_0 R}{L_1 L_2 C_1}\left(C_0 R\left[L_1 K^2 + L_2 (1-K)^2\right] + C_1 L_1\right)}\right] \tag{6.14}$$

where s_{i_2} is defined as the root square term of (6.14) .

$$s_{i_2} = 1 - 4\frac{C_0 R}{L_1 L_2 C_1}\left(C_0 R\left[L_1 K^2 + L_2 (1-K)^2\right] + C_1 L_1\right)$$

According to BIBO stability LTI (Linear time invariant) system is stable for negative real parts of poles. The system becomes more stable for high negative real values. (6.13) and (6.14) has always negative real parts if s_{i_1} and s_{i_2} are negative. In this case roots of $|s_{i_1}|$ and $|s_{i_2}|$ compose imaginary parts of poles. Positive values of s_{i_1} and s_{i_2} are in the range $[0,1]$. For s_{i_1} and s_{i_2} equal to one, according to (6.13) and

(6.14) one of the pole of each equation is zero. However s_{i_1} and s_{i_2} are equal to one only in case that some component do not exist, which is not meaningful. Thus real values of poles are small than zero for all cases. As a resullt open loop system is stable for all cases.

Quality factors Q_1, Q_2 and corner frequencies w_{0_1} and w_{0_2} are derived interms of circuit parameters as following;

$$w_{0_1} = \sqrt{\frac{a_0}{a_2}} = \sqrt{\frac{1}{C_0 L_1 \frac{K^2}{(1-.K)^2} + C_0 L_2 + \frac{1}{(1-.K)^2} C_1 L_1}} \tag{6.15}$$

$$w_{0_2} = \sqrt{\frac{a_0 a_2}{a_4}} = \sqrt{\frac{C_0 L_1 K^2 + L_2 (1-K)^2 + C_1 L_1}{L_1 L_2 C_1 C_0}}$$

$$= \sqrt{\frac{K^2}{L_2 C_1} + \frac{(1-K)^2}{L_1 C_1} + \frac{1}{L_2 C_0}} \tag{6.16}$$

$$Q_1 = \frac{a_0}{a_1 w_{0_1}}$$

$$= \frac{(1-K)^2 R}{L_1 K^2 + L_2 (1-K)^2} \sqrt{C_0 L_1 \frac{K^2}{(1-.K)^2} + C_0 L_2 + \frac{1}{(1-.K)^2} C_1 L_1} \tag{6.17}$$

$$Q_2 = \frac{a_0 a_2}{a_3 w_{0_2}}$$

$$= (C_0 R \left[\frac{K^2}{L_2 C_1} + \frac{(1-K)^2}{L_1 C_1} \right] + \frac{R}{L_2}) \frac{1}{\sqrt{\frac{K^2}{L_2 C_1} + \frac{(1-K)^2}{L_1 C_1} + \frac{1}{L_2 C_0}}} \tag{6.18}$$

[8] states that for $Q_{1,2} < 0.5$ poles are real valued. Thus transient response is exponential decaying function. For $Q_{1,2} = 0.5$ system is critical damped. But for $Q_{1,2} > 0.5$ the poles are comlex. Even real parts of poles are negative, in other words system is stable, transient response has oscillations with decaying amplitude and causes overshooting. Also it is stated that high Q causes high overshoots, such as overshoot of Q=1 is about 16.3% while overshoot of Q=2 is 44.4%.

Conversion ratio *g*, of duty-ratio k to output voltage v_0 for small signal operation is defined as output voltage v_0 over duty-ratio k for zero small signal input voltage e_1. Control to output transfer function is defined as output voltage over duty ratio while input voltage is zero.

$$g = \left.\frac{v_0(s)}{k(s)}\right|_{e_1=0} \tag{6.19}$$

By setting small signal input voltage e_1 to zero in (6.2) conversion ratio *g* is obtained as following;

$$\frac{v_0}{k} = \frac{(d_0 + d_1 s + d_2 s^2)}{(1-K)^2 (a_0 + a_1.s + a_2 s^2 + a_3 s^3 + a_4 s^4)} \tag{6.20}$$

(6.20) has same denominator with voltage conversion ratio *m* in (6.4). Thus they both present same stability characteristics. Different from (6.4), (6.20) contains 2 zeros. According to solution of second order equation zeros are;

$$s_{z_{1,2}} = -\frac{d_1}{2d_2}\left[1 \pm \sqrt{1 - \frac{4d_2 d_0}{{d_1}^2}}\right] \tag{6.21}$$

d_1 is negative for all combinations of circuit components. According to statement made for poles in previous lines zeros have always pozitive real parts. It is declared in [8] that zeros are effective at frequencies higher than zeros and positive zeros cause initail response of the transfer function to be in opposite direction with the input effect. In other words for increase in k, output voltage reflects initially with decrease because of zeros.

6.2 Stability Analysis of Cuk Converter with Ideal Elements for Discontinuous Inductor Current Mode Operation

Applying Laplace transformation to small signal model (3.48) for discontinuous inductor current mode operation variables are obtained as following;

$$i_{L_1} = \frac{1}{sL_1}\left[\frac{K_1}{(K+K_1)}v_{C_1} + e_1 + \frac{K_1}{(K+K_1)^2}V_{C_1}k\right]$$

$$v_{C_1} = \frac{1}{sC_1}\left[\frac{K_1}{(K+K_1)}i_{L_1} - \frac{K}{(K+K_1)}i_{L_2} + \frac{K_1}{(K+K_1)^2}(I_{L_2} - I_{L_1})k\right]$$

$$i_{L_2} = \frac{1}{sL_2}\left[\frac{K}{(K+K_1)}v_{C_1} - v_0 - \frac{K_1}{(K+K_1)^2}V_{C_1}k\right]$$

$$v_0 = \frac{R}{(sC_0R+1)}i_{L_2} \qquad (6.22)$$

One can write output voltage in terms of input voltage and duty ratio variations as follows:

$$v_0 = \frac{1}{(K+K_1)^2(a_0 + a_1.s + a_2s^2 + a_3s^3 + a_4s^4)}\left[KK_1e_1 + (d_0 + d_1s + d_2s^2)k\right] \qquad (6.23)$$

where; $a_0 = \dfrac{K_1^{\,2}}{(K+K_1)^2}$

$$a_1 = \frac{1}{(K+K_1)^2R}\left[L_1K^2 + L_2K_1^{\,2}\right]$$

$$a_2 = \frac{1}{(K+K_1)^2}C_0\left[L_1K^2 + L_2K_1^{\,2}\right] + C_1L_1$$

$$a_3 = \frac{1}{R}L_1L_2C_1$$

$$a_4 = L_1L_2C_1C_0$$

$$d_0 = \frac{K_1^{\,2}}{(K+K_1)}V_{C_1}$$

$$d_1 = -\frac{KK_1}{(K+K_1)^2}L_1(I_{L_1} + I_{L_2})$$

$$d_2 = KL_1C_1V_{C_1}$$

Voltage conversion ratio *m*, for discontinuous inductor current mode from (6.23) considering definition (6.3) as following;

$$\frac{v_0}{e_1} = \frac{KK_1}{(K+K_1)^2(a_0 + a_1.s + a_2 s^2 + a_3 s^3 + a_4 s^4)} \tag{6.24}$$

The system has four poles while it has no zeros. The condition for approximate separation, separate corner frequencies, can be modified for (6.24) as following;

$$\frac{1}{C_0 L_1 K^2 + C_0 L_2 K_1^2 + (K+K_1)^2 C_1 L_1} << \frac{1}{(K+K_1)^4}\left(\frac{K^2}{L_2 C_1} + \frac{K_1^2}{L_1 C_1} + \frac{(K+K_1)^2}{L_2 C_0}\right) \tag{6.25}$$

This yields;

$$1 << \left[\begin{array}{l} \frac{1}{(K+K_1)^4}(2K_1^2(K+K_1)^2 + K^4\frac{C_0 L_1}{C_1 L_2} + K_1^4\frac{C_0 L_2}{C_1 L_1} + (K+K_1)^4\frac{L_1 C_1}{L_2 C_0} + \\ 2K^2(K+K_1)^2\frac{L_1}{L_2} + 2K^2 K_1^2\frac{C_0}{C_1} \end{array}\right] \tag{6.26}$$

(6.26) is satisfied incase $C_0 > C_1$, $L_1 > L_2$ and $C_0 L_2 > L_1 C_1$ or $C_0 L_2 < L_1 C_1$. For discontinuous inductor current mode operation inductance inequality is already satisfied in (3.28). Also because of high output current ripple in discontinuous inductor current mode output capacitance is greater capacitance required for continuous inductor current mode. Thus capacitance inequality is already satisfied.

After separation denominator of (6.24), it becomes in the form of (6.5).

Pole equivalents from (6.11) and (6.12) are obtained as follows:

$$s_{1,2} = -\frac{1}{2C_0 R + \frac{2L_1 C_1 R(K+K_1)^2}{L_1 K^2 + L_2 K_1^2}}\left[1 \pm \sqrt{1 - 4K_1^2(C_0 \blacksquare_1 K^2 + L_2 K_1^2 \bar{} + (K+K_1)^2 C_1 L_1)\frac{R^2}{\blacksquare_1 K^2 + L_2 K_1^{2\,\bar{2}}}}\right] \tag{6.27}$$

$$s_{3,4} = -\frac{1}{2C_0 R}\left[1 \pm \sqrt{1 - \frac{4K_1^2 C_0 R^2}{(K+K_1)^4}\frac{C_0(L_1 K^2 + L_2 K_1^2) + L_1 C_1 (K+K_1)^2}{L_1 L_2 C_1}}\right] \tag{6.28}$$

According to statement made in the previous part for poles of continuous inductor current mode, (6.27) and (6.28) have negative real parts for all combinations of circuit elements. Thus according to BIBO stability system is stable.

Quality factors Q_1, Q_2 and corner frequencies w_{0_1} and w_{0_2} interms of circuit parameters are as following;

$$w_{0_1} = \sqrt{\frac{a_0}{a_2}}$$

$$= \sqrt{\frac{K_1^2}{C_0 L_1 K^2 + C_0 L_2 K_1^2 + (K+K_1)^2 C_1 L_1}} \tag{6.29}$$

$$w_{0_2} = \sqrt{\frac{a_0 a_2}{a_4}}$$

$$= \sqrt{\frac{K_1^2}{(K+K_1)^4} \frac{C_0 L_1 K^2 + L_2 K_1^2 + (K+K_1)^2 C_1 L_1}{L_1 L_2 C_1 C_0}}$$

$$= \sqrt{\frac{K_1^2}{(K+K_1)^4} \left(\frac{K^2}{L_2 C_1} + \frac{K_1^2}{L_1 C_1} + \frac{(K+K_1)^2}{L_2 C_0}\right)} \tag{6.30}$$

$$Q_1 = \frac{a_0}{a_1 w_{0_1}}$$

$$= \frac{K_1^2 R}{L_1 K^2 + L_2 K_1^2} \sqrt{\frac{C_0 L_1 K^2 + C_0 L_2 K_1^2 + (K+K_1)^2 C_1 L_1}{K_1^2}} \tag{6.31}$$

$$Q_2 = \frac{a_0 a_2}{a_3 w_{0_2}}$$

$$= \frac{K_1^2}{(K+K_1)^4} \left(C_0 R \left[\frac{K^2}{L_2 C_1} + \frac{K_1^2}{L_1 C_1}\right] + \frac{R(K+K_1)^2}{L_2}\right) \frac{1}{\sqrt{\frac{K_1^2}{(K+K_1)^4} \left(\frac{K^2}{L_2 C_1} + \frac{K_1^2}{L_1 C_1} + \frac{(K+K_1)^2}{L_2 C_0}\right)}} \tag{6.32}$$

Behavior of conversion ratios *m* and *g* according to Q_1 and Q_2 stated in continuous inductor current mode operation is valid for discontinuous inductor current mode operation too.

Small signal duty-ratio k to output voltage v_0 coversion ratio, *g* for discontinuous iductor current mode is derided from (6.23) by the definition (6.19) as follows;

$$g = \frac{v_0}{k} = \frac{(d_0 + d_1 s + d_2 s^2)}{(K + K_1)^2 (a_0 + a_1.s + a_2 s^2 + a_3 s^3 + a_4 s^4)} \tag{6.33}$$

(6.33) has same denominator with the line to output transfer function (6.24). Thus they both present same stability characteristics. (6.33) contains 2 zeros. Coefficients of nominator in (6.33) are given in (6.23). Zeros are equal to solution of second order equation given in (6.19). d_1 is negative for all combinations of circuit components. According to statement made for poles in previous lines zeros have always pozitive real parts. Thus both control to output transfer functions for continuous inductor current mode and discontinuous inductor current mode presents same charteristics regarding zeros.

6.3 Parasitic Resistance Effects on Stability of Cuk Converter at Continuous Inductor Current Mode Operation

Small signal model variables according to the model (4.25) are expressed as following after laplace transformation is applied.

$$i_{L_1} = \frac{1}{(sL_1 + r_{L_1} + Kr_{ds} + (1-K)r_{C_1 ESR} + (1-K)r_D)} \begin{bmatrix} -(1-K)v_{C_1} - (Kr_{ds} + (1-K)r_D)i_{L_2} + e_1 \\ +(V_{C_1} + e_D + r_{C_1 ESR} I_{L_1} + (r_D - r_{ds})(I_{L_1} + I_{L_2}))k \end{bmatrix}$$

$$v_{C_1} = \frac{1}{sC_1} \left[(1-K)i_{L_1} - Ki_{L_2} - (I_{L_1} + I_{L_2})\hat{k} \right]$$

$$i_{L_2} = \frac{1}{(sL_2 + r_{L_2} + Kr_{ds} + Kr_{C_1 ESR} + (1-K)r_D)} \begin{bmatrix} Kv_{C_1} - (Kr_{ds} + (1-K)r_D)i_{L_1} - v_0 + \\ (V_{C_1} + (r_D - r_{ds})(I_{L_1} + I_{L_2}) - r_{C_1 ESR} I_{L_2} + e_D)k \end{bmatrix}$$

$$v_0 = \frac{sC_0 R r_{C_0 ESR} + R}{(sC_0 (R + r_{C_0 ESR}) + 1)} i_{L_2} \tag{6.34}$$

(6.34) leads to relationship between output voltage, input voltage and duty-ratio as following;

$$v_0 = \frac{1}{(1-K)^2 (a_0 + a_1.s + a_2 s^2 + a_3 s^3 + a_4 s^4)} \left[K(1-K)(1+b_1 s)(1-b_2 s)e_1 + (d_0 + d_1 s + d_2 s^2)(1+b_1 s)k \right] \tag{6.35}$$

where;

$$a_0 = \frac{1}{(1-K)^2 R}\left[K^2 r_{L_1} + (1-K)^2 r_{L_2} + K r_{ds} + K(1-K) r_{C_1 ESR} + (1-K) r_D + 1\right]$$

$$a_1 = \frac{1}{(1-K)^2 R}\left[\begin{array}{l} L_1 K^2 + L_2 (1-K)^2 + C_0 (R + r_{C_0 ESR})(K^2 r_{L_1} + (1-K)^2 r_{L_2} + K r_{ds} + \\ K(1-K) r_{C_1 ESR} + (1-K) r_D) + C_1((r_{L_2} + K r_{C_1 ESR} + R)(r_{L_1} + (1-K) r_{C_1 ESR}) + \\ (r_{L_1} + r_{L_2} + r_{C_1 ESR} + R)(K r_{ds} + (1-K) r_D)) + C_0 R r_{C_0 ESR}(1-K)^2 \end{array}\right]$$

$$a_2 = \frac{1}{(1-K)^2 R} C_0 (R + r_{C_0 ESR})\left[\begin{array}{l} L_1 K^2 + L_2 (1-K)^2 + C_1((r_{L_2} + K r_{C_1 ESR})(r_{L_1} + (1-K) r_{C_1 ESR}) + \\ (r_{L_1} + r_{L_2} + r_{C_1 ESR})(K r_{ds} + (1-K) r_D)) \end{array}\right]$$

$$+ \frac{1}{(1-K)^2 R} C_1\left[\begin{array}{l} L_1 (r_{L_2} + K r_{ds} + K r_{C_1 ESR} + (1-K) r_D + R) + \\ (L_2 + C_0 R r_{C_0 ESR})(r_{L_1} + K r_{ds} + (1-K) r_{C_1 ESR} + (1-K) r_D) \end{array}\right]$$

$$a_3 = \frac{1}{(1-K)^2 R}\left[\begin{array}{l} C_0 C_1 (R + r_{C_0 ESR})\left[L_1 (r_{L_2} + K r_{ds} + K r_{C_1 ESR} + (1-K) r_D) + \right. \\ \left. L_2 (r_{L_1} + K r_{ds} + (1-K) r_{C_1 ESR} + (1-K) r_D)\right] + L_1 L_2 C_1 + L_1 C_0 C_1 R r_{C_0 ESR} \end{array}\right]$$

$$a_4 = \frac{1}{(1-K)^2 R} L_1 L_2 C_1 C_0 (R + r_{C_0 ESR})$$

$$b_1 = C_0 r_{C_0 ESR}$$

$$b_2 = C_1 \left(\frac{r_{ds}}{(1-K)} + \frac{r_D}{K}\right)$$

$$d_0 = (1-K)(V_{C_1} + e_D) - r_{ds}(I_{L_1} + I_{L_2}) - (1-K) r_{C_1 ESR} I_{L_2} - K r_{L_1}(I_{L_1} + I_{L_2})$$

$$d_1 = \left[\begin{array}{l} C_1 (r_{L_1}(r_D - r_{ds})(I_{L_1} + I_{L_2}) + (r_{L_1} + (1-K) r_{C_1 ESR})(V_{C_1} + e_D - r_{C_1 ESR} I_{L_2}) \\ - r_{ds} r_{C_1 ESR}(I_{L_1} + I_{L_2})) - K L_1 (I_{L_1} + I_{L_2}) \end{array}\right]$$

$$d_2 = L_1 C_1 (V_{C_1} + e_D + (r_D - r_{ds})(I_{L_1} + I_{L_2}) - r_{C_1 ESR} I_{L_2})$$

Small signal voltage conversion ratio, for continuous inductor current mode with parasitic resistances effect, is derived from (6.35) by setting small signal duty ratio k to zero according to definition (6.3).

$$m = \frac{v_0}{e_1} = \frac{K(1 + b_1 s)(1 - b_2 s)}{(1-K)(a_0 + a_1 . s + a_2 s^2 + a_3 s^3 + a_4 s^4)} \qquad (6.36)$$

The conversion ratio (6.36) has four poles and two zeros. However small signal voltage conversion ratio for ideal case (6.4) does not have any zeros. So, parasitic resistances add two zeros to the system. Zeros are given in (6.37).

$$s_{z_1} = -\frac{1}{b_1}$$
$$s_{z_2} = \frac{1}{b_2} \tag{6.37}$$

Supposing that the approximating method condition (6.8) is satisfied, one can derive corner frequencies of the system (6.38) and (6.39).

$$w_{0_1} = \sqrt{\frac{a_0}{a_2}}$$
$$= \sqrt{\frac{K^2 r_{L_1} + (1-K)^2 r_{L_2} + K r_{ds} + K(1-K) r_{C_1 ESR} + (1-K) r_D + (1-K)^2 R}{C_0 (R + r_{C_0 ESR}) \left[L_1 K^2 + L_2 (1-K)^2 + C_1 ((r_{L_2} + K r_{C_1 ESR})(r_{L_1} + (1-K) r_{C_1 ESR}) + (r_{L_1} + r_{L_2} + r_{C_1 ESR})(K r_{ds} + (1-K) r_D)) \right] + C_1 L_1 (r_{L_2} + K r_{ds} + K r_{C_1 ESR} + (1-K) r_D + R) + (L_2 + C_0 R r_{C_0 ESR})(r_{L_1} + K r_{ds} + (1-K) r_{C_1 ESR} + (1-K) r_D)}} \tag{6.38}$$

$$w_{0_2} = \sqrt{\frac{a_0 a_2}{a_4}}$$
$$= \sqrt{\frac{\left[C_0 (R + r_{C_0 ESR}) \left[L_1 K^2 + L_2 (1-K)^2 + C_1 ((r_{L_2} + K r_{C_1 ESR})(r_{L_1} + (1-K) r_{C_1 ESR}) + (r_{L_1} + r_{L_2} + r_{C_1 ESR})(K r_{ds} + (1-K) r_D)) \right] + C_1 L_1 (r_{L_2} + K r_{ds} + K r_{C_1 ESR} + (1-K) r_D + R) + (L_2 + C_0 R r_{C_0 ESR})(r_{L_1} + K r_{ds} + (1-K) r_{C_1 ESR} + (1-K) r_D) \right] a_0}{L_1 L_2 C_1 C_0}} \tag{6.39}$$

To make corner frequency expressions meaningful for comparison, (6.38) and (6.39) is simplified with approximations. Simplification is used for analysis in [11] too.

Approximations made for (6.43);

$$\frac{1}{R}\left[K^2 r_{L_1}+(1-K)^2 r_{L_2}+Kr_{ds}+K(1-K)r_{C_1ESR}+(1-K)r_D\right]+(1-K)^2 \approx$$

$$((r_{L_2}+Kr_{C_1ESR})(r_{L_1}+(1-K)r_{C_1ESR})+(r_{L_1}+r_{L_2}+r_{C_1ESR})(Kr_{ds}+(1-K)r_D)) \tag{6.40}$$

$$\frac{1}{R}\left[K^2 r_{L_1}+(1-K)^2 r_{L_2}+Kr_{ds}+K(1-K)r_{C_1ESR}+(1-K)r_D\right]+(1-K)^2 \approx$$

$$(r_{L_2}+Kr_{ds}+Kr_{C_1ESR}+(1-K)r_D) \tag{6.41}$$

$$\frac{1}{R}\left[K^2 r_{L_1}+(1-K)^2 r_{L_2}+Kr_{ds}+K(1-K)r_{C_1ESR}+(1-K)r_D\right]+(1-K)^2 \approx$$

$$(r_{L_1}+Kr_{ds}+(1-K)r_{C_1ESR}+(1-K)r_D)(1+C_0 R r_{C_0ESR}) \tag{6.42}$$

and by neglecting

$\left[K^2 r_{L_1}+(1-K)^2 r_{L_2}+Kr_{ds}+K(1-K)r_{C_1ESR}+(1-K)r_D\right]$ in numerator and r_{C_0ESR} in denumarator to maintain 3 terms same as in the w_{01}. Approximations for (6.44) are $a_0 \approx 1$ and $r_{C_0ESR} \approx 0$. Resultant exrpressions (6.43) and (6.44) are obtained for corner frequencies;

$$w_{0_1} = \sqrt{\frac{1}{\frac{C_0 L_1 K^2}{(1-K)^2}+C_0 L_2+\frac{C_1 L_1}{(1-K)^2}+\frac{C_0 C_1}{R}+\frac{C_1(L_1+L_2)}{R}}} \tag{6.43}$$

$$w_{0_2} = \sqrt{\begin{array}{l}\frac{K^2}{L_2 C_1}+\frac{(1-K)^2}{L_1 C_1}+\frac{1}{L_2 C_0}+\frac{(r_{L_2}+Kr_{C_1ESR})(r_{L_1}+(1-K)r_{C_1ESR})+(r_{L_1}+r_{L_2}+r_{C_1ESR})(Kr_{ds}+(1-K)r_D)}{L_1 L_2} \\ +\frac{(r_{L_2}+Kr_{ds}+Kr_{C_1ESR}+(1-K)r_D)}{RL_2 C_0}+\frac{(r_{L_1}+Kr_{ds}+(1-K)r_{C_1ESR}+(1-K)r_D)}{L_1 C_0 R}\end{array}} \tag{6.44}$$

When they are compared with (6.14) and (6.15) it reveals that parasitic resistances tend to separate corner frequencies, increasing high frequency and decreasing low frequency.

By approximations;

$$\frac{1}{R}\left[K^2 r_{L_1}+(1-K)^2 r_{L_2}+Kr_{ds}+K(1-K)r_{C_1ESR}+(1-K)r_D\right]+(1-K)^2 \approx$$

$$\left[K^2 r_{L_1}+(1-K)^2 r_{L_2}+Kr_{ds}+K(1-K)r_{C_1ESR}+(1-K)r_D\right] \tag{6.45}$$

$$\frac{1}{R}\left[K^2 r_{L_1} + (1-K)^2 r_{L_2} + K r_{ds} + K(1-K) r_{C_1 ESR} + (1-K) r_D + (1-K)^2 \right] \approx$$

$$\left[r_{L_1} + K r_{ds} + (1-K) r_{C_1 ESR} + (1-K) r_D \right] \tag{6.46}$$

for Q_1 and $r_{C_0 ESR} \approx 0$ and $K r_{C_1 ESR} = (1-K) r_{C_1 ESR}$ for Q_2, quality factors expression is obtaing as following;

$$Q_1 = \frac{a_0}{a_1 w_{0_1}}$$

$$\approx \frac{(1-K)^2 R}{\left[L_1 K^2 + L_2 (1-K)^2 + C_0 R (1-K)^2 + C_1 R (1-K)^2 + C_1 (1-K)^2\right] w_{0_1}} \tag{6.47}$$

$$Q_2 = \frac{a_0 a_2}{a_3 w_{0_2}}$$

$$\approx (C_0 R\left[\frac{K^2}{L_2 C_1} + \frac{(1-K)^2}{L_1 C_1}\right] + \frac{R}{L_2} + \frac{\begin{array}{c} C_1 (r_{L_1}{}^2 + r_{L_1} r_{C_1 ESR} + K(1-K) r_{C_1 ESR}{}^2 + \\ (2K r_{L_1} + r_{C_1 ESR})(K r_{ds} + (1-K) r_D)) \end{array}}{\begin{array}{c} C_0 C_1 R (L_1 + L_2)(r_{L_1} + K r_{ds} + K r_{C_1 ESR} + (1-K) r_D) \\ + L_1 L_2 C_1 \end{array}}) \frac{1}{w_{0_2}} \tag{6.48}$$

Since nominator and denominator increases with inclusion of the parasitic resistances, general statement about parasitic resistance effects can not be derived.

All denominator coefficients of (6.18) increase with parasitic resistance effects. Considering pole equivalents (6.11), (6.12) and coefficients of (6.33), exact statement for increase or decrease of pole real parts can not be made. However BIBO stability criteria negative real parts of poles are satisfied for all cases, according to statement made for ideal case poles. Thus system remains open loop stability in case of parasitic resistances.

Small signal duty-ratio k to output voltage v_0 conversion ratio *g*, for continuous inductor current mode with parasitic resistances effect, is derived as;

$$g = \frac{v_0}{k} = \frac{(d_0 + d_1 s + d_2 s^2)(1 + b_1 s)}{(1-K)^2 (a_0 + a_1 . s + a_2 s^2 + a_3 s^3 + a_4 s^4)} \tag{6.49}$$

(6.49) has same denominator with the line to output transfer function (6.36). Thus they both present same stability characteristics. Transfer function (6.49) has three zeros, while its ideal form (6.20) contains two. Coefficients of nominator in (6.49) are given in (6.35). According to solution of second order equation two zeros are;

$$s_{z_{1,2}} = -\frac{d_1}{2d_2}\left[1 \pm \sqrt{1 - \frac{4d_2 d_0}{{d_1}^2}}\right] \tag{6.50}$$

Because of parasitic resistances, negative d_1 and positive d_0, d_2 tends to decrease in magnutude. However zeros remain their real parts pozitive. Additional negative zero is pleced because of output filters parasitic resistance, it is given in (6.51).

$$s_{z_3} = -\frac{1}{b_1} \tag{6.51}$$

6.4 Parasitic Resistance Effects on Stability of Cuk Converter at Discontinuous Inductor Current Mode Operation

The relation for input and output variables given in small signal model in (4.41) in laplace form can be derived as following;

$$v_0 = \frac{1}{(K+K_1){K_1}^2(a_0 + a_1.s + a_2 s^2 + a_3 s^3 + a_4 s^4)}\left[KK_1(1+b_1 s)(1-b_2 s)e_1 + (d_0 + d_1 s + d_2 s^2)(1+b_1 s)k\right] \tag{6.52}$$

where;

$$a_0 = \frac{1}{{K_1}^2 R}\left[K^2 r_{L_1} + {K_1}^2 r_{L_2} + (K+K_1)Kr_{ds} + KK_1 r_{C_1 ESR} + (K+K_1)K_1 r_D + 1\right]$$

$$a_1 = \frac{1}{{K_1}^2 R}\left[\begin{array}{l} L_1 K^2 + L_2 {K_1}^2 + C_0(R + r_{C_0 ESR})(K^2 r_{L_1} + {K_1}^2 r_{L_2} + (K+K_1)Kr_{ds} + KK_1 r_{C_1 ESR} + (K+K_1)K_1 r_D) + \\ C_1(((K+K_1)r_{L_2} + Kr_{C_1 ESR} + R)(r_{L_1} + K_1 r_{C_1 ESR}) + ((K+K_1)(r_{L_1} + r_{L_2} + r_{C_1 ESR}) + R)(Kr_{ds} + K_1 r_D)) + \\ C_0 R r_{C_0 ESR}\dfrac{{K_1}^2}{(K+K_1)} \end{array}\right]$$

$$a_2 = \frac{1}{{K_1}^2 R}C_0(R + r_{C_0 ESR})\left[\begin{array}{l} L_1 K^2 + L_2 {K_1}^2 + C_1(((K+K_1)r_{L_2} + Kr_{C_1 ESR})((K+K_1)r_{L_1} + K_1 r_{C_1 ESR}) \\ + (K+K_1)(r_{L_1} + r_{L_2} + r_{C_1 ESR})(Kr_{ds} + K_1 r_D)) \end{array}\right]$$

$$+\frac{1}{K_1{}^2R}C_1(K+K_1)\begin{bmatrix}L_1((K+K_1)r_{L_2}+Kr_{ds}+Kr_{C_1ESR}+K_1r_D+R)+\\(L_2+\frac{C_0Rr_{C_0ESR}}{(K+K_1)})((K+K_1)r_{L_1}+Kr_{ds}+K_1r_{C_1ESR}+K_1r_D)\end{bmatrix}$$

$$a_3=\frac{1}{K_1{}^2R}\begin{bmatrix}C_0C_1(R+r_{C_0ESR})(K+K_1)\blacksquare_1((K+K_1)r_{L_2}+Kr_{ds}+Kr_{C_1ESR}+K_1r_D)\\+L_2((K+K_1)r_{L_1}+Kr_{ds}+K_1r_{C_1ESR}+K_1r_D)\\+(K+K_1)^2L_1L_2C_1+(K+K_1)L_1C_0C_1Rr_{C_0ESR}\end{bmatrix}$$

$$a_4=\frac{1}{K_1{}^2R}(K+K_1)^2L_1L_2C_1C_0(R+r_{C_0ESR})$$

$$b_1=C_0r_{C_0ESR}$$

$$b_2=C_1(K+K_1)(\frac{r_{ds}}{K_1}+\frac{r_D}{K})$$

$$d_0=(K+K_1)\begin{bmatrix}K_1(K+K_1)(V_{C_1}+e_D)-(K+K_1)^2r_{ds}(I_{L_1}+I_{L_2})\\-(K+K_1)K_1r_{C_1ESR}I_{L_2}-(K+K_1)Kr_{L_1}(I_{L_1}+I_{L_2})\end{bmatrix}$$

$$d_1=(K+K_1)\begin{bmatrix}C_1((K+K_1)r_{L_1}(r_D-r_{ds})(I_{L_1}+I_{L_2})+((K+K_1)r_{L_1}+K_1r_{C_1ESR})(V_{C_1}+e_D-r_{C_1ESR}I_{L_2})\\-(K+K_1)r_{ds}r_{C_1ESR}(I_{L_1}+I_{L_2}))-KL_1(I_{L_1}+I_{L_2})\end{bmatrix}$$

$$d_2=(K+K_1)^2L_1C_1(V_{C_1}+e_D+(r_D-r_{ds})(I_{L_1}+I_{L_2})-r_{C_1ESR}I_{L_2})$$

Small signal voltage conversion ratio *m*, for discontinuous inductor current mode with parasitic resistance effect, is obtained as following from (6.52) by setting small signal duty-ratio to zero;

$$m=\frac{v_0}{e_1}=\frac{KK_1(1+b_1s)(1-b_2s)}{(K+K_1)K_1{}^2(a_0+a_1.s+a_2s^2+a_3s^3+a_4s^4)} \tag{6.53}$$

The transfer function has four poles as transfer function of ideal case. But differently from ideal case (6.53) has two zeros. Zeros are given in (6.54).

$$\begin{aligned}s_{z_1}&=-\frac{1}{b_1}\\s_{z_2}&=\frac{1}{b_2}\end{aligned} \tag{6.54}$$

Considering that approximating condition is satisfied and denominator become in the form of (6.5), function parameters are derived.

Corner frequencies of the system:

$$w_{0_1} = \sqrt{\frac{a_0}{a_2}}$$

$$\approx \sqrt{\frac{K^2 r_{L_1} + K_1^2 r_{L_2} + (K+K_1)Kr_{ds} + KK_1 r_{C_1ESR} + (K+K_1)K_1 r_D + K_1^2 R}{C_0(R+r_{C_0ESR})\left[\begin{array}{l} L_1K^2 + L_2K_1^2 + C_1(((K+K_1)r_{L_2} + Kr_{C_1ESR})((K+K_1)r_{L_1} + K_1 r_{C_1ESR}) + \\ (K+K_1)(r_{L_1} + r_{L_2} + r_{C_1ESR})(Kr_{ds} + K_1 r_D)) \end{array}\right] + C_1(K+K_1)\left[\begin{array}{l} L_1((K+K_1)r_{L_2} + Kr_{ds} + Kr_{C_1ESR} + K_1 r_D + R) + \\ (L_2 + \frac{C_0 R r_{C_0ESR}}{(K+K_1)})((K+K_1)r_{L_1} + Kr_{ds} + K_1 r_{C_1ESR} + K_1 r_D) \end{array}\right]}} \tag{6.55}$$

$$w_{0_2} = \sqrt{\frac{a_0 a_2}{a_4}}$$

$$\approx \sqrt{\frac{\left[\begin{array}{l} C_0(R+r_{C_0ESR})\left[\begin{array}{l} L_1K^2 + L_2K_1^2 + C_1(((K+K_1)r_{L_2} + Kr_{C_1ESR})((K+K_1)r_{L_1} + K_1 r_{C_1ESR}) + \\ (K+K_1)(r_{L_1} + r_{L_2} + r_{C_1ESR})(Kr_{ds} + K_1 r_D)) \end{array}\right] \\ + C_1(K+K_1)\left[\begin{array}{l} L_1((K+K_1)r_{L_2} + Kr_{ds} + Kr_{C_1ESR} + K_1 r_D + R) + \\ (L_2 + \frac{C_0 R r_{C_0ESR}}{(K+K_1)})((K+K_1)r_{L_1} + Kr_{ds} + K_1 r_{C_1ESR} + K_1 r_D) \end{array}\right] \end{array}\right] a_0}{(K+K_1)^2 L_1 L_2 C_1 C_0 (R+r_{C_0ESR})}} \tag{6.56}$$

With following approximations, corner frequency w_{0_1} is simplified to get meaningful expression.

$$\frac{1}{R}\left[K^2 r_{L_1} + K_1^2 r_{L_2} + (K+K_1)Kr_{ds} + KK_1 r_{C_1ESR} + (K+K_1)K_1 r_D + K_1^2\right] \approx$$

$$(((K+K_1)r_{L_2} + Kr_{C_1ESR})((K+K_1)r_{L_1} + K_1 r_{C_1ESR}) + (K+K_1)(r_{L_1} + r_{L_2} + r_{C_1ESR})(Kr_{ds} + K_1 r_D)) \tag{6.57}$$

$$\frac{1}{R}\left[K^2 r_{L_1} + K_1^2 r_{L_2} + (K+K_1)Kr_{ds} + KK_1 r_{C_1ESR} + (K+K_1)K_1 r_D + K_1^2\right] \approx$$

$$((K+K_1)r_{L_2} + Kr_{ds} + Kr_{C_1ESR} + K_1 r_D) \tag{6.58}$$

$$\frac{1}{R}\sqrt{K^2 r_{L_1} + K_1^2 r_{L_2} + (K+K_1)Kr_{ds} + KK_1 r_{C_1 ESR} + (K+K_1)K_1 r_D + K_1^2} \approx$$

$$((K+K_1)r_{L_1} + Kr_{ds} + K_1 r_{C_1 ESR} + K_1 r_D)(1 + \frac{C_0 R r_{C_0 ESR}}{(K+K_1)}) \qquad (6.59)$$

and by neglecting

$\sqrt{K^2 r_{L_1} + K_1^2 r_{L_2} + (K+K_1)Kr_{ds} + KK_1 r_{C_1 ESR} + (K+K_1)K_1 r_D}$ in numarator and $r_{C_0 ESR}$ in denumarator to maintain 3 terms same as in the w_{01}. Resultant expression for w_{0_1} is

$$w_{0_1} \approx \sqrt{\frac{1}{\frac{C_0 L_1 K^2}{K_1^2} + C_0 L_2 + \frac{C_1 L_1 (K+K_1)}{K_1^2} + \frac{C_0 C_1}{R} + \frac{C_1 (L_1 + L_2)(K+K_1)}{R}}} \qquad (6.60)$$

By approximating $a_0 \approx 1$ and $r_{C_0 ESR} \approx 0$ expression for w_{0_2} is simplified as following;

$$w_{0_2} \approx \sqrt{\begin{array}{l} \frac{K^2}{(K+K_1)^2 L_2 C_1} + \frac{K_1^2}{(K+K_1)^2 L_1 C_1} + \frac{1}{(K+K_1)L_2 C_0} + \\ \frac{((K+K_1)r_{L_2} + Kr_{C_1 ESR})(r_{L_1} + K_1 r_{C_1 ESR}) + (K+K_1)(r_{L_1} + r_{L_2} + r_{C_1 ESR})(Kr_{ds} + K_1 r_D)}{(K+K_1)^2 L_1 L_2} \\ + \frac{((K+K_1)r_{L_2} + Kr_{ds} + Kr_{C_1 ESR} + K_1 r_D)}{(K+K_1)RL_2 C_0} + \frac{((K+K_1)r_{L_1} + Kr_{ds} + K_1 r_{C_1 ESR} + K_1 r_D)}{(K+K_1)L_1 C_0 R} \end{array}} \qquad (6.61)$$

Parasitic resistances add terms to denominator of w_{0_1} and to nominator of w_{0_2}. It means that parasitic resistances tend to separate corner frequencies.

With approximations, quality factor Q_1 and Q_2 simple expressions (6.64) and (6.65) are obtained.

Aproximations for Q_1;

$$\frac{1}{R}\sqrt{K^2 r_{L_1} + K_1^2 r_{L_2} + (K+K_1)Kr_{ds} + KK_1 r_{C_1 ESR} + (K+K_1)K_1 r_D + K_1^2} \approx$$

$$K^2 r_{L_1} + K_1^2 r_{L_2} + (K+K_1)Kr_{ds} + KK_1 r_{C_1 ESR} + (K+K_1)K_1 r_D \qquad (6.62)$$

$$\frac{1}{R}\left[K^2 r_{L_1} + {K_1}^2 r_{L_2} + (K+K_1)Kr_{ds} + KK_1 r_{C_1 ESR} + (K+K_1)K_1 r_D\right] + {K_1}^2 \approx$$

$$(K+K_1)r_{L_1} + Kr_{ds} + K_1 r_{C_1 ESR} + K_1 r_D \tag{6.63}$$

and (6.57) and $r_{C_0 ESR} \approx 0$.

$$Q_1 = \frac{a_0}{a_1 w_{0_1}}$$

$$\approx \frac{{K_1}^2 R}{\left[L_1 K^2 + L_2 {K_1}^2 + C_0 R {K_1}^2 + C_1 R {K_1}^2 + C_1 {K_1}^2\right]} \frac{1}{w_{0_1}} \tag{6.64}$$

Approximations for Q_2 are $r_{C_0 ESR} \approx 0$, $r_{L_1} \approx r_{L_2}$ and $Kr_{C_1 ESR} = K_1 r_{C_1 ESR}$, so that

$$Q_2 = \frac{a_0 a_2}{a_3 w_{0_2}}$$

$$\approx \left[C_0 R\left[\frac{K^2}{(K+K_1)^2 L_2 C_1} + \frac{{K_1}^2}{(K+K_1)^2 L_1 C_1}\right] + \frac{R}{(K+K_1)^2 C_1 L_2} + \frac{\left[\begin{array}{l} C_1((K+K_1)^2 {r_{L_1}}^2 + (K+K_1) r_{L_1} r_{C_1 ESR} + K^2 {r_{C_1 ESR}}^2 + \\ (K+K_1)(2r_{L_1} + r_{C_1 ESR})(Kr_{ds} + K_1 r_D) + \\ (K+K_1)(L_1+L_2)(r_{L_1} + Kr_{ds} + Kr_{C_1 ESR} + K_1 r_D)) \end{array}\right]}{(K+K_1)C_0 C_1 R(L_1+L_2)(r_{L_1} + Kr_{ds} + Kr_{C_1 ESR} + K_1 r_D) + (K+K_1)^2 L_1 L_2 C_1} \right] \frac{1}{w_{0_2}} \tag{6.65}$$

All denominator coefficients of (6.23) ideal case, increase with parasitic resistance effects. Considering pole equivalents (6.11), (6.12) and coefficients of (6.52), exact statement for increase or decrease of pole real parts can not be made. However BIBO stability criteria, negative real parts of poles are satisfied for all cases, according to statement made for ideal case poles. Thus system remains open loop stability in case of parasitic resistances.

Small signal duty-ratio k to output voltage v_0 conversion ratio *g*, for discontinuous inductor current mode operation with parasitic effects is obtained as following, from (6.52) by setting small signal input voltage to zero;

$$\frac{v_0}{k} = \frac{(d_0 + d_1 s + d_2 s^2)(1 + b_1 s)}{(K + K_1)K_1^{\,2}(a_0 + a_1.s + a_2 s^2 + a_3 s^3 + a_4 s^4)} \tag{6.66}$$

(6.66) present same stability characteristics with line to output transfer function (6.53), because they both has same denominator. Ideal and non ideal control to output transfer functions is different in zero numbers also. Parasitic resistances add another zero to the system. It is (6.67).

$$s_{z_3} = -\frac{1}{b_1} \tag{6.67}$$

Already existing zeros equivalents have same representations with (6.47). Considering coefficients of (6.52) and (6.50) it reveals that because of parasitic resistances, negative d_1 and positive d_0, d_2 tends to decrease in magnutude. However zeros remain their real parts pozitive.

6.5 Critical Points for Open Loop Operation

Satisfying only stability criteria do not provide desired dynamic behaviour. Listed critical points below have significant effects on dynamic behaviour:

i. It was stated in [4] that the resonant frequency of C_1, L_1 and L_2 must be greater than the line frequency, to avoid input current oscillations (w_L), if the source varies periodically.

$$w_L << \frac{1}{\sqrt{L_1 C_1}} \tag{6.68}$$

ii. According to [4] resonant frequency C_1, L_2 must be lower than the switching frequency (w_S), to provide constant voltage in a switching period.

$$w_S >> \frac{1}{\sqrt{L_2 C_1}} \tag{6.69}$$

iii. The output filter C_0, L_2 should be determined such that its resonant frequency is too small from the switching frequency. Thus the oscillations are eliminated.

$$w_S >> \frac{1}{\sqrt{L_2 C_0}} \tag{6.70}$$

CHAPTER 7

DESIGN AND SIMULATIONS

Simulations are run with SIMPLORER 7.0 Student Version.

7.1 Design and Simulations for Continuous Inductor Current Mode Operation

Circuit elements for the converter are given in Table 7.1. Steady-state operating point of the converter is given in Table 7.2. The circuit used in the simulation is shown in Fig.7.1. Switch S switches at a period T=0.025 ms, with a duty-ratio K=0.4. It is driven with PWM1 module. Dot shown in the figure indicates that the current enters the element at that terminal. Simulation is done in transient mode of the Simplorer which yields results in real time.

Table 7.1 Components of the converter

Component	L_1 / mH	L_2 / mH	C_1 /μF	C_0 /μF	R / Ω
Size	2	2	150	200	5

Table 7.2 Steady State Operating Points

Parameter	E_1 / V	V_0 / V	K	I_{L_2} / A	I_{L_1} / A
Magnitude	100	67	0.4	13.4	8.9

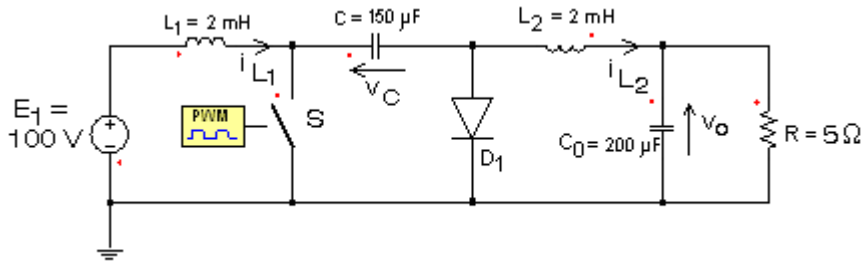

Fig. 7.1 The circuit simulated

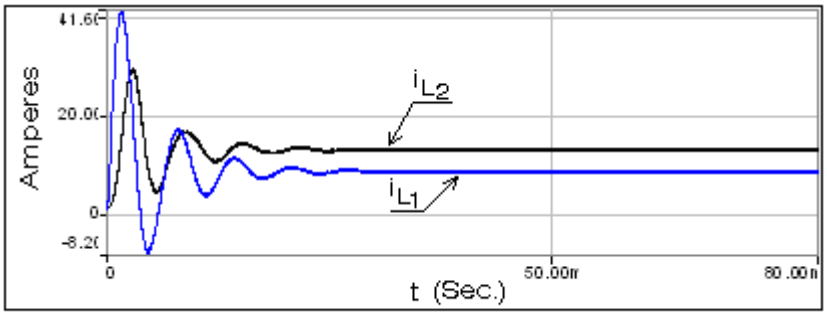

Fig. 7.2 (a) Input and output inductor current i_{L_1}, i_{L_2}.

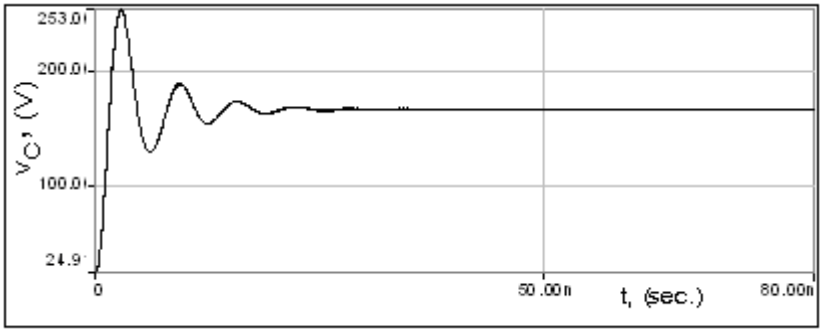

Fig. 7.2 (b) Energy transferring capacitor v_{C_1}.

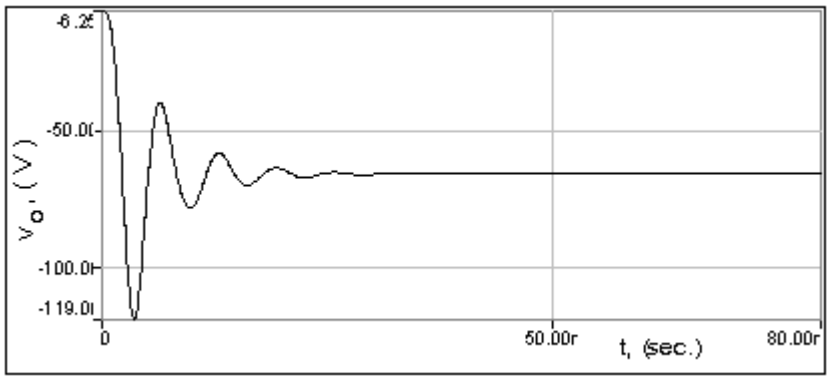

Fig. 7.2 (c) Output voltage v_0 simulation results.

The response obtained in the transient mode is from the start up instant onward. Thus the simulation includes both transient and steady-state behaviours. Fig. 7.2 (a) shows the inductor currents i_{L1} and i_{L2} in time resulting from the simulation of the circuit shown in Fig.7.1. The system settles down to its steady-state operating point within

30 msec. The oscillation in the currents at starting, are indications of the presence of the poles of the system located on the imaginary axis. The results presented here cover the first 80 msec. of the simulation. Fig.7.2(b) shows the capacitor voltage v_{C1} and Fig.7.2.(c) shows the output voltage v_o. Note that the average output voltage is negative in polarity at the designed value -67 V.

The steady-state behaviours are shown in Fig.7.3 (a) – (c). The data displayed here are extracted from the complete response shown in Fig.7.2(a) – (c) around t = 50 msec. Fig.7.3 (a) shows the inductor current variations i_{L1} and i_{L2} for a period of a few cycles around t=50 msec. Figs.7.3(b) and (c) show similar detailed variations at

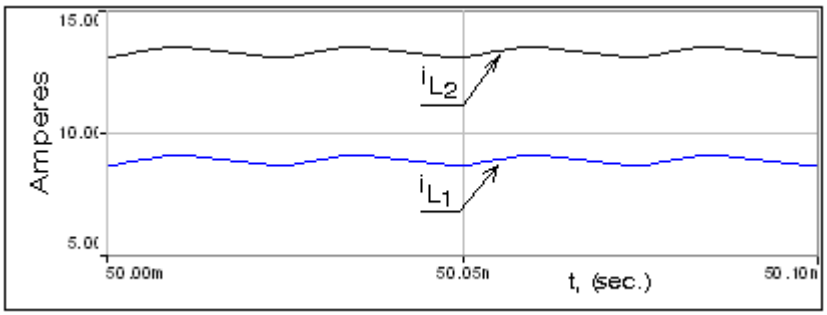

7.3 (a) inductor currents i_{L_1}, i_{L_2} in detail for a few cycles.

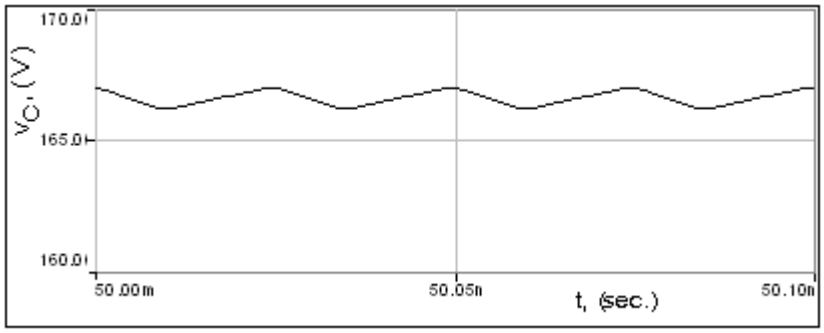

7.3 (b) detailed capacitor voltage v_{C_1} for a few cycles.

the same time interval for the capacitor voltage v_{C_1} and the output voltage v_0, respectively. The computed ripple magnitudes for the capacitor voltage, the output voltage, and the inductor currents are given in Table 7.3.

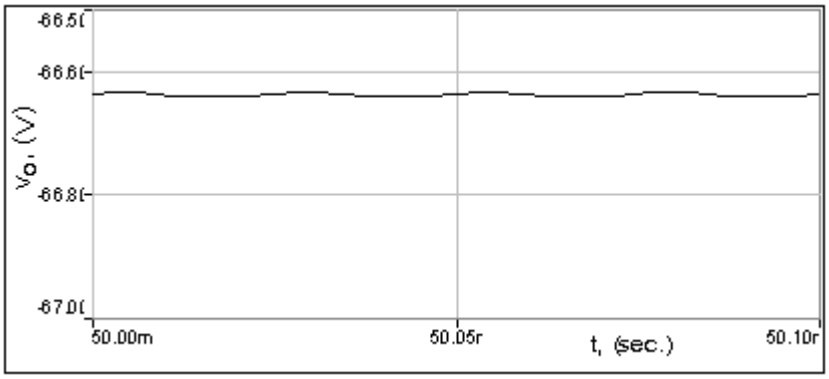

7.3 (c) detailed output voltage v_0 for a few cycles.

Table 7.3 Ripple magnitudes at steady-state

Peak-to-Peak Ripple	ΔV_C / V	ΔV_0 / mV	ΔI_{L1} / A	ΔI_{L2} / A
Magnitude	0.59	9.76	0.5	0.5

7.2 Design and Simulations for Discontinuous Inductor Current Mode Operation

In simulating the circuit in continuous conduction mode operation M conversion-ratio and conduction parameter K_a were found as given in Table 7.4.

Table 7.4 Conversion ratio and Conduction parameter

Parameter	Value
K_a	16
M	0.67

The discontinuous conduction mode operation for the same conversion ratio M, conduction parameter K_a must be lower than 0.35 according to the criteria developed previously for discontinuous conduction mode operation. Since K_a depends on the equivalent inductance L_{eq}, it can be decreased to 0.35 by changing L_{eq}. The critical value of the equivalent inductance L_{eq} for M=0.67 is calculated as

$21.8*10^{-6}H$, so that $L_{eq} < 21.8*10^{-6}H$. Conduction parameter K_a can also be modified by decreasing both the output current magnitude and the switching frequency. However, here both the current demand and switching frequency are considered constant.

In accordance with (3.22) the order of magnitude of L_1 remained same, although it is reduced to 1mH. In order to obtain the desired L_{eq} a higher value has been adopted for L_2. Hence, $L_2 < 21.5\mu H$ is found. Consequently, parameters of the converter that operates in discontinuous conduction mode have been modified to those given in Table 7.5. The other parameters of the circuit remain same as given in Table 7.6. Input and output current ripples resulting in the discontinuous inductor current mode of operation are given in Table 7.7.

Table 7.5 Parameters for Discontinuous Inductor Current Mode

Parameter	L_{eq} /μH	L_1/mH	L_2/μH	K_a	M	K	K_1
Value	14.77	1	15	0.236	0.67	0.32	0.48

Table 7.6 Other Circuit Parameters

Component	C /μF	C_o /μF	R / Ω
Size	150	200	5

Table 7.7 Input and output ripple currents

Variable	ΔI_{L1} / A	ΔI_{L2} / A
Magnitude	0.8	53

The implemented circuit for the simulation is shown in Fig. 7.4. Switch S is driven with PWM module switches with a period T=0.025 ms, and K=0.32 duty-

ratio. Simulation results for transient mode are given in Fig. 7.5. It takes about 6 msec to settle down to the steady-state operating point. Simulation is made for 80 msec in length. It is observed that the output current waveform has a large envelope due to high magnitude of the current ripple.

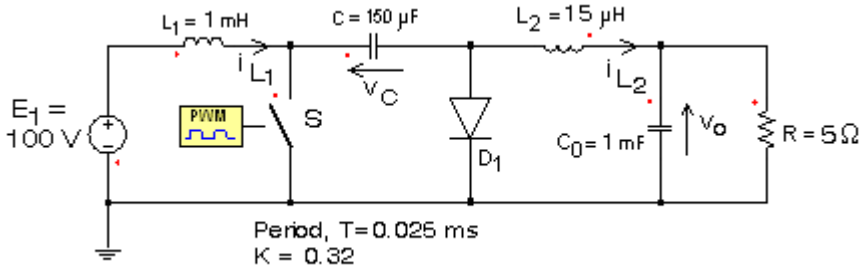

Fig. 7.4. The circuit simulated

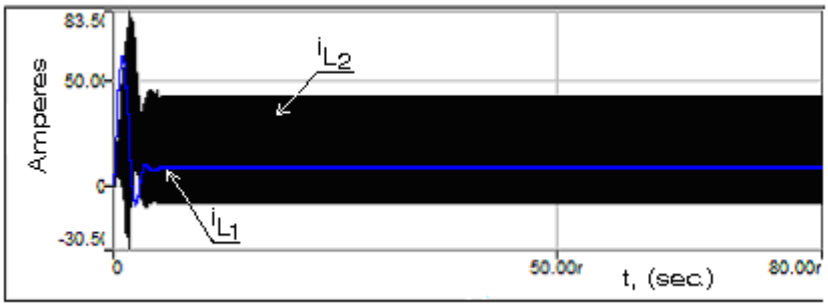

Fig. 7.5 (a) Input and output inductor current i_{L_1}, i_{L_2}.

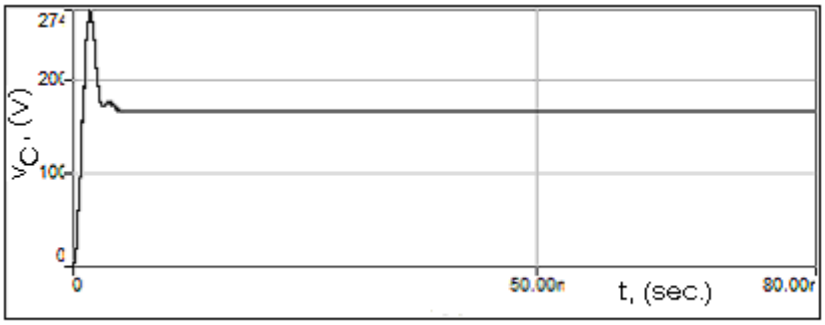

Fig. 7.5 (b) Energy transferring capacitor v_{C_1}.

The steady-state responses for a few cycles around t= 50.0 ms are shown in Fig. 7.6 (a) – (c). They are the current waveforms for the inductors, the diode current waveform, the energy transfer capacitor's voltage waveform and the output voltage waveform.

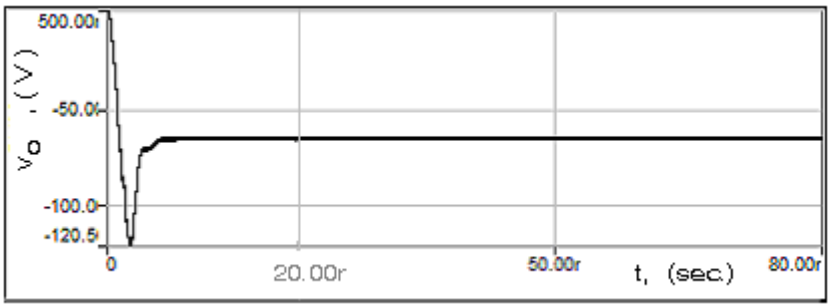

Fig. 7.5 (c) Output voltage v_0 simulation results.

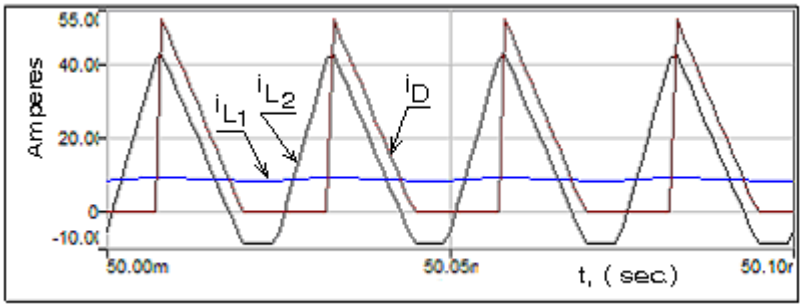

Fig. 7.6 (a) Simulation results of input and output inductor current i_{L_1}, i_{L_2} and diode current i_D scaled for few cycles.

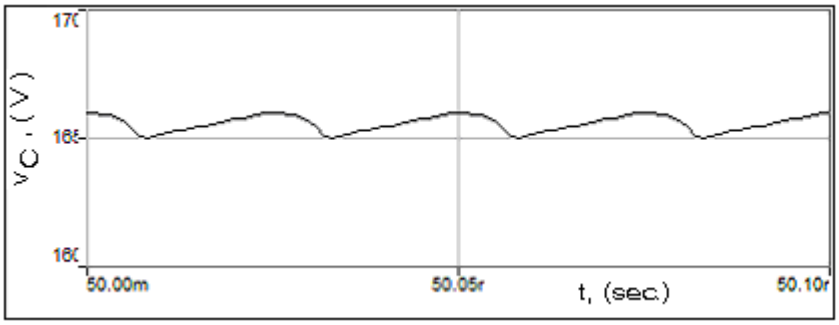

Fig. 7.6 (b) Simulation results of energy transfering capacitor voltage v_{C_1} scaled for few cycles.

In the analysis the voltage ripple of the energy transferring capacitor within the interval $(K+K_1)T, T$ is ignored except the derivation of I_f expression. Note that this voltage ripple ignored here is directly related with I_f. From simulation

results of the energy transferring capacitor, it is obviously seen that the voltage of the capacitor increases slightly at the state 'S off, D_1 off'.

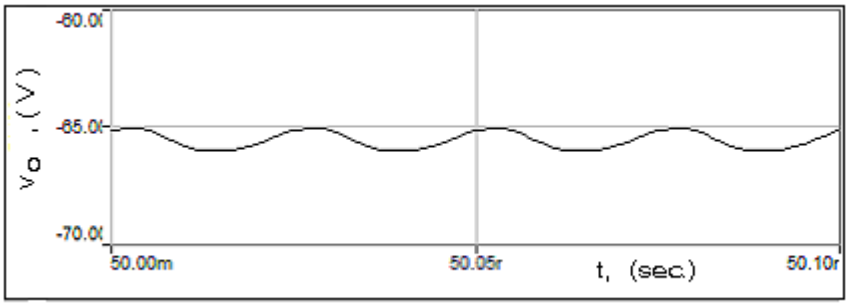

Fig. 7.6 (c) Simulation results of output voltage v_0 scaled for few cycles.

The output voltage waveform shown in simulation results has higher ripple than that obtained in the continuous conduction mode. The reason for this is the reduced size of the output inductance L_2. Thus the corner frequency of the output filter L_2-C_0 increases and it can not, therefore, filter ripples as did before. To reduce the ripple at discontinuous conduction mode the output filter corner frequency needs to be reduced by increasing capacitor value. This, however, violates the condition to be satisfied of the item 3 in Part 6.3.

The simulation is repeated with a large output capacitor of C_o =1 mF to yield us the steady-state responses shown in Fig.7.7(a) –(c).

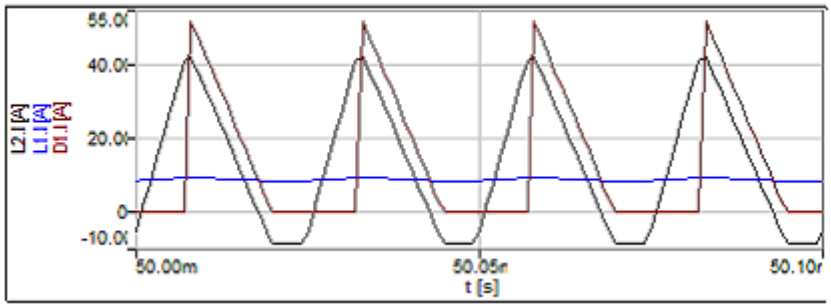

Fig. 7.7 (a) Simulation results of input and output inductor current i_{L_1}, i_{L_2} and diode current i_D scaled for few cycles.

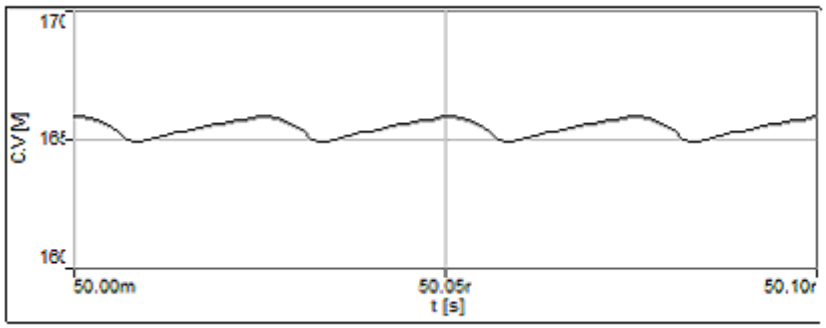

Fig. 7.7 (b) Simulation results of energy transferring capacitor voltage v_{C_1} scaled for few cycles.

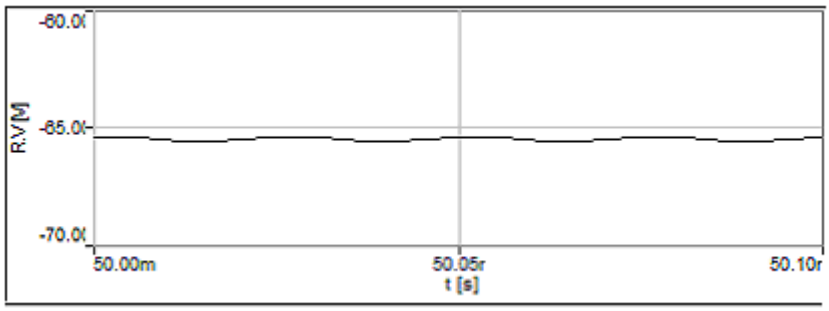

Fig. 7.7 (c) Simulation results of output voltage v_0 scaled for few cycles.

7.3 Design and Simulations for Application of Cuk Converter as Power Factor Preregulator

The circuit elements that are already modified in part 7.2 so that the converter runs in discontinuous inductor current mode are given together in table 7.8.

Table 7.8 Modified circuit elements for Discontinuous Inductor Current Mode

Component	L_1 / mH	L_2 / μH	C / μF	C_0 / mF	R / Ω
Size	1	15	150	1	5

A bridge rectifier, supplied from RMS 220 V AC, is used as a dc source. Required output voltage is 100 V. Load is considered constant, so parameter K_a is constant for this case. Conversion-ratio M for input peak voltage 311 V is 0.32. According to (3.56) K_a satisfies the condition $K_a < 0.28$. K_a parameter for the considered circuit is 0.236, so the circuit parameters are not modified. For given parameters K_a and M duty-ratio K_1 is calculated as 0.24. The parameters are given in Table 7.9.

Table 7.9 Conduction parameters and Duty ratios for the circuit

Parameter	M	K_a	K_1
Value	0.32	0.236	0.24

As stated before input voltage of the converter has periodical waveform. According to the item one and two of '6.3 Critical Points for Open Loop Operation' (6.68) and (6.69) must be satisfied. For the proposed circuit the calculated variables of (6.68), (6.69), (6.70) are given in the table 7.10. (6.69) is satisfied by the parameters of the circuit. Resonant frequency of input inductor and energy storage capacitor is 4 times greater than input line frequency. Thus (6.68) is not satisfied. This causes oscillation in input current.

The constructed circuit for simulation is shown in Fig. 7.8. Simulation results for transient mode are given in Fig. 7.9.

Table 7.10 Parameters for the proposed circuit

Parameter	w_L	w_S	$\frac{1}{\sqrt{L_1 C_1}}$	$\frac{1}{\sqrt{L_2 C_1}}$
Value	628	251327	2582	21082

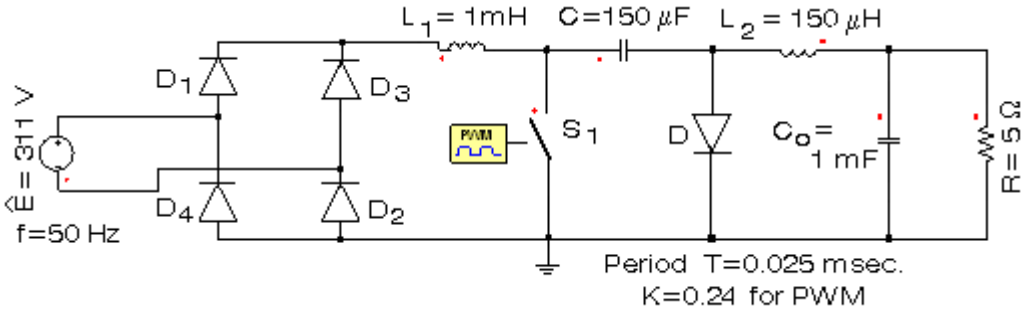

Fig. 7.8 The constructed circuit for the simulation.

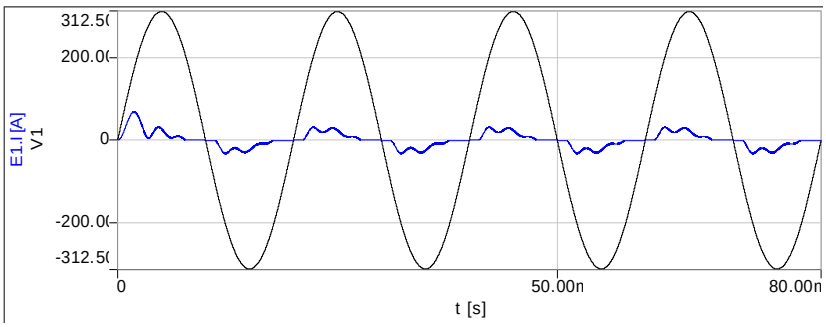

Fig. 7.9 (a) Current and voltage waveforms of the supply E_1

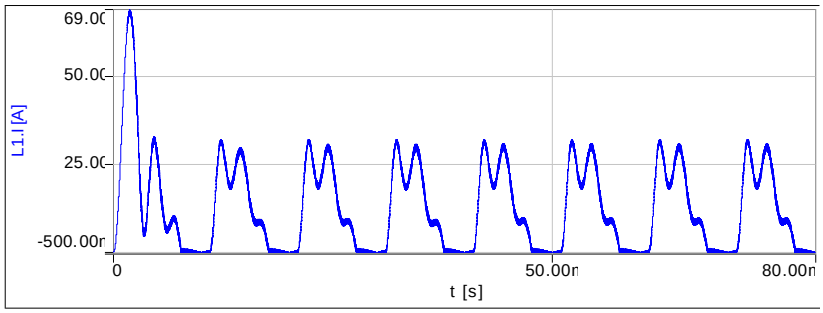

Fig. 7.9 (b) Input inductor current, i_{L_1} waveform.

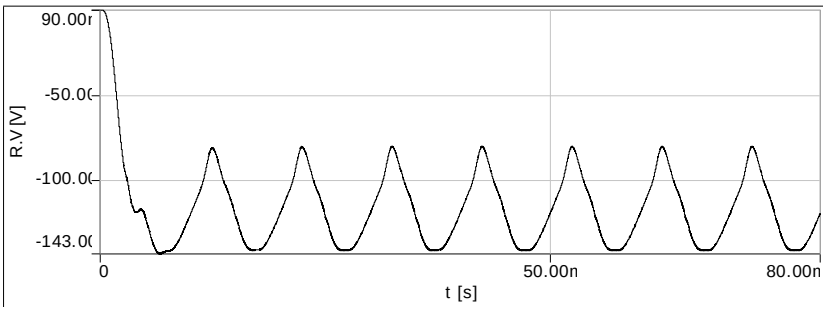

Fig. 7.9 (c) Output voltage, v_0 waveform.

It is obviously seen from results that input current oscillates at the proposed frequency. Also the output voltage has ripples at the frequency of the input voltage. This is due to the inability of the filter made of the output inductor and the output capacitor. To reduce the input current oscillations, the angular frequency $\frac{1}{\sqrt{L_1 C_1}}$ is to be modified to satisfy the item one of 'Critical Points for Open Loop Operation'. Modified values for components are:

Table 7.11 Modified Component values

Component	Value
L_1	200uH
C_1	7 uF
C_0	5 mF

As stated in [4] the existing capacitor is calculated to filter switching frequency ripple. Another capacitor, as practically applied, is used to filter out the line frequency ripple. In the simulation the size of the output capacitor is modified instead of adding a capacitor. After the modification, calculated parameters for discontinuous inductor current mode operation are given in Table 7.12. Simulation results are given in Fig. 7.10.

Table 7.12 Conduction parameters and duty-ratios for the circuit

Parameter	Value
M	0.36
K_a	0.22
K_1	0.24

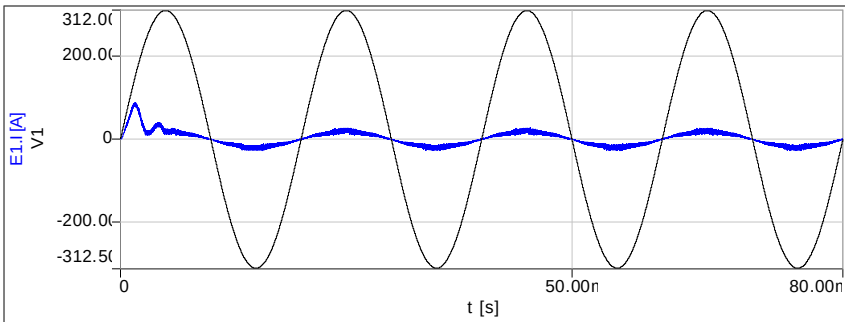

Fig. 7.10 (a) Supply E_1 voltage and current waveform for PFP operation

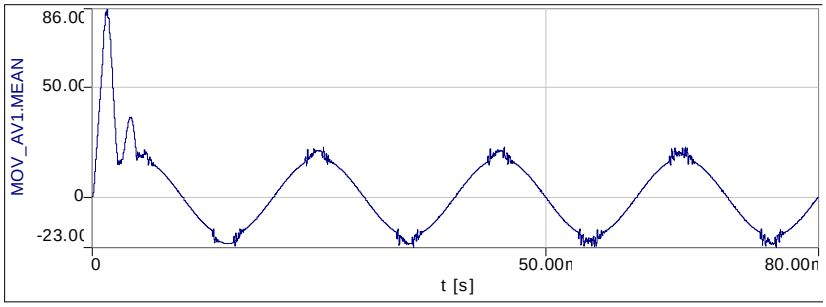

Fig. 7.10 (b) Supply E_1 current waveform averaged for a period for PFP operation

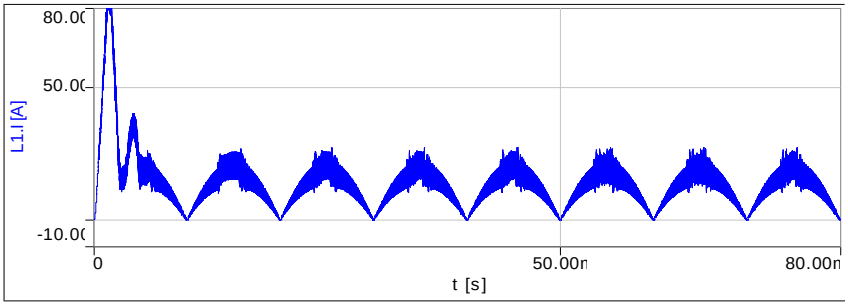

Fig. 7.10 (c) Input inductor current i_{L_1} waveform for PFP operation

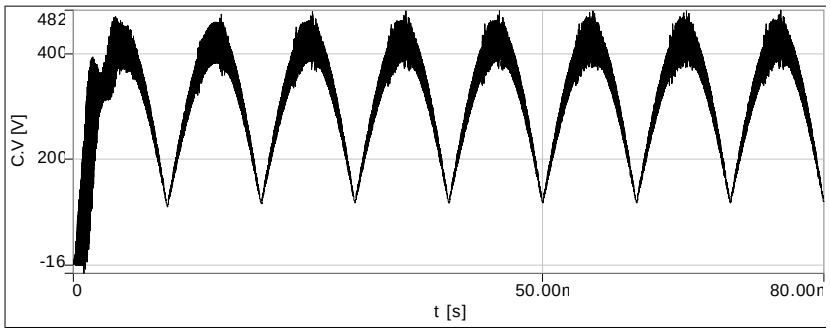

Fig. 7.10 (d) Voltage v_{C_1} waveform of energy transferring capacitor for PFP operation

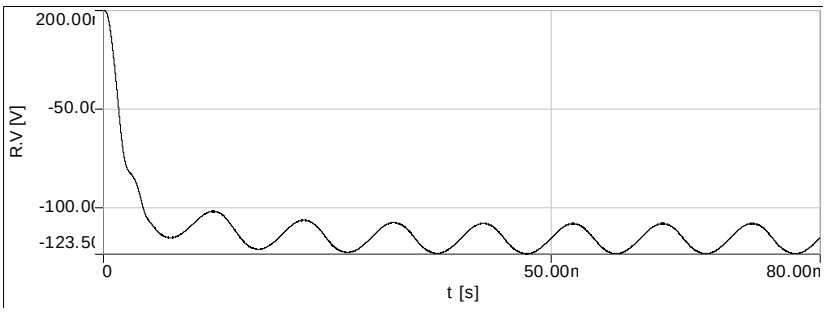

Fig 7.10 (e) Output voltage v_0 waveform for PFP operation

Power factor at the supply is calculated by simulator as 0.815.

7.4 Design and Simulations for Dynamic Models

7.4.1 Continuous Inductor Current Mode Simulations

The ideal circuit proposed for continuous inductor current mode analysis in Table 7.1 is considered for simulation of dynamic models. Its line to output voltage transfer function is obtained as:

$$\frac{v_0(s)}{e_1(s)} = \frac{0.6667}{0.333*10^{-12}s^4 + 0.333*10^{-9}s^3 + 1.41*10^{-6}s^2 + 0.5824*10^{-3}s + 1} \qquad (7.1)$$

The circuit do not satisfy criteria determined for separate corner frequencies since elements L_1 is equal to L_2. Bode plot of the line to output transfer (7.1) is given in

Fig. 7.11. Bode plot shown that corner frequencies are not separate as predicted. Step response of the line to output voltage transfer function is given below in Fig.7.12.

The circuit given in Table 7.1 is modified to satisfy separate corner frequencies criteria:

Table 7.13 Modified circuit parameters for separate corner frequencies.

Component	L_1 / mH	L_2 /mH	C_1 /μF	C_0 /μF	R /Ω
Size	2	0.5	150	500	5

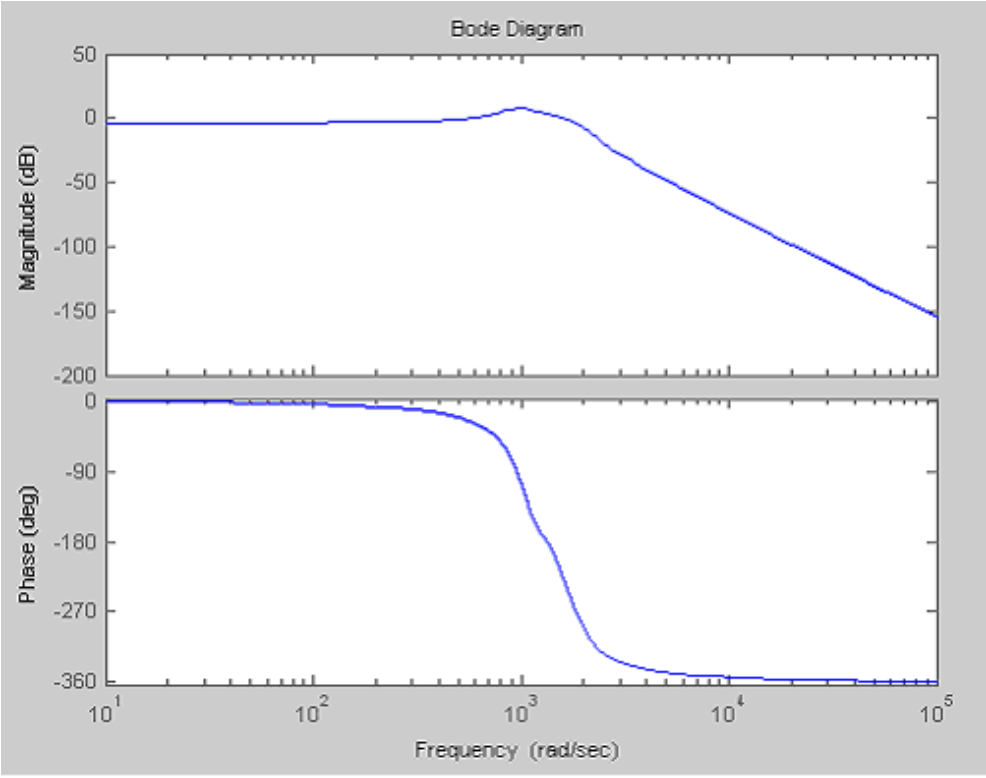

Fig. 7.11. Bode plot of the transfer function (7.1)

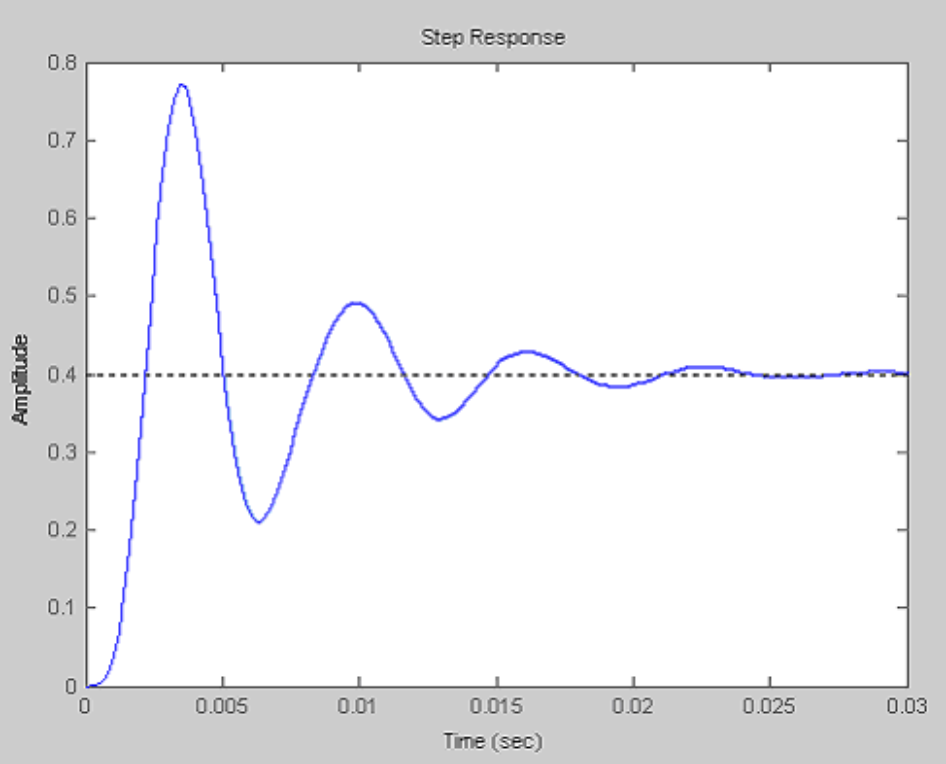

Fig. 7.12. Step response of the transfer function (7.1)

Line to output voltage transfer function for the circuit given in table 7.13 is obtained as following:

$$\frac{v_0(s)}{e_1(s)} = \frac{0.6667}{0.208*10^{-12}s^4 + 0.083*10^{-9}s^3 + 1.113*10^{-6}s^2 + 0.28*10^{-3}s + 1} \tag{7.2}$$

Poles for the transfer function with approximation method (6.5) are obtained:

$$s_{1,2} = -90{,}90 \pm 8.8430i$$

$$s_{3,4} = -200 \pm 10.11i \tag{7.3}$$

Bode plot for approximate and original transfer functions are obtained in Fig. 7.13. Graph plotted with blue shows results of original transfer function. Green graph was plotted for transfer funtion obtained or approximate solution. Approximating tends to separate corner frequencies.

7.4.1.1 Parasitic Resistance Effects

Parasitic resistances are considered as follows:

Table 7.14. Parasitic resistances considered for continuous inductor current mode

Parameter	r_{L_1} / Ω	r_{L_2} / Ω	r_{ds} / Ω	e_D / V	r_D / Ω	r_{C_1ESR} / Ω	r_D / Ω
Value	0.5	0.5	0.05	0.7	0.01	0.01	0.01

Line to output transfer function in (6.36) is obtained as following for parameters given table 7.13 and 7.14:

$$\frac{v_0(s)}{e_1(s)} = \frac{0.6667(1-11*10^{-6}s-80*10^{-12}s^2)}{0.209*10^{-12}s^4+0.364*10^{-9}s^3+1.696*10^{-6}s^2+0.648*10^{-3}s+1.160} \quad (7.4)$$

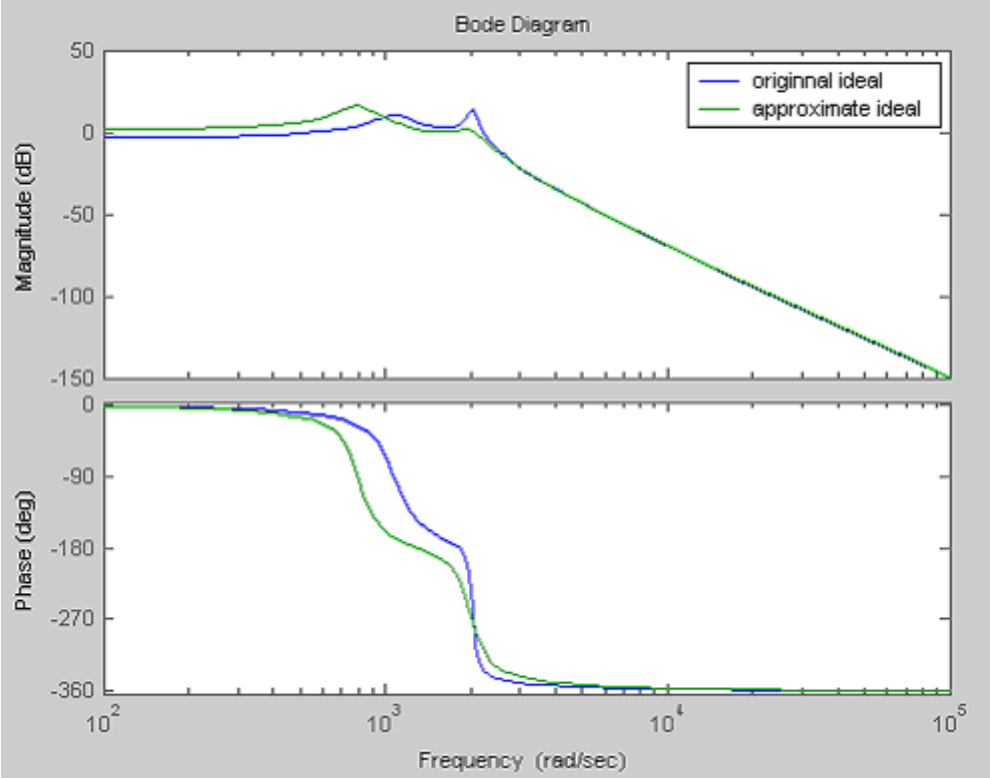

Fig. 7.13 Bode plots of line to output transfer function (7.2) and line to output transfer function obtained for approximate poles (7.3).

Bode plots for transfer functions (7.2) ideal case and (7.4) with parasitic resistances are given in Fig. 7.14. Bode plots of Fig. 7.14 shows that quality factors Q for the system decrease considerably with parasitic effects.

Step responses of both functions are shown in Fig.7.15. It is clearly seen that in ideal case the response settles to higher steady-state value following large oscillations. This implies that quality factor Q is high for the ideal case and parasitic resistances cause extra damping.

7.4.2 Discontinuous Inductor Current Mode Simulations

The ideal circuit proposed for discontinuous inductor current mode analysis in Table 7.5 is considered for simulation of dynamic models. Line to output transfer function for the proposed circuit is obtained as;

$$\frac{v_0(s)}{e_1(s)} = \frac{0.24}{2.250*10^{-15}s^4 + 0.450*10^{-12}s^3 + 0.315*10^{-6}s^2 + 0.033*10^{-3}s + 0.36} \quad (7.5)$$

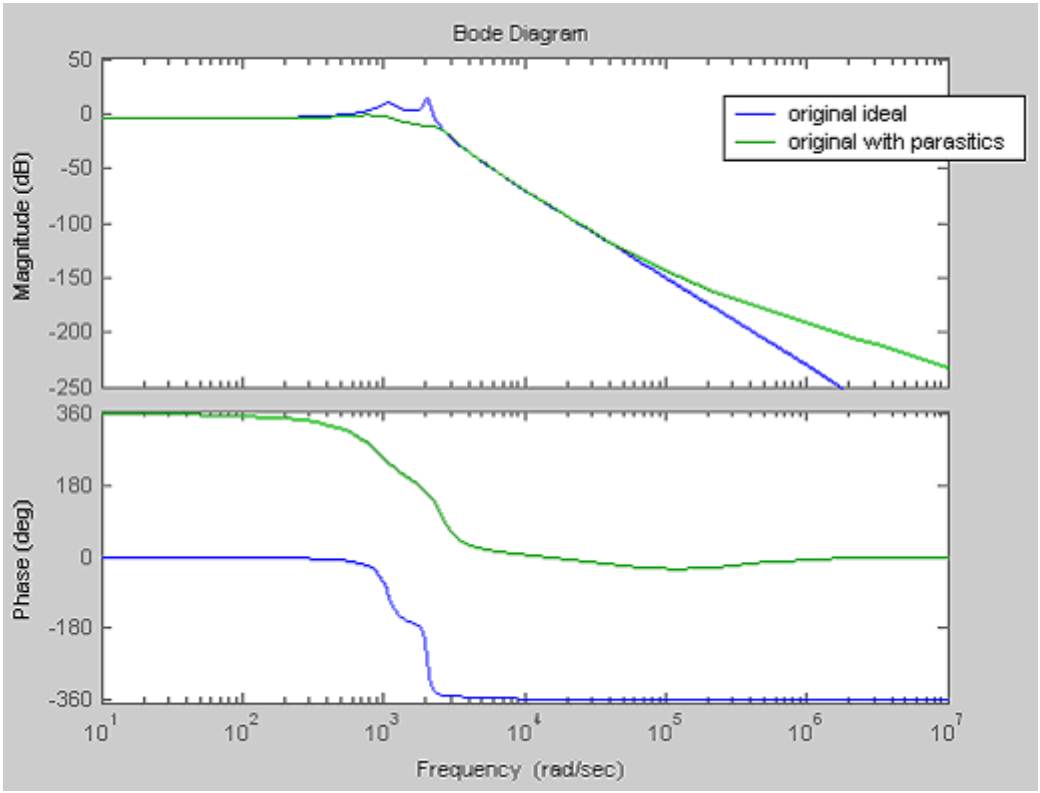

Fig. 7.14 Bode plots of line to output transfer function (7.2) ideal case and line to output transfer function (7.4) with parasitic resistances.

The separate corner frequency criteria is satisfied by parameters of the circuit in Table 7.5. Poles of transfer function (7.5) with approximation method (6.5) are obtained as:

$$s_{1,2} = -52.44 \pm 20.3480i$$

$$s_{3,4} = -100 \pm 71.03i \quad . \tag{7.6}$$

Bode plot for transfer function with approximate poles (7.6) and transfer function (7.5) are plot in Fig.7.16. Graph plotted with blue is a result of transfer function (7.5). Green graph was plotted for transfer function obtained for approximate poles (7.6).

7.4.2.1 Parasitic Resistance Effects

Parasitic resistances are considered as given in Table 7.15. Approximate solution for discontinuous inductor current mode tends to close up corner frequencies.

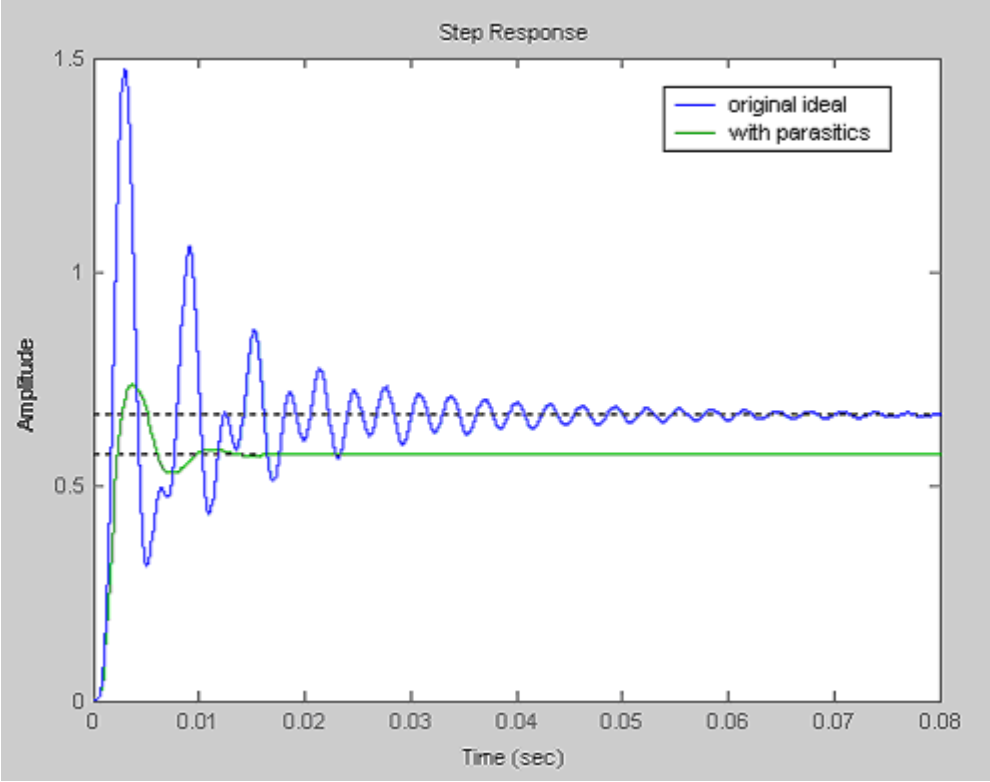

Fig. 7.15 Step response of line to output transfer function (7.2) ideal case and line to output transfer function (7.4) with parasitic resistances.

Table 7.15. Parasitic resistancec considered for continuous inductor current mode

Parameter	r_{L_1}/Ω	r_{L_2}/Ω	r_{ds}/Ω	e_D/V	r_D/Ω	r_{C_1ESR}/Ω	r_{C_0ESR}/Ω
Value	0.1	0.5	0.05	0.7	0.01	0.01	0.01

Line to output transfer function in (6.53) is obtained as following for parameters given Table 7.5 and Table 7.15:

$$\frac{v_0(s)}{e_1(s)} = \frac{1.041(1 - 6.25*10^{-6}s - 1.625*10^{-12}s^2)}{0.626*10^{-12}s^4 + 0.065*10^{-9}s^3 + 1.024*10^{-6}s^2 + 0.440*10^{-3}s + 1.08} \quad (7.7)$$

Bode plots for ideal case discontinuous inductor current mode operation transfer function (7.5) and transfer function for discontinuous inductor current mode with parasitic resistances (7.7) are obtained. According to Fig.7.17 corner frequencies are

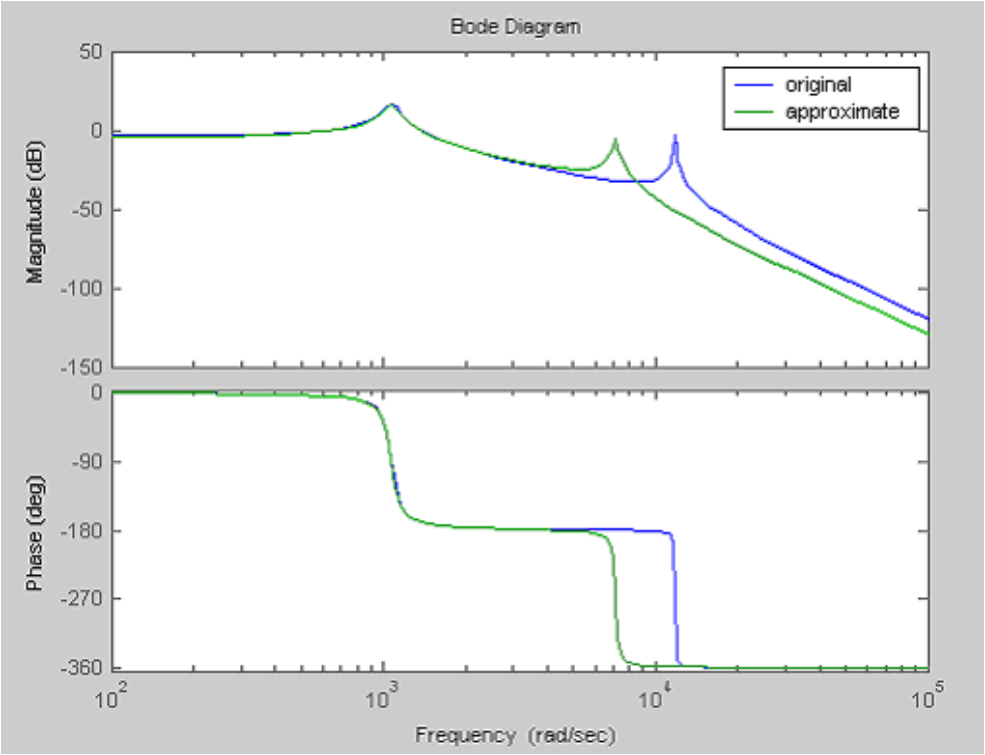

Fig. 7.16 Bode plot for transfer function with approximate poles (7.6) and transfer function (7.5).

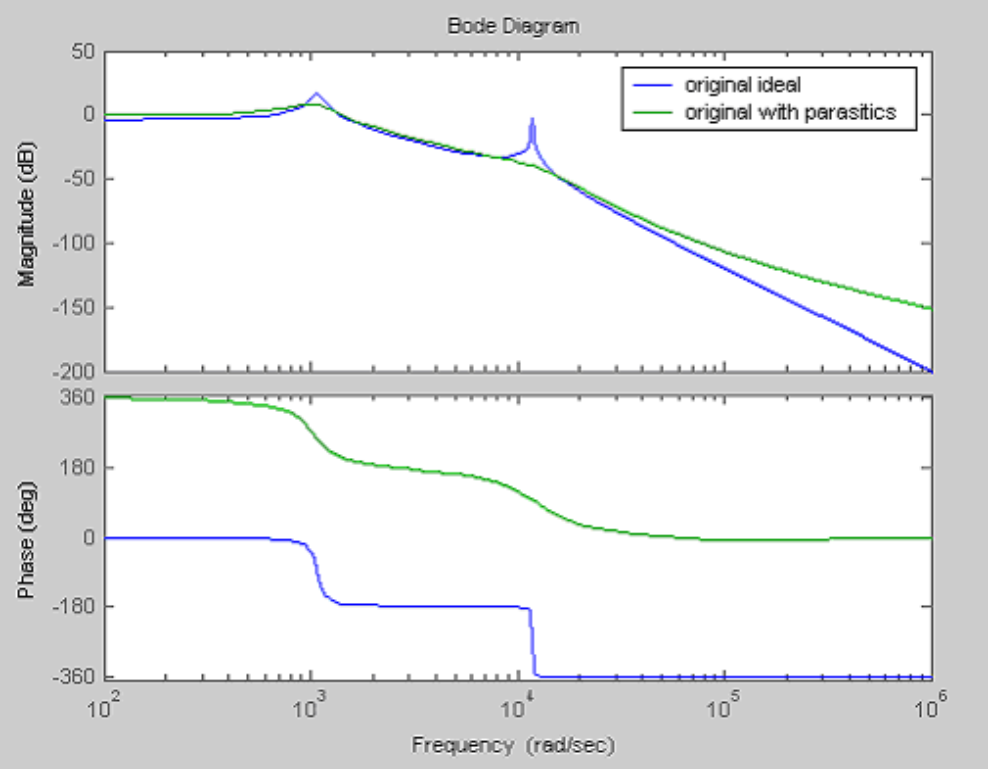

Fig. 7.17 Bode plots for ideal case discontinuous inductor current mode operation transfer function (7.5) and transfer function for discontinuous inductor current mode with parasitic resistances (7.7)

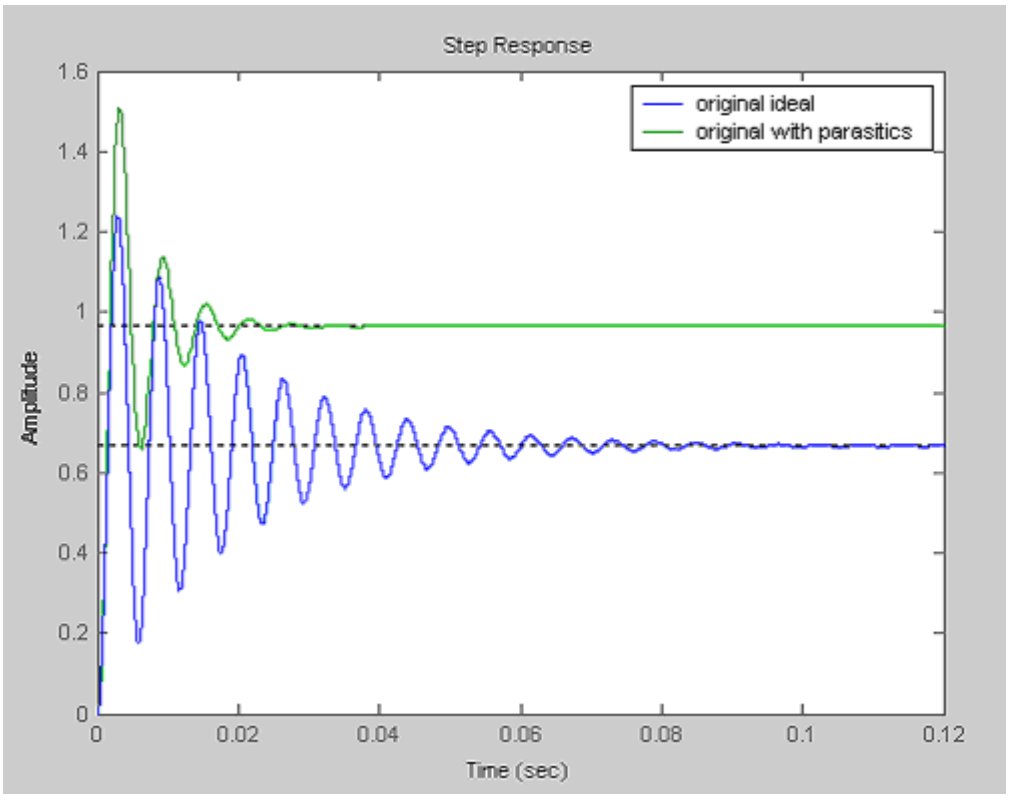

Fig. 7.18 Step responses of the functions (7.5) and (7.7)

not affected by parasitic resistances. But parasitic resistances tend to increase magnitude, according to simulation results. That is not expected result. Step responses of the functions (7.5) and (7.7) are shown in Fig.7.18. Increases in the magnitude and in the peak values are also observed for parasitic resistance case. This is not an expected result also.

General case observed for all transfer function is the shift of the phase by -180 degree resulting for frequencies between the two corner frequencies.

CHAPTER 8

CONCLUSION

The study introduced in this thesis compiles the results of studies made related to Cuk converters. The summary of the compilation can be given as follows:

The steady-state and dynamic models are derived using the state-space averaged models. Stability and small signal behavior are analyzed through open loop dynamic voltage conversion ratios and control to output dynamic conversion ratios, where conventional definition of the dynamic conversion ratios is transfer functions.

Derivations are repeated for the topology of Cuk converter including parasitic resistances. Losses of parasitic resistances and switching are determined and overall efficiency expression is obtained.

Consequently with a designed converter theoretical analysis are investigated through simulations.

Current and voltage ripples at steady-state are analyzed using state equations. It is shown in the study that equations governing the operation of the converter at steady-state are equal to those derived from volt-second and current-charge balancing. One point of interest is that, these equations do not include capacitors and inductors present in the converter. Thus the steady-state operating point is not determined by the capacitors and inductors of the system.

The thesis tries to give quite detailed analysis of the Cuk converter in discontinuous inductor current mode. It is seen that the converter is forced to operate in discontinuous inductor current mode if the size of the output inductance is decreased to a sufficiently low value or the switching frequency is decreased to a sufficiently low value. The followings have been noted in the operation at this mode; two of the three states of operation resulting in this mode are similar to those obtained in continuous inductor current mode operation, whereas the third state in the

discontinuous mode of operation does yield significant difference in the state variable, and the input current freewheels.

Compared to the continuous inductor current mode operation, the output inductor current ripple for discontinuous inductor current mode results is high. Also, the output inductor current ripple magnitude comes out greater than the average output inductor current.

The ability of Cuk converter to operate satisfactorily in discontinuous inductor current mode makes them a choice to be used as a Power Factor Preregulator. Noting that the input voltage for them in these applications are half sinusoidal waveform, the discontinuous inductor current mode operation together with half sinusoidal input voltage put the converter into worst case operational condition.

The thesis accounts for the effects of parasitic resistances on the steady-state and dynamic models for both operation modes. Static parasitic resistance of switches and elements are determined. Steady-state and dynamic models are obtained for the modified topology with parasitic resistances. It is noted in the study that the steady-state conversion ratios for both continuous and discontinuous modes of operations are reduced by the presence of the parasitic resistances.

The thesis pays attention to the overall efficiency issue as well. Expressions, regarding to the overall efficiency of Cuk converter, are derived while it is operating in continuous inductor current mode and discontinuous inductor current mode. It is made clear that parasitic resistances, non ideality of the magnetic core material used for inductances, and switching loss resulting from simultaneous current and voltage transitions in switching elements are primary causes for losses in the Cuk converter. Within this context we note that losses in the magnetic core material and during the turning off transition period of the switch are high for discontinuous inductor current mode compared to the losses of continuous inductor current mode. Whereas for discontinuous inductor mode, losses resulting during diode conductions and in turning on transition period of the switches are nearly zero. The effect of increasing

switching frequency on the efficiency for operations in both modes can be simply summarized as a decrease.

Considerations regarding to the stability and dynamic behavior of the Cuk converter are based on dynamic conversion ratios which are conventionally called transfer functions in the thesis work. General stability criteria for the Cuk converter are established so that separate corner frequencies are to be satisfied. Such a condition accounts for the poles of the system can be approximated in case of separate corner frequencies. Otherwise, the stability analysis can only be made for a given specific numerical set of the elements. It is seen in this part of thesis work Cuk converter while operating in discontinuous inductor current mode already satisfies separate corner frequencies condition. However, for continuous inductor current mode operation the criterion needs to be checked whether it is being satisfied for the given set of converter parameters. Note that for the open-loop operation Cuk converter, with separate corner frequency condition being satisfied, is stable for all cases. Parasitic resistances tend to separate corner frequencies and add zeros to conversion ratios of the system for both operation modes. Parasitic resistance effect in quality factor Q can not be stated obviously according to the obtained expressions. Also the thesis work refers to the critical points that affect dynamic behavior of the converter.

Simulations of a Cuk converter made in the thesis work show that Cuk converter is stable for both operating modes. Simulations with parasitic resistances included indicate that the quality factor Q decreases with increasing amount of parasitic resistances. However, increasing presence of them do not significantly affect corner frequencies. For continuous inductor current mode the magnitude of step response for ideal case is greater than the magnitude of step response for the case including parasitic resistances. However, for discontinuous inductor current mode the magnitude of step response for ideal case is smaller than the magnitude of step response for the case including parasitic resistances.

REFERENCES

[1] Cuk, Slobodan M., *Modeling, Analysis and Design of Switching Converters, Ph.D. Theses,* California Institude of Technology, Pasadena, California, 1977.

[2] Middlebrook R.D., Cuk Slobodan, *A General Unified Approach to Modeling Switchin- Converter Power Stages.* IEEE Power Electronics Specialist Conference, pp. 73-86 , Cleveland , June 1976.

[3] Sebastian, J., Cobos J. A., Lopera J. M. And Uceda J. *The determination of the Boundaries Between Continuous and Discontinuous Conduction Modes in PWM Dc-to-Dc Converters Used as Power Factor Preregulators.* IEEE Transactions on Power Electronics, Vol. 10, No.5, September 1995.

[4] Simonetti, D. S. L., Sebastian, J. and Uceda, J. *The Discontinuous Conduction Mode Sepic and Cuk Power factor Preregulators: Analysis and design.* IEEE Transactions on Industrial Electronics, Vol. 44, No.5, October 1977.

[5] Brokovic, Milivoje, Cuk, Slobodan. *Input Current Shaper Using Cuk Converter,* Telecommunications Energy Conference, pp. 532-539, 1992. INTELEC '92., 14th International.

[6] Maksimovic, Dragan, Cuk, Slobodan. *A unified analysis of PWM Converters in Discontinuous Modes.* IEEE Transactions on Power Electronics, Vol. 6, No.3, July 1991.

[7] Rashid, Muhmmed H., *Power Electronics, 2nd Ed.,* Printice-Hall, Inc., New Jersey, 1998.

[8] Erickson, Robert W. , Maksimovic, Dragan. *Fundamentals of Power Electronics.* 2nd ed. Kluwer academic Publishers, 2003.

[9] Krein, Philip T. *Elements of Power Electronics.* Oxford University Press, 1998.

[10] Rashid, Muhammad H. *Power Electronics Handbook.* Academic Press, 2001.

[11] Vorperian, Vatche. *The effects of Magnetizing Inductance on the Small- Signal Dynamics of the Isolated Cuk converter.* IEEE Transactions on Aerospace and Electronic Systems, Vol. 32, No.3, pp. 967-983, July 1996.

[12] L. Malesani, L. Rosseto, G. Spiazzi, P. Tenti, *Performance Optimization of Cuk Converters by sliding Mode Control.* IEEE Transactions on Power Electronics, Vol. 10, No. 3, pp. 395-402, 1992

[13] J. Mahdavi, A. Emadi, H.A. Toliyat, *Appliction of State Space Averaging Method to Sliding Mode Control of PWM DC/DC Converters,* Industry Applications Conference, Thirty-Second IAS Annual Meeting, IAS '97., Conference Record of the 1997 IEEE, pp. 820-827, 1997.

[14] Y. Fuad, W. L. de Koning and J. W. van der Woude, *Pulse-width modulated d.c.–d.c. converters,* International Journal of Electrical Engineering Education, Vol. 38, No. 1, pp. 54-79, 2001.

[15] Y. Fuad, W. L. de Koning and J. W. van der Woude, *On the Stability of Pulsewidth-Modulated Cuk Converter,* IEEE Transactions on Circuits and Systems-II: Express Briefs, Vol. 51, No. 8, 2004.

[16] G. Spiazzi, P. Mattavelli, *Design Criteria for Power Factor Preregulators Based on Sepic and Cuk Converters in Continuous Conduction Mode,* Industry Applications Society Annual Meeting, 1994., Conference Record of the 1994 IEEE, Vol. 2, pp. 1084 - 1089, 2-6 Oct 1994.

[17] Bo-Tao Lin, Yim-Shu Lee, *Power Factor Correction Using Cuk Converters in Discontinuous-Capacitor-Voltage Mode Operation,* , IEEE Transactions on Industrial Electronics, Vol. 44, Issue 5, pp. 648 – 653, 1997.

[18] Oppenheimer, M. , Husain, I., Elbuluk, M., De Abreu Garcia, J.A., *Sliding Mode Control of the Cuk Converter,* Power Electronics Specialists Conference PESC '96 Record., 27th Annual IEEE, Vol. 2, pp. 1519-1526, 1996.

[19] Santi, E., Cuk, S., *Modeling of One-Cycle Controlled Switching Converters,* Telecommunications Energy Conference, INTELEC apos;92., 14th International, pp. 131 – 138, 1992 .

[20] Smedley, K.M., Cuk, S., *Dynamics of One-Cycle Controlled Cuk Converters,* IEEE Transactions on Power Electronics, Vol. 10, Issue 6, pp. 634 – 639, 1995.

[21] Tse, C.K., Chan, W.C.Y., *Instability and Chaos in a Current-Mode Controlled Cuk Converter*, Power Electronics Specialists Conference, PESC apos;95 Record., 26th Annual IEEE, Vol. 1, pp. 608 – 613, 1995.

[22] Yi Jia, Wei Xueye, *Chaos in Switch Control of a Current-Mode Cuk Converter*, The 2nd International Workshop on Autonomous Decentralized System, pp. 267 – 272, 2002.

[23] Tse, C.K., Lai, Y.M., Iu, H.H.C., *Hopf Bifurcation and Chaos in a Free-Running Current-Controlled Cuk Switching Regulator*, IEEE Transactions on Circuits and Systems I: Fundamental Theory and Applications, Vol. 47, Issue 4, pp. 448 – 457, 2000.

[24] Cuk, S., *A New Zero-Ripple Switching DC-to-DC converter and Integrated Magnetics*, IEEE Transactions on Magnetics, Vol. 19, Issue 2, pp. 57- 75, 1983.

[25] Cuk, S., *New Magnetic Structures for Switching Converters*, IEEE Transactions on Magnetics, Vol. 19, Issue 2, pp. 75 – 83, 1983.